Performance Prediction, Parameter Selection, and Channel Adaptation in the Line-of-Sight Outdoors Optical Wireless Channels Using Intelligent Systems

By

Adnan El. Yakzan

A thesis submitted in partial fulfillment of the requirements for the degree of

Doctor of Philosophy

School of Engineering
August 2013

THE UNIVERSITY OF WARWICK

For my Family

Table of Contents

List of Figures

List of Tables

Acknowledgements

I would like to express my sincere appreciation to my supervisors, Prof. Roger J. Green, and Prof. Evor L. Hines for their valuable guidance and excellent support during the entire period of my PhD studies and writing of my thesis.

I would like to express my heartfelt gratitude to my parents for their support and patience through my academic endeavors. Special thanks to my sister Nadia Elberjaoui Yakzan for herencouragement through the entire period of my PhD.

I also acknowledge and appreciate the help rendered by Dr. Maaruf Ali, and my labmates: Mr. Rana Atif Khan, Mr. Hussein Kusetogullari, and Mr. Bilal Chehab, for their fruitful discussion and support through the good and bad times.

Declaration

This thesis is presented in accordance with the regulations for the degree of doctor of philosophy. This work described and reported is entirely original and my own, except where otherwise indicated.

List of Publications

Journal Papers

A. El. Yakzan, R.J. Green and E. L. Hines, "Performance Prediction and Parameter Selectionof LOS Optical Wireless Channel using Genetic Algorithm", *Submitted to IEEE Wireless Communications Magazine***,** 2013.

A. El. Yakzan, R.J. Green and E. L. Hines, "Artificial Neural Network for BER Prediction, and Adaptive Neuro-Fuzzy Inference System (ANFIS) for Channel Adaptation, utilizing ASGA Generated Data in Optical Wireless Communication", *Submitted to Jounal of Optical Communication and Networking(JOCN), 2013*.

Conferences

A. El. Yakzan, R.J. Green and E. L. Hines, "On the Performance of Shot and Johnson Noises in the LOS- Optical Wireless Channel under Sensible Selection Requirements of an Application- Specific Genetic Algorithm**",** 15th International Conference on Transparent Optical Networks, Spain, 2013.

A. El. Yakzan, R.J. Green and E. L. Hines, "Application-Specific Genetic Algorithm Targeting the Complexity of Parameter Selection in LOS Outdoors Optical Wireless Channel", *UKSim 15th International Conference on Mathematical/Analytical Modelling and Computer Simulation*, Cambridge, UK, 2013.

A. El. Yakzan, R.J. Green and E. L. Hines, "A Genetic Algorithm based Selection of a Transmission Wavelength in the LOS Optical Wireless Channel", *International Conference on Transparent Optical Networks*, Warwick, UK, July, 2012.

A. El. Yakzan, R.J. Green, E.L. Hines and M. Ali, " An Intelligent Approach to Link Parameter Estimation for Outdoor Optical Wireless Channels", *2012 Mediterranean Conference on Embedded Computing, Montenegro*, 2012.

A. El. Yakzan, R.J. Green, E.L. Hines "A Neuro-Genetic Hybrid Algorithm Utilizing Outdoors LOS Optical Wireless Channels", *4th International Conference on Computational Intelligence, Communication Systems and Networks*, Phuket, Thailand, 2012.

Abstract

With the increased usage of optical wireless communication, finding appropriate parameters for reliable transmission and providing efficient channel performance have become of challenging interest in research and industry. This has been a strong motivation to examine and develop methods and techniques to find suitable link parameters to increase the channel availability. This thesis is mainly concerned with designing, implementing and adapting intelligent algorithms to solve for parameter selection, channel prediction, and channel adaptation in dynamic optical wireless channels. The problem could be solved with other methods such as binary and sequential search; however, intelligent systems have the ability to find optimal results with more reliability, time efficiency and increased flexibility. The research focuses on single and multi-objective selection techniques using application-specific genetic algorithm (ASGA) in the outdoors line-of-sight (LOS) optical wireless channel where parameters have different effects on the channel performance and may affect the behaviour of other channel parameters. The technique is well-established at pre-installation stages of the channel, and could be also applied at run-time if a reconfigurable hardware is installed.

An intelligent system, which uses a genetic algorithm predicted and optimized optical wireless channel in the (LOS) field, is presented. The prediction technique is proposed to estimate the bit error rate (BER) at the receiver, and suggests appropriate selection of link parameters. In this research, the work is developed based on on-off keying (OOK) modulation, and makes use of different weather conditions for channel modeling. A first attempt is made with a GA-based selection for transmission wavelengths (700nm to 1600nm), the overall deterministic attenuations

being estimated by a visibility model, where the changes in visibility decide about the wavelength control margin. The research is then extended to consider various external link parameters scaled by look-up tables that meet the optical wireless industry. It shows that the transmission power should not always be the only costin the channel, and there are other parameters worthy of control. Principal Component Analysis is applied targeting the ASGA selected datasets to extract the contribution of each parameter to the output, and the implicit relations that exist among data sets to achieve a certain bit-error-rate. An Artificial Neural Network (ANN) is then applied to the channel for *BER* prediction; this may also validate the pre-installation advice done by PCA. Finally, a two-stage modelling using a neuro-fuzzy hybrid algorithm used for adapting the channel by monitoring the link range and total attenuations in the channel.

Through analysing the simulation results using these intelligent systems algorithms, the thesis aims at providing maximum utilization of channel parameters for achieving optimum channel performance and increased availability under the application of various intelligent systems, which demonstrate their efficiency and effectiveness as compared with other techniques.

Glossary of Terms

2G	Second Generation
3G	Third Generation
ANN	Artificial Neural Network
ANFIS	Adaptive Neuro-Fuzzy Inference System
ANSI	American National Standards Institute
APD	Avalanche Photodiode
ASGA	Application-Specific Genetic Algorithm
AWGN	Additive White Gaussian Noise
BER	Bit Error Rate
BPSK	Binary Phase Shift Keying
BW	Bandwidth
CATV	Cable Television
CCA	Canonical Correlation Analysis
CDMA	Code Division Multiple Access
CDR	Clock and Data Recovery
CMA	Clock Manipulation Unit
CSI	Channel State Information
DBIR	Directed Beam Infrared
DC	Direct Current
DMD	Deformable Mirror Devices
DMUX	Demultiplexer
EA	Evolutionary Algorithm
EC	Electric Current
EM	Electromagnetic
EMI	Electromagnetic Interference
FIS	Fuzzy Inference System

FM	Frequency Modulation
FOV	Field of View
FSO	Free Space Optics
FSO/RF	Free Space Optics/Radio Frequency
GA	Genetic Algorithm
Gbps	Gigabits per second
GP	Genetic Programming
GPS	Global Positioning System
HDTV	High Definition Television
IEC	International Electrotechnical Commission
IM/DD	Intensity Modulation/Direct Detection
IR	Infrared
IrDA	Infrared Data Association
ISI	Inter-symbol Interference
Kbps	kilobits per second
LAN	Local Area Network
LB	Lower Bound
LCD	Liquid Crystal Display
LD	Laser Diode
LED	Light Emitting Diode
LM	Levenberg-Marquadt
LN	Lognormal
LOS	Line of Sight
LSM	Line Strip Multibeam
LTCC	Low Temperature Co-fired Ceramic
MAN	Metropolitan Area Network
Mbps	Megabits per second

MEM	Micro-Electromechanical
MF	Membership Function
MHz	Mega Hertz
MIMO	Multiple-In Multiple-Out
ML	Maximum Likelihood
MLP	Multilayer Perceptron
MSD	Multi-spot Diffusing
MSE	Mean Square Error
MSM	Multiple Sub-carrier Modulation
MSM PD	Metal-semiconductor Photodiode
MUX	Multiplexer
NIR	Near Infrared
NLOS	Non Line of Sight
NN	Neural Network
NRZ	Non-Return-to-Zero
OOK	On-Off Keying
OW	Optical Wireless
PAM	Pulse Amplitude Modulation
PAR	Peak-to-Average Power Ratio
PCA	Principal Component Analysis
PD	Photodiode
PDAs	Personal Digital Assistant
PDF	Probability Density Function
PM	Pulse Modulation
PPM	Pulse Position Modulation
QE	Quantum Efficiency
QoS	Quality of Service

QPSK	Quadrature Phase Shift Keying
RF	Radio Frequency
RMA	Receiver Main Amplifier
SA	Simulated Annealing
SI	Scintillation Index
SIR	Short range Infrared
SNR	Signal-to-Noise Ratio
Tbps	Terabits per second
UB	Upper Bound
UV	Ultra Violet
WAN	Wide Area Network
W-CDMA	Wideband Code Division Muliplexing

CHAPTER I: Introduction

1.1 Introduction

Optical wireless is one of the latest approaches for telecommunications. It refers to a technology lying between two technologies: the radio communications and the optical fibre communications. Radio frequency (RF) and optical fiber technology have the potential of providing data capacity of the order of Gbps and Tbps respectively. The requirements of broadband wireless system can be met through the integration of the optical fibre with millimeter wave wireless systems, which is the subject of the latest area of telecommunications research, addressing the need for both the reliability and the confidentiality of multimedia services. The increasing demand on bandwidth in wireless communication has driven researchers to explore new technologies to accommodate more data throughput over the decades and has become a hot area of research and application. Optical Wireless, based on free-space optics (FSO), is becoming an attractive alternative for indoor and outdoor communications because of its wide bandwidth, high speed, low cost, license free spectrum and interference security. The direct interception of an optical wireless beam between the two remote networking locations is basically impossible because any individual attempts to block the beam would occur near the optical wireless equipment terminus point. Consequently, it is not necessary currently to add security protocols, especially when higher layer protocols (transport layer) can be used in conjunction with layer one optical wireless technology to encrypt sensitive network information and to provide additional encapsulation.

The transmission process in optical wireless imposes many challenges in the outdoor environment that threaten its survivability, such as adverse weather conditions, vibrations of buildings, eye safety requirements, passing obstacles, and multipath effects occur in the indoor environment. Several approaches discussed in the literature have been analyzed in order to propose ways of treating these challenges. In this thesis, different weather models designed for analyzing the optical wireless performance are used in order to concentrate on external channel parameters that could be controlled when the signal to noise ratio or the bit error rate at the receiver are considered.

The research utilizes the concept of evolutionary algorithms to analyse, predict, and select channel parameters in the outdoors optical wireless environment. Meta-heuristic designates a computational technique to optimize a search space problem and iteratively improving a solution of candidate based on the given measure of quality. In this thesis, the work builds on OOK modulation and uses the power of intelligent system techniques to develop multiple scenarios of selection and adaptation, which will be able to learn about the short range wireless optical medium according to different weather models, assign reliable parameters of transmission, update the layer with the various changes, and propose different optimization levels.

1.2 Optical Wireless Communication

The history of optical wireless communication goes back to 1960 when the laser as source light was invented by Dr. T. Mainman. In 1965, a beam guide system and the space propagation system which emits light to free space were being studied to use laser for free space optical communication, known as FSO nowadays [1.1]. For indoors optical wireless communications, the modern era was initiated by F. R.

Gfeller in 1979, who suggested the use of diffuse optical radiation in the near infrared to interconnect a cluster of terminals in the same room [1.2]. The growth of FSO technology has taken an exponential shape over the last few years especially for "last mile" applications, where FSO links provide the transmission capacity to overcome information bottlenecks. Optical wireless communication is a technology that uses modulated optical beams generated by light emitting diodes (LEDs) and lasers to transmit information in line-of-sight through the atmosphere. In comparison to RF, optical wireless communication is characterized by lower implementation cost, unregulated spectrum, high capacity, and security. However, the transmission process imposes many challenges in the outdoor environment that threaten its viability, due to bad weather conditions, building sway, obstacles, and multipath effects in the indoor environment [1.3].

1.2.1 Configuration of Optical Wireless Channel

Optical wireless communication consists of a transmission unit and a receiving unit. In the transmission unit, a light emitting source (LED) is modulated by a time-varying electrical current (EC) signals, and the receiving unit uses photodiodes (PIN or APD) to generate EC signals according to the instantaneous optical received power after traversing the medium (outdoor or indoor) [1.4]. The physical properties of the link and the dynamics of link characteristics require careful selection of modulation and reception techniques. One important method is the intensity modulation and direct detection IM/DD, as depicted in figure 1.1.

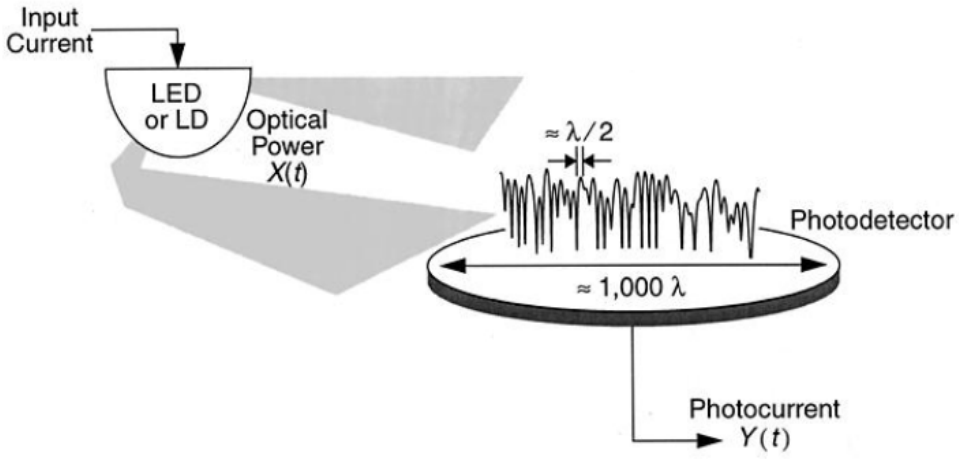

Figure 1.1 IM/DD Transmission and reception in an infrared link, adapted from [1.4].

$X(t)$ represents the instantaneous optical power from the emitter, $Y(t)$ represents the instantaneous current generated at the receiver photodiode. The optical link will not suffer from multipath fading effects that are usually experienced by the RF system since the surface of the photodetector is millions of square wavelengths of that of the received optical signal [1.5]. The differences between RF and IM/DD-IR can be summarized in table 1.1. Amplifier and filter modules are also used at both transmitter and receiver units to improve noise immunity and system throughput.

Table 1.1 Comparison between radio and IM/DD infrared systems for indoor wireless communications, adapted from [1.6].

Property of Medium	Radio	IM/DD Infrared	Implication for IR
Bandwidth Regulation	Yes	No	Approval not required. Worldwide compatibility
Passes Through walls	Yes	No	IR more easily secured. Independent links in different rooms.
Multipath Fading	Yes	No	Simple link design
Multipath distortion	Yes	Yes	
Path Loss	High	High	
Dominant Noise	Other Users	Background Light	Limited range
Input X(t) represents	Amplitude	Power	Difficult to operate outdoors
SNR proportional to	$\int \lvert X(t)\rvert^2 dt$	$\int \lvert X(t)\rvert^2 dt$	High transmitter Power requirement
Average power proportional to	$\int \lvert X(t)\rvert^2 dt$	$\int \lvert X(t)\rvert dt$	Choose waveform X(t) with high peak-to-average ratio.

The transmitter and receiver are both calibrated to maintain the connection; the optical link can be classified as LOS or diffuse (non-LOS). In LOS links, the transmitter and receiver are aligned to give the maximum power efficiency. Line-of-sight (LOS) links offer higher transmission speed due to the lower path loss and narrow field of view (FOV) of the optical receiver in outdoors communication. Despite the advanced technology in optical wireless, LOS cannot support full mobility purposes. Nevertheless, diffuse systems are used when transmitter-receiver alignment is not possible; it depends on reflecting the signal from multi-surfaces until it reaches the receiver; this can achieve a reliable communication as long as the receiver lies in the illumination area, characterized by a wide FOV [1.7].

The optical link is divided into 3 categories: directed, hybrid and non-directed, according to the orientation between the transmitter and the receiver. Different configurations of optical wireless systems for indoor and outdoor communication can be arranged depending on the specific requirements of a system as shown in figure 1.2. The directed link is used when the transmitter and receivers are pointing towards each other for both LOS and diffuse systems. In LOS topologies, the transmitter and the receiver are in direct view of each other, without any obstacle between them. Non-LOS systems however, may have objects blocking the straight path. These configurations depend on the use of reflective surfaces to create an alternative path for the link. A hybrid link can provide some degree of directionality, for a receiver which employs a wide angle FOV to receive the optical signal. When the emitted beam from the transmitter and the field-of-view (FOV) of the receiver are narrow, the system is considered "directed." If only one of them is narrow, then the system is classified as "hybrid". On the other hand, when both the receiver and the transmitter have a wide FOV and a wide emission beam, the system is considered "non-directed". LOS configurations improve power efficiency and minimize multipath effects. The flexibility of some LOS-based systems is restricted due to the fact that the alignment between the transmitter and the receiver is required. Consequently, non-LOS topologies sometimes increase link robustness because they allow the system to operate even when obstacles are blocking the direct path between the transmitter and the receiver [1.6].

The disadvantage of the non-LOS topologies is that when reflective surfaces are being used to create alternative paths between transmitter and receiver, multipath effects takes place. Therefore, the maximum power efficiency is concentrated in an emission that takes the shape of a narrow cone, this is a directed-LOS topology

called “directed beam infrared” (DBIR) [1.8], and a good source for providing such a narrow beam is the laser [1.9]. In return, the receiver allows in this case a narrow FOV in order to minimize the probability of receiving unwanted wavelengths and increase the power budget in the same time. The receivers incorporate imaging or non-imaging high-gain concentrators that allow the use of smaller photo detectors with reduced capacitance, which increases the speed of the system. Besides, a directed-LOS system requires a lower transmission power maintaining more power flux density at the receiver. The disadvantages of the directed-LOS configuration include its susceptibility to blocking, and its restricted mobility due to the necessity of the alignment [1.4]. Tracked systems are a special case of the directed-LOS configuration, where the transmitter and the receiver are made to move by mechanical or electro-optical means to maintain a continuous reception while providing some level of mobility. This offers maximum power efficiency, high bit rates, and wide coverage. The transmitted power required for a tracked system, is several orders of magnitude smaller than the power required (table 1.2) by a diffuse system for a specific data rate and range. A directed-LOS configuration could be of a cellular topology, where cells of energy are created by semi-directive LOS transmitters, thus, providing mobility and maintaining reasonable power efficiency. Although cellular systems can provide high mobility, improved power budget, and minimum multipath distortion, they are still susceptible to blocking from passing objects. The problem can be resolved by overlapping the cells in a way that allows the connection to find alternative paths [1.4].

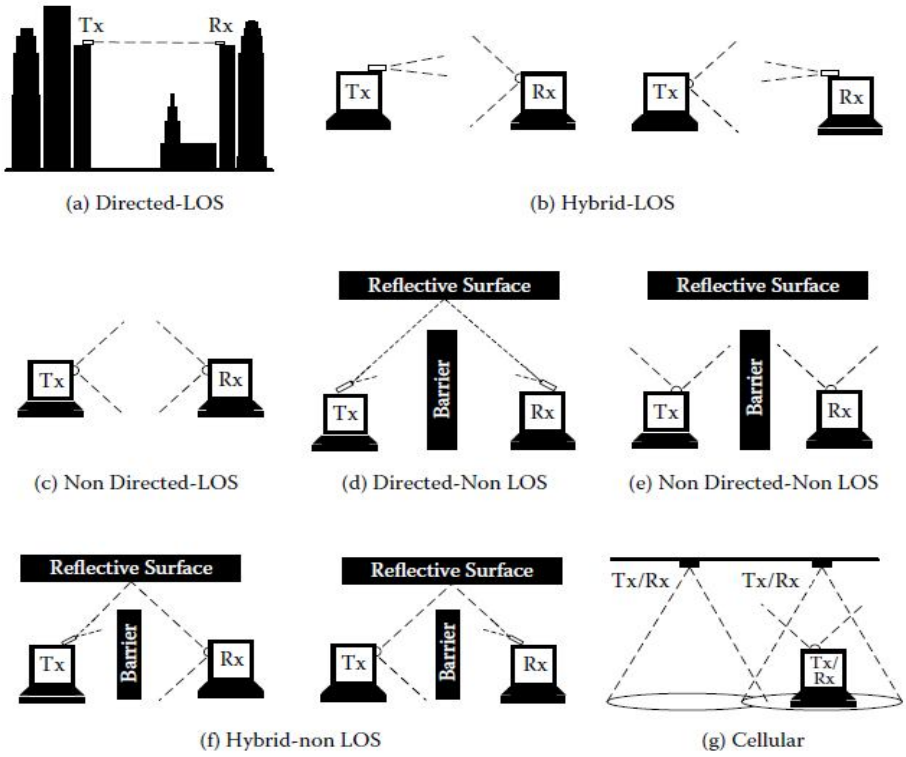

Figure 1.2 Different configurations of wireless IR links (adapted from [1.4]).

Table1.2 Values of transmitted Power for tracked, diffuse, and cellular topologies (adapted from [1.9]).

Data Bit Rate (Mbps)	Optical Power (Diffuse System)	Optical Power (Tracked System)	Optical Power (Cellular System)
0.1	$3 \times 10^{-2}\ W$	$6 \times 10^{-7}\ W$	$3 \times 10^{-3}\ W$
0.5	$6 \times 10^{-2}\ W$	$8 \times 10^{-7}\ W$	$5.8 \times 10^{-3}\ W$
1	$8 \times 10^{-2}\ W$	$1 \times 10^{-6}\ W$	$8 \times 10^{-3}\ W$
5	$1 \times 10^{-1}\ W$	$3 \times 10^{-6}\ W$	$1 \times 10^{-2}\ W$
10	$2.5 \times 10^{-1}\ W$	$6 \times 10^{-6}\ W$	$2 \times 10^{-2}\ W$
50	$6 \times 10^{-1}\ W$	$9 \times 10^{-6}\ W$	$2 \times 10^{-2}\ W$

1.2.1.1 Optical transmitter Hardware

The transmitter of an optical wireless system could be a laser diode (LD) or light emitting diode (LED). Laser, or "light amplification by stimulated emission of radiation", was invented in 1960 using a ruby crystal and nowadays, it is able to provide optical power ranging from few milliwatts to few thousands of watts,

operating in a wavelength range from 350nm to the near infrared (NIR ~ 1.6μm) [1.10]. Depending on the requirement, the LED and LD can be applied according to the applications achieved for optical wireless links. Laser diodes usually have higher optical power outputs, and more optical modulation bandwidth with a relatively linear responsivity (electrical-to-optical conversion) above the lasing threshold, which allow multilevel modulation techniques [1.11]. However, the LED is more eye safe and cheaper in production; a comparison is depicted in table 1.3.

Table 1.3 Comparison between LED and LD (adapted from [1.11-1.12]).

Characteristics	LED	LD
Optical Spectral Width	$25 - 100nm$	$< 10^{-5} - 5\,nm$
Modulation Bandwidth	Tens of KHz to Hundreds of MHz	Tens of KHz to Tens of GHz
Spectral Circuitry Required	None	Threshold and Temperature Compensation Circuitry
Eye Safety	Considered Eye Safe	Must be Rendered Eye Safe
Reliability	High	Moderate
E/O Conversion Effiecency	10-20%	30-70%
Cost	Low	Moderate to High

1.2.1.2 Optical Wireless Channel

Optical wireless communication uses intensity modulation direct detection (IM/DD) in most of its applications due to its simplicity and ease of implementation. It is a form of modulation in which the optical output power of a source is varied in accordance with some characteristic of the modulating signal. By varying the bias current of the transmitter device, it modulates the data onto the instantaneous power of the infrared carrier. Recovery of the modulating signal is by direct detection, where the photodetector generates current proportional to the optical received power.

When intensity modulation is used, the channel model depends on the level of the background noise. For low illumination, a Poisson process could be used with rate $\lambda s(t) + \lambda n$, where, $\lambda n$is proportional to the power of the background illumination and $\lambda s(t)$ is proportional to the instantaneous optical power of the received signal [1.13]. For high illumination, the shot noise at the receiver is dominating, and it can be modeled as an additive white Gaussian noise (AWGN) plus a DC offset. The channel could be installed in indoor or outdoor environments (Discussed in Chapter 2). Eye and skin safety requirements are major constraints that need to be considered for optical wireless applications. The choice and operation of optoelectronics is also significant, it requires a pre-estimation of the channel characteristics using mathematical models. The thesis will focus on outdoors LOS optical wireless communications, considering different weather models, and the internal and external effects that might improve or worsen the channel performance.

1.2.1.3 Optical Receiver Hardware

Optical receivers are based on solid state devices, which perform the inverse operation of light emitting devices, (LEDs) or laser diode (LDs) by converting the incident radiant light into an electrical current. The receivers in optical wireless system have tended to adopt PIN diodes or avalanche photodiodes (APD). PIN diodes have been employed in most applications due to their low bias voltage requirements and tolerance to temperature fluctuations [1.14]. APDs are usually 10 to 15 dB more sensitive than PINs, and therefore are more expensive, with higher bias voltage requirements and temperature-dependent gain [1.6]. Photodetectors are essentially reverse biased diodes on which the radiant optical energy is incident. The incident photons, if they have sufficient energy, generate free electron hole pairs. The

drift or diffusion of these carriers to the contacts of the device constitutes the detected photocurrent.

1.2.2 Integration of RF and Optical Wireless Networks

Wireless systems are of great concern in industry and undergoing rapid technological changes. Since the 1980's, the development of a variety of devices have revolutionized the wireless communication systems. For every development stage, the core of this industry centres around the development of a high capacity, reliable, and secure wireless field. Thanks to the previous achievements in the 2G (9.6–14.4 Kb/s) and backbone of the 3G (64 Kbps– 2 Mbps) networks, they have proved to be highly competitive and feasible in the time, and have prepared for a newly different way of data manipulation. Consequently, communication systems require a higher standard in order to support HDTV (4-20 Mb/s) and various broadband wireless services, such as high-speed Internet access (1- 100 Mb/s), several multimedia, video conferencing, and computer network applications [1.15-1.18]. In comparison with 3G networks, the increasing bandwidth demands in future wireless service, the increasingly large number of users, and the responsibility towards them, are shifting interests towards a new paradigm. In fact, the existing wireless systems are no longer able to fulfill the demands of higher bandwidth, and require new considerations on the direction of technology. Consequently, free space optics (FSO) has emerged for such a great need to provide high speed telecommunications at the highest achievable bandwidth, encapsulating data in a secure medium [1.19-1.21]. Meanwhile, RF technology suffers from congestion, and the desire to extend high-speed internet access has supported much of this growth; as a result, the primary focus of most FSO research and development has been toward the transmission of digital signalling formats. On the other hand, the performance of optical wireless networks is highly

dynamic because of changing atmospheric and platform conditions. RF/FSO approach is on the edge to provide improved network performance in worst cases of congestion and weather conditions. It is emerging as a technology for achieving survivable optical networking based on dynamic and autonomous topology reconfigurations. RF/FSO investigates the use of FSO technology to transport modulated radio frequency (RF) analog signals. The transmission of RF intensity-modulated signals over FSO links has the following advantages [1.22, 1.23].

1- FSO is immune to interference that comes from electromagnetic (EM) signals and other sources of radiation [1.24].
2- FSO/RF requires no licensing, and provides higher transmission bandwidth.
3- FSO transmission links can be deployed faster, and sometimes cheaper than optical fibre links.
4- Connecting nearby islands or deployment of CATV links in areas where installing fibre infrastructure is very expensive [1.25].
5- FSO provides a viable transport medium for transporting IS-95 CDMA signals to base stations from macro and microcell sites and can reduce the setup costs of temporary microcells deployed for special events, (football game, shows, speeches, etc) by eliminating the need for a directional microwave link or connecting cable [1.26].
6- Another benefit of using IR compared to RF is the health concerns. Side effects caused by exposure to electromagnetic (EM) radiation are still ongoing research topics. Since the human nervous system receives and interprets information via electrical signals, possible carcinogenic, reproductive and neurological effects may indeed develop due to exposure to intense EM radiations [1.27-1.28].

The major concern for optical links is their failure because of atmospheric obscuration, so there are hybrid optical/RF links in which high performance RF provides a "backup" connection in optically obscured conditions, such as in figure 1.3. The RF can also assist in pointing, acquisition, and tracking of the optical beams during network setup, using either RF direction finding, or the RF broadcast of the GPS locations of transceivers [1.28].

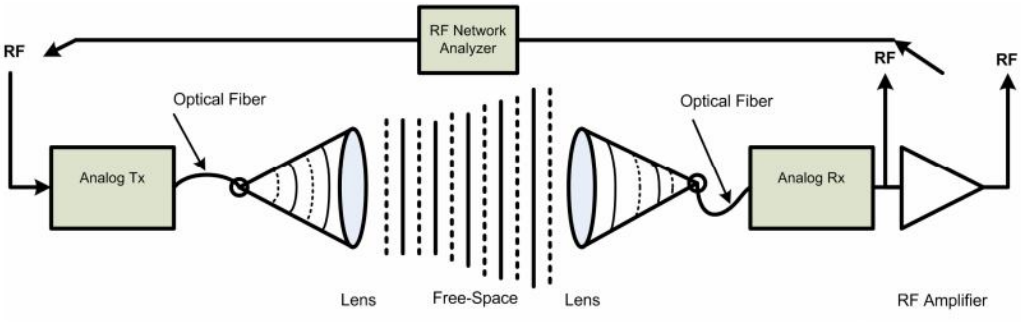

Figure 1.3 RF Setup Utilizing FSO technology, edited from [1.29].

1.3 Research Motivation

Short range optical wireless links are commonly implemented in contemporary networks and will have promising impact on the future of wireless communications. Their significance is revealed in bringing broadband to home as well as a high bandwidth bridge between LANs, MANs and WANs, commercially used at a distance of 1 km range in companies like Cable Free in the UK, and Light Point in the USA. Rapid technical progress and innovations in technologies are increasing interest in networking and communications. Furthermore, the wireless communication industry is moving towards increased performance, better quality of service (*QoS*), higher reliability, reduced costs, and greater security. In outdoor optical wireless technology, major atmospheric attenuations are caused due to absorption, scattering and shimmer of the optical signals (See Figure 1.4).

Absorption takes place due to the presence of carbon dioxide and water droplets. Scattering occurs in the presence of fog, haze, rain and snow. It allows a portion of light traveling from a source to deflect away from the intended receiver in a divergence related to the wavelength and the size of the fog particle. Shimmer is caused by a combination of light refraction, atmospheric turbulence, air density cloud cover, and wind. These challenges impose an increasing interest to adapt the overall effects that might mimic the throughput and BER of the optical wireless link, as well as the signal-to-noise ratio (SNR) and the received power (P_{RX}), which are of direct proportional relation. In addition to the previous achievements in industry and research, the practical deployments of optical wireless can achieve per-link availability figures from 99.7 to 99.99% depending on range and geographical region. Large investments are being deployed to raise overall availability up to the 99.999%. Unrealistic expectations have harmed the credibility of the industry and only reliable communication will be adopted in the mainstream telecommunication industry. This fact is tackled in the research and several intelligent techniques are exploited in order to optimize the channel performance and recruit for efficiency, survivability, and upgradeability of data in the short range outdoors LOS optical wireless communication.

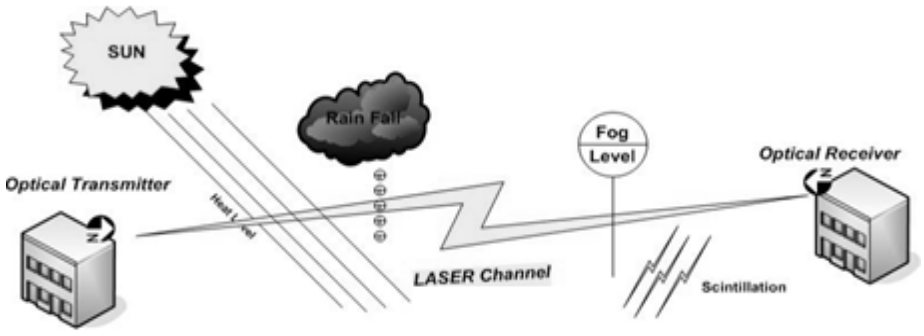

Figure 1.4 Challenges in the outdoors optical wireless channel.

1.4 Thesis Structure

The thesis mainly consists of three parts: Introduction to optical wireless communication and its fundamentals, the use of several intelligent systems to tackle the problem in the outdoors LOS optical wireless channels, and the last part manipulates results, evaluates the achievements, and sheds light on future research areas.

The first chapter is the introduction, mainly providing the background about optical wireless communications. It states the motivation around the project, and suggests the main problem to be solved throughout the thesis.

The second chapter concentrates on indoor and outdoor infrared communications, the design technology, service disruption on the physical layer, and optical security. The problem is stated, and the research is narrowed with a set of contributions discussed.

Chapter three consists of a literature review and discusses the recent contributions related to the optical wireless communication. It stresses the achievements of intelligent systems for power and SNR optimizations using genetic algorithms, artificial neural network, fuzzy logic, and hybrid algorithms.

The fourth chapter discusses the methodology that will be used for the subsequent chapters. This chapter includes the first attempt of using a genetic algorithm for a transmission wavelength selection in NIR systems. The selection targets several weather conditions based on the international code of visibility.

Chapter five shows the model of the optical wireless channel considering atmospheric attenuations (deterministic) and turbulence (scintillation) conditions. It discusses the parameters and selection functions that a genetic algorithm makes use of, and then simulates an original coded program that utilizes the concept of

evolutionary algorithms. It shows the fitness function, and various simulation results covering overall link characteristics. An application-specific genetic algorithm is presented, but, prior to this process, the generated code is compared against the complexity of the MATLAB GA tool box to assure its reliability in solving the designated problem.

Chapter six shows a multivariate data analysis of the application-specific generated data sets studied using principal component analysis (PCA) to find correlations among parameters and map them to the real channel.

The seventh chapter discusses a fuzzy-neuro approach. An Artificial Neural Network (ANN) is firstly used for *BER* prediction to validate the results obtained by the previous methods and could also be applied to estimate the BER of optical wireless channel model deploying different cross-sections of transceivers; and then a hybrid model using adaptive neuro-fuzzy inference system (ANFIS) is modelled and used for channel adaptation by monitoring the link range and total attenuations in the channel.

Chapter eight concludes the research, and sheds light on possible future work. Important results and methodology obtained from previous chapters are summarized and the possibilities for future directions are discussed.

References

[1.1] J. Hecht, “City of Light: The Story of Fiber Optics”, *Oxford University PressInc.*, 1999.

[1.2] F. R. Gfeller, U. Bapst, "Wireless in-house data communication via diffuse Infrared radiation," *Proceedings of the IEEE,* vol. 67, pp. 1474-1486, November, 1979.

[1.3] A. Jabeena, M. J. P. Priyadarsini, PRV Bharat, V. Radhakrishna, and A.Salma, “Effect of Atmospheric Turbulence on Wireless Optical Link”, *in International Journal of Engineering and Technology (IJET), 2013.*

[1.4] J. R. Barry, “Wireless Infrared communications”, Boston: *Kluwer Academic Publishers*, 1994.

[1.5] M. Bass, W. Eric, V. Stryland, D. R. Williams, and W. L .Wolfe, “Handbook of Optics: Fundamentals, Techniques, and Design”, vol.1, 2nd Edition, *McGraw-Hill*, New York, 1995.

[1.6] J. M. Kahn, J. R. Barry, "Wireless Infrared communications," *Proceedings of the IEEE,* vol. 85, pp. 265-298, Feb, 1997.

[1.7] R. J. Green, H. Joshi, M. D. Higgins, and M. S. Leeson, "Recent developments in indoor optical wireless systems," *, IETCommunications,* vol. 2, pp. 3-10, 2008.

[1.8] C. Singh, J. John, Y.N. Singh, and K.K. Tripathi, “Indoor Optical Wireless Systems: Design Challenges”, Mitigating Techniques and Future Prospects, *IETE TechnicalReview*, 21(2), 101–117, 2004.

[1.9] P.P. Smyth, P.L. Eardley, K.T. Dalton, D.R. Wisely, P. McKee, and D. Wood, “Optical Wireless — A Prognosis”, *presented at SPIE*, 1995, pp. 212–225.

[1.10] S. Hranilovic, “Wireless optical communication systems”, *Springer*, New York, 2005.

[1.11] J. J. Chaturi Singh, K.K.Tripathi, "A Review of Indoor Optical Wireless Systems," *IETE Technical Review,* vol. 19, pp. 3-17, January-April 2002.

[1.12] V. Jungnickel, T. Haustein, A. Forck, and C. V. Helmolt, "155 Mbit/s wireless transmission with imaging Infrared receiver," *Electronics Letters,* vol. 37, pp. 314-315, 1 March 2001.

[1.13] H. Park, J. R. Barry, “Performance of Multiple Pulse Position Modulation on Multipath Channels”, *IEE Proceedings in Optoelectronics*, 143(6), 360–364, 1996.

[1.14] R. R. Iniguez, R. J. Green, "Indoor optical wireless communications," *IEEE Colloquium on Optical Wireless Communications(Ref. No. 1999/128),*pp. 14/1-14/7, 1999.

[1.15] T. S. Rappaport, "Wireless personal communications: trends and challenges," *IEEE Antennas and Propagation Magazine,* vol. 33, pp. 19-29, 1991.

[1.16] M. Macedonia, "Why digital entertainment drives the need for speed" *Computer,* vol. 33, pp. 124-127, 2000.

[1.17] T. H. Meng, B. M. Gordon, E. K. Tsern, A. C. Hung, "Portable videoon-demand in wireless communication," *Proceedings of the IEEE,* vol. 83,pp. 659-680, April 1995.

[1.18] R. Dawson, "LED bandwidth improvement by bipolar pulsing," *IEEE Journal of Quantum Electronics,* vol. 16, pp. 697-699, Jul 1980.

[1.19] W. A. Gambling, "The rise and rise of optical fibers," *IEEE Journal of,Selected Topics in Quantum Electronics, ,* vol. 6, pp. 1084-1093, 2000.

[1.20] J. Beckett, "The Internet phenomenon," *Engineering Science and Education Journal* vol. 5, pp. 102-104, June 1996.

[1.21] W. A. Gambling, "Possibilities of optical communications," *Engineering,* vol. 198, p. 776, 1964.

[1.22] W. S. C. Chang, "RF photonic technology in optical fiber links", *chap.1*, *Cambridge University Press,*Cambridge, 2002.

[1.23] D. Ngo, H. Nguyen, M. Atiquzzaman, J. J. SlussJr, and Hazem. H. Refai, "The Application of Fiber Optic Wavelength Division Multiplexing in RF Avionics", *23rd Digital Avionics Systems Conference*, Oct 24-28, 2004, Salt Lake City, UT, 14 p. NASA/TM-2004-213377, 2004.

[1.24] Hakki H. Refai, J. J. SlussJr, and Hazem H. Refai, "Optical interference on free-space optical transceivers," *Frontiers in Optics* – 87th Optical Society of America Annual Meeting, Tucson, AZ., 2003.

[1.25] Hakki H. Refai, J.J.SlussJr, and Hazem H. Refai, "The use of free-space optical links for CATV applications," *accepted to SPIE Opto Ireland*, Dublin, Ireland, April 4-5, 2005.

[1.26] Hakki H. Refai, J. J. SlussJr, and Hazem H. Refai, "Interconnection of IS-95 CDMA microcells using free-space optical links," *in proc. of the 1st IEEE and IFIP International Conference on Wireless and Optical Communications Networks (WOCN 2004)*, Muscat, Oman, June 7-10, pp. 78-81, 2004.

[1.27] WHO – World Health Organization, "2006 WHO Research Agenda for Radio Frequency Fields", Geneva. Available: <http://www.who.int/peh-emf/research/rf_research_agenda_2006.pdf>, Accessed: [05 May 2013].

[1.28] NatašaĐinđić, JovicaJovanović, VladicaVeličko, vićIvanaDamnjanović, Boris Đinđić, and andJelenaRadović, "Radiofrequency and Microwave Radiation and Occupational Exposure", *ActaMedicaMedianae*, Serbia, 2011.

[1.29] Hakki H. Refai, J. J. SlussJr, Hazem H. Refai, and M. Atiquzzaman "Transporting RF Signals over Free-Space Optical Links" School of Electrical and Computer Engineering, Free-Space Laser Communication Technologies XVII, edited by G. Stephen Mecherle, *Proceedings of SPIE* Vol. 5712, (SPIE, Bellingham, WA, 2005), Oklahoma, USA, 2005.

CHAPTER II: Fundamentals of Optical Wireless Communication

2.1 Introduction

This chapter discusses the fundamentals of optical wireless communication, its transmitter and receiver hardware, and the channel of propagation for indoor and outdoor communications. The chapter talks about the design considerations and concentrates on atmospheric channel limitations; it then mentions the problem statement and sheds light on contributions and possible solutions.

2.2 Basics of Optical Wireless Communication

An optical wireless system involvesmulti-disciplines involving several areas such as the optical design, electronics design, channel modeling, communication theory, optoelectronics, modulation/demodulation techniques, and network architecture. The design of communication algorithms for any channel first requires knowledge of the channel internal and external characteristics, the basic operation of optoelectronic devices, and the amplitude constraints that they introduce. Moreover, power constraints, eye and skin safety are significant topics carefully treated where different classes of laser are considered for transmission. These constraints are fundamental to wireless optical intensity channels and do not allow the direct application of conventional RF signaling techniques. The propagation characteristics of optical radiation in indoor environments, in comparison to RF channels, are a hot area in technology considerations. The choice and operation of typical optoelectronics used in wireless optical links, and the various noise sources are analyzed before the channel is established. Different mathematical models are considered depending on channel propagation characteristics with a consideration to a variety of channel

topologies. The modern era of wireless optical communications was initiated in 1979 by F.R. Gfeller and U. Bapst by suggesting the use of diffuse emissions in the infrared band for indoor communications [2.1]. Since that time, much work has been done in characterizing optical wireless channels, designing receiver and transmitter optics and electronics, developing novel channel topologies as well as in the area of communications system design.

2.2.1 Indoors Wireless Communication

Indoor optical wireless communication has penetrated homes and offices after Gfeller and Bapst [2.1], and engaged a range of institutions, such as IrDA,serving TVs, mobile phones, PDAs, laptops and cameras. 200 Million units of IrDA ports are installed every year with 40% yearly growing rate with low-cost IR data interconnection [2.2]. The IrDA (875 nm +-30 nm) based standard uses diffuse optical communication link with a wide field of view (FOV) emitted radiation to overcome the limiting factors of shadowing and misalignment, which can hinder communications. As the diffuse system architecture supports one to many, many to one communications, it can also be used in the establishment of ad-hoc- and local area networks [2.3], where light scatters off walls and ceilings creating multiple paths from the sources to the receiver.Indoor optical wireless systems are characterized by smaller distances free from environmental degradation, and the loss in the indoor link takes place only due to free space loss. Different configurations of wireless IR links are shown in figure 1.2. The main source of noise in indoor optical wireless systems is the ambient light, which is a combination of incandescent light, fluorescent light and sunlight. The Signal to noise ratio at the receiver side is basically threatened by the ambient light, and is monitored for an acceptable channel performance. Kahn and Barry [2.4] found that the intensity of direct sunlight is

greater than the incandescent and fluorescent lights since it produces an interfering sinusoid signal of 100 Hz with a few harmonics. Other challenges in designing indoor optical wireless systems is the pulse shape of the received signal, power amplitude, eye safety, shadowing effect, and background interference.

2.2.2 Outdoors Wireless Communication

Outdoor optical wireless communications, referred to as free space optics (FSO), were developed more than 30 years by the military and NASA. It includes the long range and short range optical wireless channels. The Long range free space is mainly used for inter-satellite networking, and to convey the data rates up to Gbits/sec. Nevertheless, the short-range links are used to maintain a high bandwidth bridge between the local and wide area networks (WANs). Most of the short-range links are now commercially available for a distance of about 1 Km [2.5-2.7]. To maintain an acceptable channel performance, the outdoor optical wireless systems must transmit sufficient power to achieve good availability in the presence of adverse weather conditions without exceeding the eye-safe limit. As the transmitting conditions of optical wireless channel in the adverse weather conditions are randomly time varying, transmission requires a strategy where data to be transmitted can be found in different frequency bands, in order to allow for an efficient reception. The atmospheric effects on the outdoors optical wireless channel are studied in section 2.3, and different weather models are used to relate different parameters. One set of practical solutions in the literature has proposed the use of a hybrid (FSO/RF) system where an RF link acts as a backup to the free space optical wireless system [2.8-2.11].

2.3 Design Technology

The optical wireless system comprises of main parts depicted in figure 2.1. The transmitter consists of an interface circuit and a source drive circuit; it converts the input electric signal to an optical signal, or, in other words, modulates it for transmission in the electromagnetic field. The drive circuit of the transmitter transforms the electrical signal to an optical signal by varying the current flow through the light source. This latter can be a light emitting diode (LED) or a laser diode (LD) (discussed in 1.2.1.1). The modulated optical field then propagates through a free-space path before it reaches the receiver, where a photodetector converts the optical signal back into an electrical form with convenient demodulation techniques [2.12].

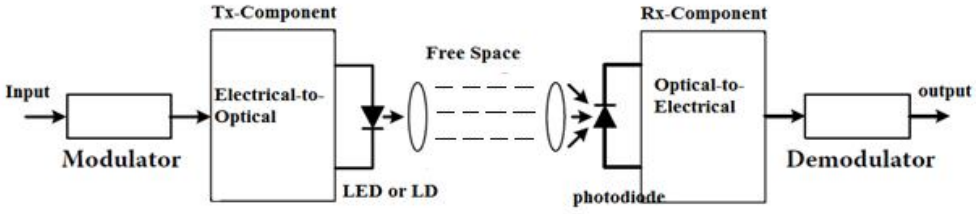

Figure 2.1 Main components of an optical wireless channel.

The receiver consists of an optical detector and a signal-conditioning circuit. The optical detector receives the optical signal, and the signal-conditioning circuit regulates the detector output to match the original input at the transmitter. However, a limitation of the signal-conditioning circuit is that it introduces signal distortion upon amplification. Thus, the lesser the noise or signal distortion induced at amplification, the better is the receiver. In practical optical wireless links, both the transmitter and the receiver blocks are developed in a single circuit called an optical

transceiver followed by a transponder for data recovery, depicted in figure 2.2, where it provides full-duplex communication [2.12].

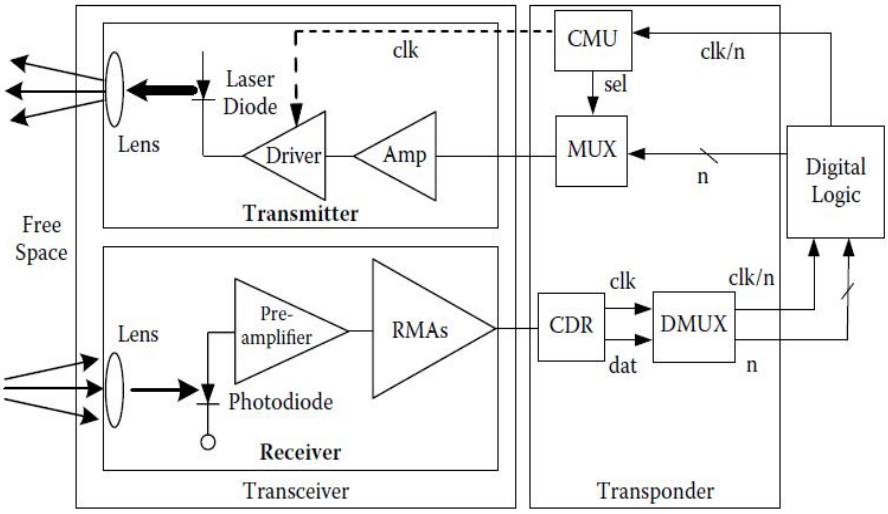

Figure 2.2 Schematic diagram of a typical optical transceiver followed by a transponder for data recovery,(adapted from [2.12]).

The development of optical fiber transmitter systems has initiated semiconductor lasers with high launch powers and broad bandwidth, with features that make them equally attractive to optical wireless applications. Nevertheless, an optical wireless transmitter suffers from eye safety restrictions and is precisely constrained to the optical power level emitted at the transmitter aperture. When it exceeds specific levels, it becomes potentially dangerous to the human eye. This situation must be taken into account, particularly for indoor free-space optic applications, where bystanders can obstruct the path and become subjected to the radiation. The appropriate light source, can be a light emitting diode (LED) or a laser diode (LD), and the photodetector at the receiver side could be avalanche photodiodes (APDs), photoconductors, metal-semiconductor metal photodiodes (MSM PDs), and PIN photodiodes (PIN PDs) chosen depending on the specific application of the system. A comparison of PIN and Avalanche photodiodes is shown in table 2.1[2.12].

Table 2.1 PIN photodiodes vs. Avalanche Photodiodes for Optical Wireless Systems (Based on [2.13-2.14]).

Characteristics	PIN Photodiode	Avalanche Photodiode
Modulation Bandwidth	Tens of Mhz to Tens of GHz	Hundreds of MHz to Tens of GHz
Photocurrent Gain	1	$10^2 - 10^4$
Special Circuitry Required	None	High Bias Voltages and Temperature Compensation Circuitry
Linearity	High	Low – suited to digital applications
Cost	Low	Moderate to High

2.3.1 Limitations on Photodetector Bandwidth

Optical receiver design is a critical procedure in optical wireless systems. It consists of a cascade of building blocks: photodetector, preamplifier, filter, main amplifier, and decision circuit. The question of how large the receiver bandwidth (BW) and what frequency response should be chosen are always treated as the basic considerations. However, this implies a control of two main effects that change in a reverse manner. For instance, if the receiver BW is wide, the receiver preserves the signal waveforms without distortion, but at the same time picks up a lot of noise, which may corrupt the signal [2.15]. If the receiver BW is made narrow, the noise decreases and the sensitivity improves. Nevertheless, signal distortions or intersymbol interference (ISI) increases. Consequently, ISI reduces sensitivity because the output swing is reduced for certain bit sequences. Thus, there is an optimum receiver BW for which the sensitivity is optimal. A rule of thumb for non-return to zero (NRZ) receivers indicates that the optimum 3 dB BW is about two thirds of the bit rate, or sometimes about 60 to 70 percent of the bit rate. The BW of the photodetector is determined by the speed with which it responds to variations of the incident optical power, known as rise time *Tr*. The combinations of the block

cascade should satisfy that BW = 2/3 Br, and several ways to achieve this consideration arediscussed in [2.16]. Based on this information, the genetic algorithm-bandwidth selection considered in chapter 5, estimates shot noise, Johnson noise, and suitable responsivity of the receiver, assuming that the bandwidth does not fall belowhalf the bit rate used for transmission.

2.3.2 Design Considerations

Optical wireless links operate in high noise environments due to ambient illumination, and consequently, an optical filter is required, to reduce the shot noise introduced at the receiver due to ambient light. Moreover, the link budget considerations require that the receiver must have a large collection area. This can be achieved through the use of optical concentrators that offer effective noiseless gain. Therefore, the design of the transmitter and receiver in the optical wireless communication should take into considerations [2.12]:

- The topology of the network to be established according to the medium.
- The power amplitude and eye safety regulations.
- For the transmitter, it is important that the light source launches its energy at angles that optimize the transmitted beam, and that the frequency response of the light source exceeds the frequency of the input signal.
- The light source should have a long lifetime, present a sufficiently high intensity, and be reasonably monochromatic.
- Small size light source, low drive voltage, and able to emit a signal at a desired wavelength or range of wavelengths, high gain bandwidth.
- The active area of the receiver photodiode, its capacitance, and its load resistance.

- The speed of processing of the transceivers, and a short response time, the gain, immunity to noise, the efficiency.
- Responsivity of the photodiode, the photo detector should be able to produce an electrical signal as high as possible for a given amount of optical power.
- High fidelity to reproduce the received signal waveform with accuracy, for analog transmission, the response of the photo detector must be linear, with regard to the optical signal, over a wide range.
- Dark currents, leakage currents, and shunt conductance must be low leading to minimal noise.

2.4 Atmospheric Transmission Limitation

In outdoor optical wireless systems, IR offers the availability of huge unregulated bandwidth, immunity to electromagnetic interference (EMI), the ease of deployment, and high security. Unfortunately, outdoor optical wireless, when compared to indoor counterparts, present additional challenges that need to be considered. Free space optics (FSO) service providers need to take into account the quality of service that can be offered under adverse atmospheric conditions, due to the effects of fog, rain, and snow on the performance of wireless IR links to different extents [2.12]. FSO service providers tend to find ways to compensate for the unwanted effects introduced by different atmospheric phenomena and by intense solar illumination. An example of one of the solutions proposed is the use of backup links like FSO/RF introduced in 1.2.2. A good understanding of the effects of fog, haze, mist, and snow, on the performance of a wireless IR link is of great importance when designing the transmitter and the receiver of an optical wireless system. Moreover, humidity, visibility, and temperature, together with the features of an FSO system and its deployment characteristics are carefully studied to model atmospheric propagation.

In this section, a variety of atmospheric phenomena and their impact on the propagation of IR radiation are presented, such as the origin and the effects of turbulence caused by scintillation, the definition of aerosol, absorption, and radiance as well as its main effect on the loss and redirection of the EM energy.

2.4.1 The Atmosphere (Aerosol, Absorption)

The atmosphere is mainly composed of 78 % Nitrogen (N_2), 21% Oxygen (O_2), and 1% Argon (Ar). However, H_2O and CO_2exist in the atmosphere with smaller amounts generated from combustion, soil, dust, and debris. The percentage of water ranges from 0 to 7 percent, and the higher the percentage, the higher the density of air.Consequently, aerosol is a suspension of solid or liquid particles in a gaseous medium. Its size has been approximated between 0.01 and 10μm by [2.17] and between 0.1 and 1μm by [2.18] and it may be considered as the main constituent of haze particles, clouds, and fog.Absorption, in the context of electromagnetic waves, is defined as the process of conversion of the energy of a photon to internal energy, When EM radiation is captured by matter, the particles in the atmosphere absorb light, and this absorption provokes excitation of particle's molecules from a lower energy level to a higher one. Light is absorbed when molecules undergo discrete energy transitions from one energy level to another and then the molecules go back to their original unexcited states. The atmospheric absorption is wavelength dependent relative to the size of the matter (gases) absorbing light from the medium, creating atmospheric windows that are taken into account when optical wireless communication is established.

2.4.2 Attenuation due to Scattering, Effect of Fog, Rain, and Mist

Water vapor is generated on the surface of the earth and the concentration of condensed water is higher at the lower part of the atmosphere, where it is present in the form of clouds or fog. Water is present in the atmosphere in the form of raindrops and snow. The droplets are formed either because of the collision of small droplets or the heterogeneous nucleation of aerosol particles that attract water vapor molecules. Several models have been developed to describe the phenomenon related to the growth of droplets like the stochastic collection model that describes the probability related to drop collision and their combination [2.17]. In general terms, fog can be considered a stratus cloud at ground level that does not produce precipitation, but that can originate drizzle.Attenuation due to water vapour in the visible and near-IR regions depends on visibility, relative humidity, and temperature, and it is directly proportional to the percentage of water droplets in the atmosphere as illustrated in figure 2.3.

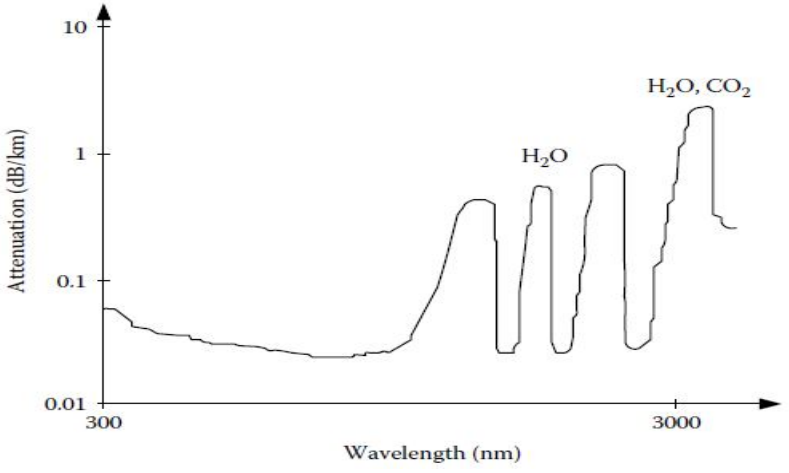

Figure 2.3 Attenuation due to atmospheric gases for visible and near-IR wavelengths (adapted from [2.17]).

An important keyword in this context is scattering; the dispersal of radiation into multiple directions as a result of physical interactions. When a particle intercepts an

EM wave, part of the wave's energy is removed by the particle and re-radiated into a solid angle centred at it with the same wavelength as the incident wave, and no energy loss happens to the particle. The level of scattering depends on the characteristics of the particle: its size in relation to the wavelength of the intercepted energy, its index of refraction, and its isotropy. Therefore, scattering is of three types: Rayleigh, Mie, and non-selective. Rayleigh scattering is mainly observed in gases, and it refers to the scattering of light by particles whose size is small compared to the wavelength of the electromagnetic radiation incident upon them. The scattering by particles with diameters larger than one tenth of the incident light wavelength up to a diameter equal to the wavelength of the incident light is known as Mie scattering [2.19]. Finally, non-selective scattering occurs to particles whose size is larger than the incident wavelength. In optical wireless communications, Rayleigh and Mie are the most relevant types of scattering, as they refer to the scattering of light from molecules of air, and other atmospheric particles such as fog, mist, and haze [2.20]. The most important factor used to study the attenuation due to fog, rain, and mist is the visibility of the eye at the most sensitive wavelength (550nm), which can be obtained from its extinction coefficient β, given by Equation (2.1) [2.18].

$$V = \frac{ln|0.02|}{\beta(\lambda = 550)} = \frac{3.91}{\beta(\lambda = 550)}(km) \qquad (2.1)$$

Therefore, the scattering coefficient can be calculated from Equation (2.2),

$$\beta_{scatt}(\lambda) = \frac{3.91}{V}\left(\frac{\lambda}{0.55}\right)^{-\delta} \qquad (2.2)$$

Where δ is a parameter depending on visibility level (δ = 1.6, 1.3, and $\delta = 0.585\sqrt[3]{V}$ for V>50km, 6km<V<50km, and V<6km respectively). Another approach

to calculate the attenuation due to scattering has been presented by Gebhart et al. [2.21] in Equation (2.3).

$$\beta_{scatt} = \frac{17}{V}\left(\frac{555}{\lambda}\right)^{0.195\,S} \tag{2.3}$$

Where λ is the wavelength in nm, and Vis the visibility in km, β_{scatt} is therefore in dB/km. The attenuation due to rain can be calculated as a function of rainfall rate. Its value has been approximated by 6 dB/km during heavy rain (10 mm/hr) [2.20, 2.21]. Others indicate that the attenuation due to rain can reach values of up to17 dB/km, while the attenuation due to snow can be as high as 60 dB/km [2.19, 2.22].Unfortunately, the relationship between attenuation and visibility in Equations (2.1, 2.2, and 2.3) do not take into account the size of the droplets. In our model, we refer to a combination of Beer-Lambert and Koschmieder methods (referenced in Chapter 4, Section 4.3) to present different size droplets and randomly generate datasets corresponding to their relative attenuation.

2.4.3 The Effect of scintillation and Channel Turbulence

Scintillation is defined as a random fluctuation on the received field strength caused by irregular changes in the transmission path over time. The optical signal is varied as it travels through air, due to small fluctuations in the index of refraction along the optical path. These fluctuations, called optical turbulence, originate from atmospheric turbulence that creates thermal inhomogeneities along the path of the transmitted optical signal. The index of refraction value in the atmosphere depends on temperature, pressure, and humidity of air and on the wavelength used for the transmission. Scintillation is a major factor that causes significant performance deterioration of an optical wireless link after fog, low clouds, and direct sunlight, mostly observed during day and night times with a low impact during sunrise and

sunset [2.23]. This problem increases when the distance between transmitter and receiver is over 4km and when the receiver has a small aperture. Attenuation due to scintillation can reach up to 20 dB; however, optical turbulence is not deterministic, but rather a probabilistic process. The intensity fluctuation of a laser beam due to atmospheric turbulence can be expressed as a probability density function (PDF) such as the lognormal PDF and the gamma-gamma PDF [2.24]. Ryotov variance is one of the most useful methods followed to calculate the strength of optical turbulence, and it is calculated in [2.25] by defining the PDF of the intensity fluctuation, the Ryotov variance is given by Equation (2.4).

$$\sigma^2 = 1.23\, C_n^2 \sqrt[6]{k^7 L^{11}} \tag{2.4}$$

$C_n^2$is the refractive index structure parameter, L is the distance of propagation, and k is the wave number. Experimental results in [2.21] report that scintillation leads to 30 dB amplitude variation for a 61 km-long wireless IR link. With a larger beam divergence, and 2.7km distance, it showed a variation up to 10dB. Their results show amplitude variations (at the receiver) originated by air turbulence during clear sky conditions of up to 30dB. It was also observed that the problem becomes more significant as the distance between the transmitter and the receiver increases and a higher fade time is indicated.

2.5 Channel Model

The optical wireless channel is affected by different optical background noise levels which depend on the deployment circumstances [2.25, 2.26]. If the background interference is low, the channel can be modeled by a Poisson process. When the background noise is relatively high and comparable with the optical signals, the channel can be modeled by an additive white Gaussian noise (AWGN) model [2.4].

2.5.1 Intensity Modulation and Direct Detection (IM/DD)

An optical wireless channel mostly refer to intensity modulation and direct detection (IM/DD) in channel modeling. The typical optical wireless system structure can be found in Figure 2.4.

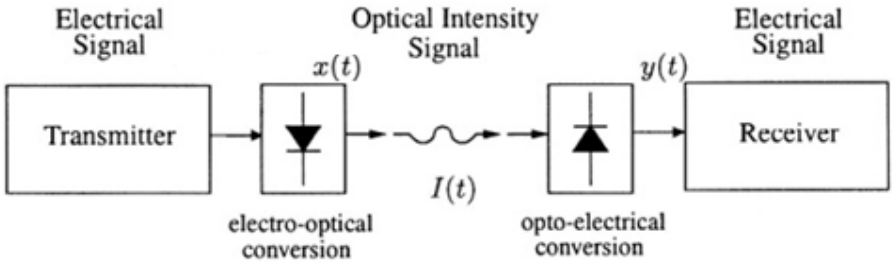

Figure 2.4 Main Components of Optical wireless system (figure adapted from [2.27]).

Intensity modulation with direct detection (IM/DD) is a major method of communication in optical wireless systems [2.28] In this mode of operation, the power of the optical source *x*(*t*) is directly modulated by changing the drive current, and a photocurrent *y*(*t*) proportional to the incident optical power is generated at the receiver. An optical wireless system using IM/DD has an equivalent model to figure 2.5, which hides the high frequency nature of the optical carrier [2.4]; h (*t*) and R represent the linear baseband channel impulse response and the photodetectorresponsivity respectively. The equivalent baseband model of an optical wireless link could be described as:

$$y(t) = R\,x(t) * h(t) + n(t) \tag{2.5}$$

Where *y(t)* is the received photocurrent and *(x(t)>0)* is the transmitted power, *n(t)* represents the shot noise with single-sided power spectral density $N_o = 2qI_B$. I_B is the DC photocurrent generated by the average combined power of the background radiation, q is the electron charge, and * denotes convolution.

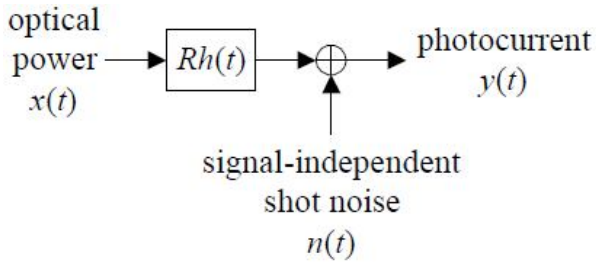

Figure 2.5 IM/DD Equivalent baseband model of an optical wireless system (adapted from [2.4]).

$I_B$is dominant over the photocurrent generated by the signal; therefore, the shot noise is independent of the received signal [2.29]. The optical wireless channel is fixed for a given position of the transmitter, receiver and intervening reflectors. It changes significantly when any of these are moved by distances in the order of centimetres. In the channel model in chapter 5, a Gaussian model will be used to study the deterministic attenuations (fog, rain, snow, mist, etc), and then the probability distribution function will be used to estimate the effect of turbulence (scintillation) on channel performance, where it will be subject to a genetic algorithm decision for selecting the best fit channel parameters.

2.5.2 Classes of Laser and Eye safety

The optical wireless channel exhibits a potential danger of eye hazard when the optical energy of the transmission signal exceeds certain levels. High energy optical sources injure the eye, so many organizations around the world adopted eye safety regulations, such as the International Electrotechnical Commission (IEC) in Switzerland and the American National Standards Institute (ANSI) in America. The optical signal is non-negative and the average transmitted optical power $x(t)$ should not exceed a predetermined value, P_{av}, and must be constrained due to eye and skin safety, where $x(t)$ must satisfy Equation (2.6) [2.12].

$$\lim_{T\to\infty} \frac{1}{2T} \int_{-T}^{T} x(t)dt \leq P_{av};\ x(t) \geq 0 \qquad (2.6)$$

Such constraints distinguish wireless infrared from the conventional linear Gaussian noise channel, where the obtained channel combines the filtered Gaussian noise characteristics of conventional wire based channels with the IM/DD constraints of fibre-optic systems [2.28]. Information about potential damage caused by different wavelength lasers can be found in Table 2.2.

Table 2.2 Types of radiation and their likely effects on the human eye (Based on [2.30]).

Name	Wavelength	Eye Damage	Example of Laser Type
Ultra-Violet 'C'	100 – 280 nm	Cornea	Argon Fluoride 193nm
Ultra-Violet 'B'	280 – 315 nm	Cornea	
Ultra-Violet 'A'	315 – 400 nm	Cornea &Lens	Nitrogen 337 nm
Visible	400 – 760 nm	Cornea &Retina	Ruby 694nm (Red)/Helium/Neon 633 nm (Red), Neodymium YAG Freq Doubled 532nm (Green) Argon 485-515 nm (Blue-Green)
Infra-Red 'A'	760nm – 1.4 µm	Cornea &Retina	Gallium Arsenide, 850 nm, Neodymium YAG 1.064 µm
Infra-Red 'B'	1.4nm – 3.0 µm	Cornea	Erbium, 1.621 µm
Infra-Red 'C'	3.0 µm – 1.0 mm	Cornea	Carbon Dioxide (CO_2), 10.6 µm

Lasers are placed into four classes as depicted in Table 2.3. Class1 is the lowest class of laser danger; it doesn't cause eye damage even when directly captured by the human eye for a long period of time. Class2 lasers emit visible radiation with low power that are eye-safe within 0.25 seconds. Class3A lasers can cause hazards in less than 0.25 seconds. These can cause permanent damage to the naked eye. Class3B lasers have very high power and can create dangerous levels of radiation even after reflection from dull surfaces [2.16].

Table 2.3 Laser safety classifications for a point-source emitter (adapted from [2.16]).

	650nm (Visible)	880nm (infrared)	1310nm (infrared	1550nm (infrared)
Class 1	Up to 0.2 mW	Up to 0.5mW	Up to 8.8 mW	Up to 10 mW
Class 2	0.2 – 1 mW	N/A	N/A	N/A
Class 3A	1 – 5mW	0.5 – 2.5 mW	8.8 – 4.5 mW	10 – 50 mW
Class 3B	5 – 500 mW	2.5– 500 mW	45 – 500 mW	50 – 500 mW

2.6 Statement of the Problem

Optical Wireless Channels suffer from adverse weather conditions. The expectations of a received signal are being threatened by the achievable link margin. Industrial companies, such as CableFree (UK) and Lightpointe (USA), nowadays do not publish enough data sets to study the effect of link parameters on one another, and thus on the signal-to-noise performance. However, they specify an output power from the transmitter laser, and a corresponding fade margin at the receiver. If the received signal falls under the fade margin, it's practically lost, regardless of the modulation techniques; however, the transmitted power should not always be the problem. It is therefore of necessity to build an algorithm that understands the environmental effects on the channel to "select" and "adapt" the appropriate parameters fordifferent link constraints and channel characteristics. Moreover, it is necessary to study how implicitly inputs are related, and also the effect of input parameters on the output itself. This will create space for the channel fade margin; the more the parameters are adjusted, the more is the control margin at the receiver photodiode. The parameters of major importance are:

- Transmitter power in Watts, or the optical power density per square meter emerging from the transmitter optics.
- Transmitter beam divergence in milliradian.
- The transmitter optical wavelength.
- The transmitter aperture.
- Modulation Bandwidth.
- The range between transmitter and receiver
- The responsivity of the receiver photodiode.
- The hardware of the receiver.
- The signal-to-noise performance.
- Shot Noise and thermal noise of white Gaussian distribution, acting in turbulent media.

2.7 Contribution and Possible Solutions

Due to the adverse weather conditions that might affect the optical wireless channel, it is worthy on the first level to study how such parameters affect the bit error rate (BER) and Signal to Noise Ratio (SNR). The ultimate goal here is to find a way of parameter selection that improves the channel performance and targets a BER of 10^{-9} at the receiver side. There are many parameter combinations that might lead to this fact, keeping in mind that the environmental conditions might be fixed external parameters or subject to instantaneous variations. The first stage of this work is to design a single/multi-objective selection algorithm able to understand all internal and external parameters. And then, an adaptation process is built to adapt the channel to the suggested parameters at run-time using an Adaptive Neuro-Fuzzy Inference System (ANFIS). The selection algorithm utilizes the concept of genetic algorithms

for sensible selection requirements at pre-installation of optical wireless channel; the adaptation algorithm works at run-time given that the channel is equipped with configurable hardware. The optimal datasets chosen by the genetic algorithm are selected for multivariate statistical analyses to extract input/input and input/output relations. The outcome will decide about criteria of parameter selection for a reliable channel performance, which may approach an improvement on the percentage availability if accurately followed.

References

[2.1] F. R. Gfeller, U. Bapst, “Wireless in-house communication via diffuse infrared radiation” *Proc. of the IEEE, 67(11): 1474–1486, November 1979.*

[2.2] J. Tajnai, H. Packard, IBM and Sharp, “Serial Infrared Physical Layer Specification”, *Version 1.4.Infrared Data Association, 2001.*

[2.3]Matt Garfield et al, “Diffuse Free Space Optical MIMO Communication for Robust Indoor Local Area Network”, Drexel, Philadelphia, 2007.

[2.4] J. M. Kahn and J. R. Barry, “Wireless infrared communications” *Proc. of the IEEE*, vol. 85, no. 2, pp. 265-298, February 1997.

[2.5] SalahuddinQazi,“Optical Communications: Challenges and Opportunities,” *in proc. of the 2006 International Conference on Wireless Networks,* ICWN 2006, Las Vegas, Nevada, USA, June 26-29, 2006

[2.6]Anthony C. Boucouvalas, “Editorial on Optical Wireless Communications,” *IEEE Proc. on Optoelectronics*, October 2003.

[2.7] Joseph N. Pelton et al “Optical Communications and Intersatellite Links*,” International Technology Research Institute* (World Technology Division) report, Dec. 1998.

[2.8]S. Qazi “White LEDs Offer Wi-fi alternative”, Newscast *The SPIE Magazine of Photonics Technologies and Applications*, US-Pakistan, 2006.

[2.9] J. P. Yao, G. Chen, and T. K. Lim, "Holographic diffuser for diffuse infrared wireless home networking," *Optical Engineering*, vol. 42, no. 2, pp. 317-324, February 2003.

[2.10] Issac I. Kim, Eric Korevaar, “Availability of Free Space Optics and Hybrid FSO/RF Systems”, in *Proc.of SPIE 4530, Optical Wireless Communications IV, 84, November 2001.*

[2.11] H. Izadpanah, “A Millimeter-Wave Broadband Wireless Access Technology Demonstrator for the Next-Generation Internet Network Reach Extension,” *IEEE Communications Magazine*, Sept. 2001.

[2.12] R. R. Iniquez, S.M. Idrus, and Z. Sun, “Optical Wireless Communications, IR for Wireless Connectivity”, *Taylor & Francis Group*, Florida, USA, 2008.

[2.13] D. P. Schinke, R. G. Smith, and A. R. Hartman.Photodetectors, in H. Kressel, editor, “Semiconductor Devices for Optical Communication”, chapter 3, pages 61–87. *Springer-Verlag*, Berlin, Germany, 1980.

[2.14] D. R. Goff. “Fiber Optic Reference Guide — A Practical Guide to the Technology”, *Focal Press*, Boston, MA, 1996.

[2.15] J.M. Senior, “Optical Fiber Communications: Principles and Practice”, *2nd ed. Prentice Hall International*, 1992.

[2.16] D. J. T. Heatley, D. R. Wisely, I. Neild, and P. Cochrane, "Optical wireless: the story so far", *Communications Magazine, IEEE,* vol. 36, pp. 72-74, 79-82, 1998.

[2.17] N.J. Veck, “AthmosphericTranmission and Natural Illumination (visible to microwave regions)”, *GEC Journal of Research*, 3(4), 209–223, 1985.

[2.18] M. Achour, “Simulating Atmospheric Free-Space Optical Propagation Part II: Haze, Fog and Low Clouds Attenuation”, *in Optical Wireless Communications V*, *Proceedings ofSPIE*, 4873, 1–12, 2002.

[2.19] P.P. Smyth, M. McCullagh, D.R. Wisely, D. Wood, S. Ritchie, P.L. Eardley, and S. Cassidy, “Optical Wireless Local Area Networks — Enabling Technologies”, *BT Technology Journal*, 11(2), 56–64, 1993.

[2.20] P.L. Eardley and D.R. Wisely, “1 Gbit/s Optical Free Space Link Operating over 40 m Systems and Applications”, *IEEE Proc. in Optoelectronics*, 143(6), 330–333, 1996.

[2.21] M. Gebhart, E. Leitgeb, and J. Bregenzer, “Atmospheric Effects on Optical Wireless links”, *7th International Conference on Telecommunications (ConTEL)*, pp. 395–401, Zagreb, Croatia, 2003.

[2.22] M.A. Bramson, “in Infrared Radiation, A Handbook for Applications”, *Plenum Press*, p. 602, 1969.

[2.23] A. Al-habasch, K.W. Fischer, C.S. Cornish, K.N. Desmet, and J. Nash, “Comparison between Experimental and Theoretical Probability of Fade for Free Space Optical Communications”, *Optical Wireless Communications V, Proceedings of SPIE*, 4873,79–89, 2002.

[2.24] R.J. Hill, R.G. Frehlich, and W.D. Otto, “The Probability Distribution of Irradiance Scintillation”, NOAA Environmental Research Laboratories, *Colorado, ERL ETL-274*, 1996.

[2.25] V. Jungnickel, V. Pohl, S. Nonnig, and C. von Helmolt, "A physical model of the wireless Infrared communication channel”, *Selected Areas inCommunications, IEEE Journal on,* vol. 20, pp. 631-640, 2002.

[2.26] G. Einarsson, “Principles of Lightwave Communications”, *John Wiley&Sons*, Chichester, New York; Brisbane; Toronto; Singapore: Wiley, 1996.

[2.27] S. Hranilovic, “Wireless optical communication systems”, Springer, New York, 2005.

[2.28] J. R. Barry, “Wireless Infrared Communications”, *Kluwer Academic Publishers*, Boston, 1994.

[2.29] E. A. Lee and D. G. Messerschmitt, “Digital Communication”, 2nd Edition. *Kluwer Academic Publisher*, 1994.

[2.30] The Royal Society for the Prevention of Accidents (ROSPA), Available: <www.lasersafety.org.uk>, Accessed: [03 June 2012].

CHAPTER III: Literature Review on Recent Achievements

3.1 Introduction

This chapter contains a literature review about the achievements in optical wireless communication. Hybrid FSO/RF technology and rate adaptive modulation are presented for improved channel availability, and propagation models for short and long outdoors optical wireless communication. The chapter concentrates on the latest achievements of intelligent systems in solving communication problems for optical wireless channels.

3.2 Optical Wireless Achievements

Adverse weather conditions that affect channel availability and bandwidth are randomly time varying; therefore, adaptive datarate, bandwidth, and power solutions have been suggested at the transmitter end.Moreover, variable FOV solutions at the receiver end have been investigated, which require bulky optical hardware in order to adapt to the channel conditions [3.1]. Fractal modulation can be used over time-varying channels and the spectral efficiency is kept constant over a broad range of rate-bandwidth ratios. To do that, data is embedded in optical ultra-short laser pulses in a homogeneous signal, using wavelet diversity strategy to help optical wireless signals penetrate rain, clouds, and fog. The pulses with waveforms like dolphin chirps are separated by holographic techniques and are transmitted at various rates [3.2, 3.3].

Kedar and Arnon [3.4] found that the scattering effect of fog could instead be used to enhance the performance of the link. This is achieved using an array of detectors, which form large FOV for capturing some of the scattered light when the unscattered light is not received. The SNR is improved; and the intersymbol interference

produced as a result of multiple scattering is reduced by the use of an adaptive decision equalizer. Line-of-sight misalignment between optical transceivers caused by the influence of wind, buildings sway (earthquakes), and passing obstacles (birds) is a source of pointing error at the beam steering stage and is a random process that affects system performance. Therefore, auto-beam tracking capabilities have been proposed by Izadpanah et al [3.5] to increase the optical power of the receiver and the footprint of the coverage. Moreover, Kedar and Arnon tackled the problem in [3.4] by suggesting an adaptive laser array transmitter and adaptive divergence beams.

Scintillation, defined in section 2.4.3, is a major contributor to wavefront distortion mainly for high frequencies and long distance communication (>500m). It is therefore necessary to reduce the shadowing effect and increase the transmitter power without causing eye hazards; thus, a multibeam transmitters technique based on multi-spot diffusing (MSD) has been proposed[3.6, 3.7]. MSD is a multi-input, multi-output (MIMO) system that utilizes multiple narrow-beam transmitters and a multi-branch angle-diversity receiver, which also promises easier alignment [3.6, 3.8]. The function of the transmitter is to generate several diffusing spots, while the receiver consists of several receiving elements with a narrow FOV. Therefore, a room ceiling could be covered with a uniform distributed optical signal. Moreover, MIMO space-time coding technique allows intelligent processing of multiple independent received signal components and is used to characterize the instantaneous state of the channel during a training period by independent data, which combat channel variations and shadowing. The results of their experimentation showed that space-time coding in hardware increased the levels of diversity and bit error performance. It also showed that bit error performance varies as a function of

transmitter array inter-element distance and transmitter to receiver distance. As in RF, MIMO techniques have the potential to improve diffuse optical links with comparable data rates with promising channel conditions [3. 9].

3.2.1 Hybrid FSO/RF Approach

The requirement of outdoor optical wireless systems mainly focuses on the sufficient power needed to insure the availability of data under adverse weather conditions without exceeding eye safety limits. It is further motivated by the need to preserve carrier class availability because of signal attenuation in the link due to heavy fog, snow and smoke. A practical solution using a hybrid system of optical and RF links is proposed, where the latter acts as a backup to the free space optical wireless system. Such a system is called a hybrid free space optics/radio frequency (FSO/RF) that employs a laser and a radio in tandem to obtain higher survivability of communication link and propose a backup plan upon FSO failure [3.10]. Experimentally, Kim and Korevar proved in [3.11] that FSO combined with a radio frequency backup can achieve better availability for much longer link distances if the free space optics link is combined with a radio frequency backup. Furthermore, Akbulut et al [3.12] developed a hybrid FSO/RF communication system between two campuses of Ankara University located at different locations in the city. The optical link is 2.9 km distant, operating at 1550nm laser source, provided a 155 Mb/sec full duplex connection with an RF feedback of 2.4 GHz Links at 11Mbps.

3.2.2 Availability Model of FSO Data Link

Alternatively, some statistical approaches for a free-space optical (FSO) data link have been negotiated in [3.13]. This model is based on the analysis of random attenuations and their fluctuations in the atmospheric transmission channel. It takes

into account the probability density function of random attenuations (SigmaX=SI), the duration of individual fade events, and the knowledge of the probability density function of fade durations, to estimate the unavailability of the link caused by specific channel properties [3.14]. Optical wireless channels are usually modelled as having a normal fading coefficient with additive white Gaussian noise (AWGN), and optimal detection of a received signal is designed based on maximum likelihood (ML), assuming the receiver has channel state information (CSI). The BER approximation is approached using Guass-Hermite Quadrature and Series approximation under some assumptions in [3.15] shown in figures 3.1 and 3.2.

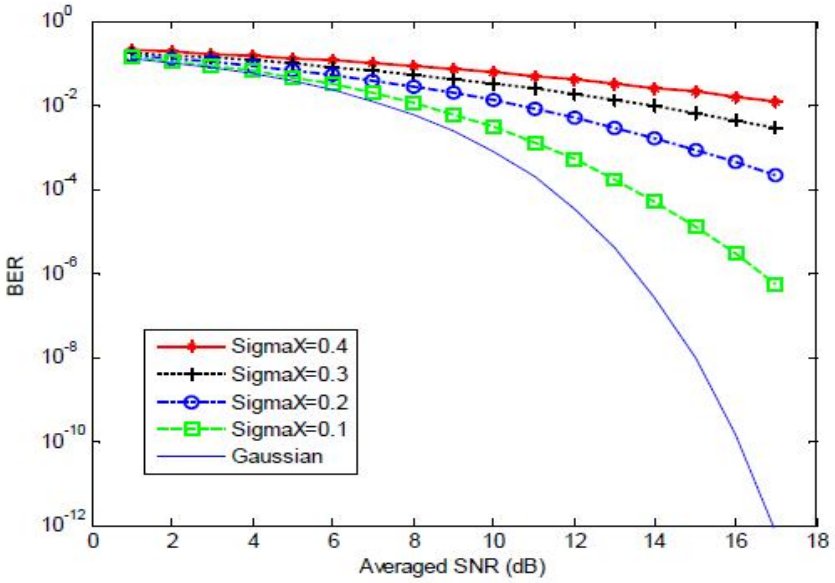

Figure 3.1 BER of lognormal channel with CSI versus SNR at different fading intensities [5.13].

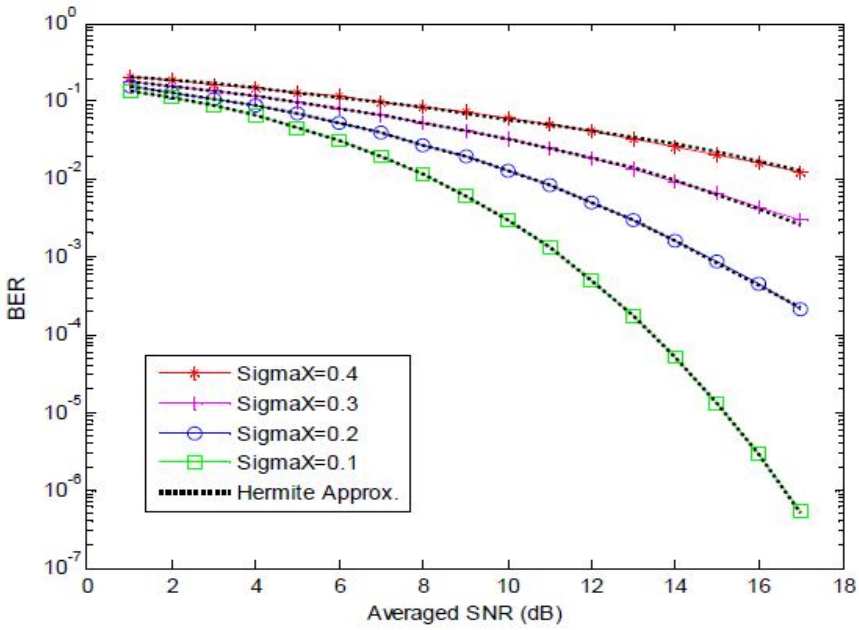

Figure 3.2 Hermite-approximated probability of error for polynomial order n=5 at different values of fading intensity [5.13].

3.2.3 Estimation of Laser Beam Pointing Parameters in the Presence of Atmospheric Turbulence

The effects of pointing errors of an FSO laser communication is considered for estimating the performance of the channel under atmospheric turbulence. Pointing errors can be thought of being composed of two components: a fixed type, called a boresight error, and a random error called jitter. One method of estimating the errors is by using a sequence of return signal values from the intended target with the aid of wave-optics based approach, as described in [3.16]. Other related topics, like the maximum likelihood (ML) symbol by symbol detection techniques for lognormal (LN) turbulence channels, and the gamma-gamma irradiance probability density function models, have been considered to model the effects of optical turbulence in [3.17, 3.18].

3.2.4 Rate-Adaptive Modulation Techniques for Infrared Wireless Communication

The type of modulation in the optical wireless link also affects the type of optimization done on several parameters, which has been discussed in [3.19]. Actually, multicarrier modulation permits transmission with minimal inter-symbol interference on selective frequency channels. Electrical multiple sub-carrier modulation (MSM) uses hundreds of carriers for modulations in the channels, but there is a drawback of high peak-to-average power ratio (PAR) that can lead to clipping and nonlinear distortions; therefore, QPSK and BPSK techniques are used to minimize this effect by selecting specific harmonics for signal recovery. Optical wireless systems using this technique involve modulation of digital and analog information from different electrical subcarriers, and then modulated onto a single optical carrier. The Multi-subcarrier system can be modulated using FM, PM, and Intensity Modulation (IM) [3.20]. The latter, along with direct detection (DD), is being used for most MSM systems, which permits asynchronous multiplexing of heterogeneous information and permits the receiver to make selective demodulation only for the streams of interest. For this advantage, MSM of IM/DD is widely used in optical transmissions of different data sources [3.21]. Basically, average power reduction techniques for intensity-modulated optical systems have been approached using multiple BPSK and QPSK subcarriers. One technique involves block coding of the data bits to be transmitted and the amplitude of symbols modulated on the subcarrier, the second replaces the fixed dc bias by a variable one that changes on symbol-to-symbol basis. These techniques applied to subcarriers originated from a single transmitter with symbol-synchronization [3.22].

3.2.5 System Model, Capacity and Coding for Long-Range Optical Wireless Channel

Intensity modulation and direct detection are used in [3.23] to understand the ultimate capacity of the outdoor long-distance optical wireless communication. The work is done so that the channel under weak atmospheric turbulence is modeled as a stationary ergodic channel with lognormal intensity fading, where signals experience asymmetric statistics due to on-off keying signaling. The channel capacity and outage probability are computed, to provide insight into the quality of this channel as well as the ultimate performance limit. The different coding schemes in OOK showed that fixed rate turbo codes can perform close to the capacity at low turbulence and variable rate adaptive coding when turbulence becomes stronger.

The deterministic attenuations related to fog and rain could be studied using gamma-gamma and lognormal distribution functions for strong-to-week and weak turbulence conditions respectively [3.24]. A statistical analysis of received signal in fog conditions is done in Graz, Austria using a sliding window [3.25], and the evaluation of optimum wavelength in free space optical transceivers is discussed in [3.26] which will be utilized to compare with the an alternative genetic algorithm approach discussed in chapter 4, for wavelength selection under certain weather limitations.

3.3 Propagation Model

The propagation of optical wireless communication signals can be expressed by several mathematical models that describe several channel topologies (section 1.2.1). Following the discussions in chapter 1, the received optical power, studied in [3.27], is independent of position and angular orientation of the photodetector. Analysis for indoors optical communication by Hash *et al* [3.28] reported the double reflection

model, and Barry in [3.27] extended the simulation to model any number of reflections. In this section, three types of models will be considered: the short range outdoors channels, the long range outdoors channels, and multiple-in multiple-out (MIMO) optical wireless channels.

3.3.1 Ultraviolet Non-LOS Short Range Optical Wireless Communication

Ultraviolet (UV) technology has unique features of NLOS connectivity and range attenuations. Using recent devices of LEDs and APDs [3.29, 3.30], the UV approach has become a good candidate for optical wireless communications [3.31].NLOS UV communication is based on scattering and absorption: scattering allows photons to reach the receiver side, while absorption blocks interception. An empirical path lost model for the prediction of the bit error rate performance in a short-range NLOS UV communication is analyzed. Such a model is shown in figure 3.3.

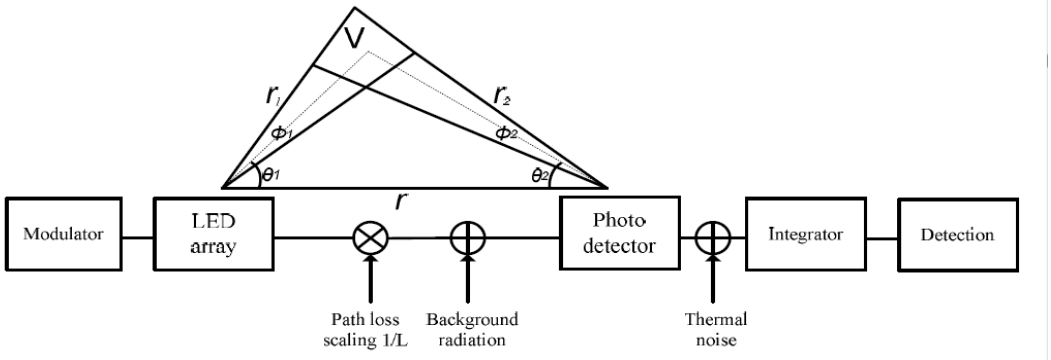

Figure 3.3 UV-NLOS optical wireless model (adapted from [3.32]).

In the model above, $\theta_1$and $\theta_2$are the transmitter and receiver apex angles, ϕ_1 and $\phi_2$are the beam divergence angles. The T_x- R_x baseline range separation is *r*, and *V* is the optical common volume, and *r1* and *r2* are the distances of the common volume to the $T_x$and R_x. Stochastic models of the detector and noise sources are

utilized, from the received optical power, the counting rate λ is modeled as Poisson process, such that,

$$\lambda_s = \eta \frac{P_r}{h\nu} = \eta \frac{P_t}{Lh\nu} \tag{3.1}$$

Knowing that the atmospheric attenuations and turbulence effects are not considered for short range communication in this model (r<500m). $P_r, L, \eta, h, and\ \nu$ represent the received power, the path loss, the quantum efficiency of the detector including optical filter and photodetector, Planck's constant, and the frequency of the optical field respectively. L is an empirical path loss model, the only contributor to attenuation, defined by α and ξ, which are the path loss exponent and the path loss factor of the unknown non-linear functions of the apex angles [3.33].

For each modulation symbol period, the integrator output is proportional to the photon count per pulse time, which is also compatible with the Poisson distribution with photon arrival rate λ, at a probability:

$$P_{k_1}(j) = \frac{\lambda^j . e^{-\lambda}}{j!} \tag{3.2}$$

Shot noise and thermal noise statistics are modeled as a mixture of Poisson point and Gaussian processes. The symbol error probability using an OOK modulation is given by:

$$P_{e-OOK} = \frac{1}{2}\sum_{k=0}^{m_T} (\lambda_s + \lambda_b)^k e^{-(\lambda_s + \lambda_b)} + \frac{1}{2}\sum_{k=m_T+1}^{\infty} \left(\frac{\lambda_b^k . e^{-\lambda_b}}{k!}\right) \tag{3.3}$$

For optimum detection and minimizing the error probability is defined by:

$m_T = floor\left(\frac{\lambda_s}{\ln(1+\lambda_s/\lambda_b)}\right)$. $\lambda = \lambda_s + \lambda_b$ when the signal is (ON) and $\lambda = \lambda_b$ when signal is (OFF), where λ_b represents background radiation photon count rate.

3.3.2 Long-distance Optical Wireless Systems Using IM/DD

The outdoor long-distance optical wireless system adapting high-speed operation (155 Mb/s or higher) requires a transmitter that usually utilizes semiconductor lasers with high launch power and broad bandwidth. The receiver then comprises between bandwidth and noise and reduces the effective capacitance of the photodiode. This is a self-sustaining process,known asbootstrapping,where optically pre-amplified PIN or APD of different dimensions are utilized. Intensity modulation direct detection method is widely deployed using OOK modulation [3.34]. The long-distance point-to-point optical wireless link is modelled using abstract and statistical models, based on figures 3.4 and 3.5.

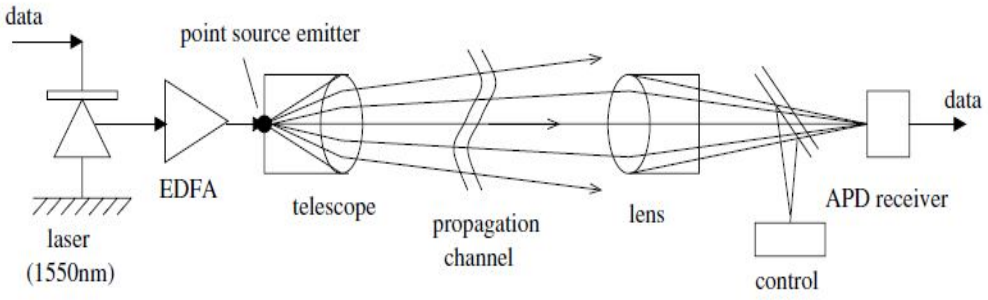

Figure 3.4 Long-distance outdoor point-to-point optical wireless system (adapted from [3.34]).

3.3.3 Multiple In-Multiple Out (MIMO) Optical Wireless Communication

The optical intensity channel consists of the incorporation of time-varying signals, and the spatial distribution of the optical intensity at the transmitter and receiver is not exploited to improve the spectral efficiency of the link due to the directed nature of the channel. Diffuse and quasi-diffuse links transmit the same signals to all locations and act as an inefficient repetition code in space. The MIMO wireless optical channel is a multi-element link, where the transmitter replaces the spatial

repetition code with a more efficient code, exploiting spatial dimensions to achieve gains in reliability and spectral efficiency. The spectral efficiency is gained by time and space codes, where the transmitter is a spatial light modulator, and the receiver is composed of a number of receive elements which detect the radiant optical power from a number of spatial modes coding [3.35]. The transmit spatial light modulator can be realized as a Liquid crystal display (LCD), or Deformable mirror devices (DMD). The latter, consist of an array of mirrors which can be deflected electrostatically to modulate a constant light source, are known as known as micro-electromechanical (MEM) devices [3.36]. MIMO optical wireless communication, not only in the infrared, has also been proposed for visible light communication arrays of white illumination LEDs to construct multi-element optical wireless links [3.37]. The use of arrays of lasers for high-speed chip-to-chip communications have been considered to improve data rates, and potential rates have achieved 500 Mbps per pixel on an array of 3×3 pixels [3.39]. A typical MIMO wireless optical channel is illustrated in Figure 3.5. In such a model, the transmitter has n_T identically shaped transmit pixels distributed and a square $n_{Tx}\ x\ n_{Ty}$grid at intervals of D_T. Due to the amplitude constraints and eye safety regulations, the transmitted amplitude at any time instant t must satisfy $a\,[\,m,n;t] \geq 0$. Therefore, the transmitted optical intensity image at time t is defined as:

$$s\,(x,y;t) = p_T\,(x,y) \otimes \sum_{m,n} a\,[\,m,n;t]\,\delta(x - m\,D_T, y - nD_T) \qquad (3.4)$$

$p_T\,(x,y)$is the optical intensity distribution associated with each transmit pixel, $\otimes$ denotes convolution, and $\delta(x,y)$ is defined by,

$$\iint f(x,y)\delta(x - x_o)(y - y_o)dxdy = f(x_o,y_o) \qquad (3.5)$$

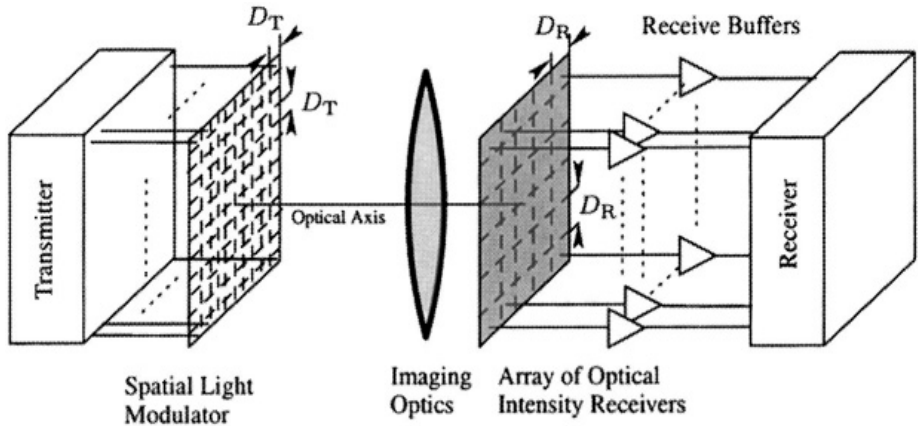

Figure 3.5 Channel Model of a MIMO wireless optical channel (adapted from [3.38]).

With a compatible time modulation format for each pixel, the receiver is positioned to collect the transmitted optical intensity image and outputs a signal representing the spatial distribution of optical power of each symbol interval on the photodetector. The receiver consists of n_R identically shaped receive pixels distributed and a square $n_{Rx}\ x\ n_{Ry}$ with interval D_R, the received output samples at each interval is given by,

$$r[k,l;iT] = \int_{t\in[iT,(i+1)T]} \int_{p_R(x-kD_R,y-lD_R)} r(x,y;t)d(x,y)dt + n[k,l;iT] \quad (3.6)$$

Where $n[k,l;iT]$is the noise at each received pixel, modelled as Gaussian due to the intense background illumination [3.40]. The channel is supposed to have static characteristics, and the transmitter and receiver are at fixed positions, and the channel characteristics which can also obey the genetic algorithm and other intelligent techniques proposed in chapters 4, 5, 6, and 7.

3.4 Achievements with Intelligent Systems

Intelligent systems have contributed to many achievements in the optical wireless industry, especially in channel optimization, noise cancellation, channel equalization, and performance estimation. Some literature appears below.

3.4.1 Genetic Algorithms for Power and SNR Optimizations

In the intelligent system approach, a genetic algorithm controlled multispot transmitter is proposed in [3.41]. It describes an alternative approach of power optimization in mobile indoors optical wireless systems. The algorithm focuses on dynamically changing the intensity of individual diffusion spots in multiple rooms, showing a negligible impact on bandwidth and rms delay spread, to emphasize the use of a more effective transmitter and receiver in various scenarios and applications. The simulations show that the dynamic range of the rooms, referenced against the peak received power, can be reduced by up to 26% when empty, and to 12% when user movement obstructs the channel. Moreover, a genetic algorithm for improving the received SNR in multi-spot diffuse infrared communication systems is proposed in [3.42]. It provides an improvement of up to 8dB compared to line strip multibeam transmitter systems (LSMS) [3.43] at a cost of about 1% overhead by adjusting the position and number of the spots on the ceiling as the receiver moves to different locations.

3.4.2 Artificial Neural Network Channel Equalization in the Bit Error Performance for PPM Diffuse Indoor Optical Channel

Channel Optimization for a PPM system is achieved in [3.44] by training a Multilayer Perceptron (MLP) artificial neural network for decision coding in different bit resolution and spread delays of the optical channels. The study shows that for a highly diffuse channel, it is required to have a 10 dB SNR to achieve an acceptable bit error rate of 10^{-5}. ANN based equalizer is 10 dB lower compared to the unequalized soft decoding at 155 Mbps data rate. The results indicate that for all ranges of delay spread, neural network equalization is an effective tool of mitigating

the ISI; the latter increases under bad weather conditions and multipath propagation. This forces the channel to change the channel parameters, especially transmission bandwidth, its effect having been studied based on Monte-Carlo simulation using the application of zero-forcing equalizer [3.45].

3.4.3 Real Time Adaptive Nonlinear Noise Cancellation using Fuzzy Logic for Optical Wireless Communication System with Multi-scattering Channel

The transmission of optical signals under adverse weather conditions causes attenuation and scattering. The atmospheric turbulence effects are analysed, and an intelligent optical receiver under multiscattering conditions is proposed in [3.46]. The train of optical pulses is transmitted and coherent detection is used in the receiver. Using the fuzzy logic concept, the receiver adapts itself by changing its sensitivity based on the value of received power and Signal to Noise Ratio (SNR) levels. Using this technique, the non-linear noises in the Additive White Gaussian Noise (AWGN) channel, incorporated in the optical signal at the receiver have been cancelled by -40dB SNR level and up-to -50dBm of received power, and proved to have high estimation and adaptability[3.46].

3.4.4 Adaptive Pulse Amplitude and Position Modulation for Optical Wireless Channel

An adaptive hybrid modulation scheme is proposed in [3.47] by considering the three major modulation schemes in the optical wireless channel. On-off keying (OOK), pulse amplitude modulation (PAM), and pulse position modulation (PPM), are analyzed in terms of their power and bandwidth requirements. The proposed modulation scheme takes the real time channel conditions into account, which is different from other schemes. By adaptively employing amplitude and position

modulation, a guaranteed system performance can be secured without compromising power and bandwidth efficiency.

3.4.5 Simulated Annealing (SA) Optimization Algorithm

A Simulated annealing algorithm (SA), proposed in [3.48-3.49], and is used as an optimization process for the diffusing pattern, in order to improve system performance. The SA finds a global minimum to optimize the hologram mask to convert a point source into an extended source with the lowest cost function. A model based on conventional square grid-type designs with 8 different lambertian spot patterns, and 5 different receiver FOVs (10, 20, 30, 45, 90) were used to determine the best results of combination of spot patterns and receiver FOV. The simulated annealing technique contributed to optimum distribution of spots for a target parameter with a 19% improvement compared to the iterative method. Moreover, 87.5% reduction over the uniform illumination pattern, and 93% reduction was observed in the standard deviation of the received signal power below that of the grid design.

3.4.6 Neuro-Genetic Hybrid Model

A neural network approach for modeling multilayer three-dimensional ceramic system-on-package inductor is developed for hardware industry in wireless applications [3.50]. A genetic algorithm based optimizer is then coupled with the neural network model obtained for subsequent design and optimization of inductor circuit model parameters. This methodology is validated by characterization data collected from multi-layer inductors fabricated in a twelve metal layer low-temperature co-fired ceramic (LTCC), which are of great interest in the W-CDMA technology. One model is used to perform sensitivity analysis and derive response

surfaces using neural networks and then a genetic algorithm model is coupled to optimize the inductor layout. The proposed neuro-genetic algorithm promises to optimize the time and cost of multilayer passive design with high accuracy.

3.5 Conclusion

The achievements discussed in the literature shows that intelligent systems are widely utilized for solving communication problems, and they were recruited for improving the performance of optical wireless channels in tremendous applications. In chapter 4, a genetic algorithm based selection of the transmission wavelength is built as a preliminary approach of selection, and it will then be extended to include various parameters of link importance.

References

[3.1] D. Kedar, S. Arnon "Optical wireless communication through fog in the presence of pointing errors", *Appl. Optics* Vol. 42, No. 24, pp 4946 - 4954, Aug. 2003.

[3.2] L. Atzori, D. D. Giusto, M. Murroni, "Performance Analysis of Fractal Modulation Transmission Over Fast-Fading Wireless Channels," *IEEE Transactions on Broadcasting, Fractal modulation*, Vol.48, No.2, June 2002.

[3.3] M. Kavehrad, B. Hamzeh, "Ultrashort Pulsed FSO Communication System With Wavelet Fractal Modulation, *Proc. SPIE 5598, Performance, Quality of Service, and Control of Next-Generation Communication Networks II*, 144, 2004.

[3.4] D. Kedar, S. Arnon, "The Positive Contribution of Fog to the Mitigation of Pointing Errors in Optical Wireless Communications," *Applied Optics*, Vol. 42, August 2003.

[3.5] H. Izadpanah et al, "High-Availability Free Space Optical and RF Hybrid Wireless Networks," *IEEE Wireless Communications*, April 2003.

[3.6] S.T. Jivkova, M. Kavehrad, " Multispot diffusing configuration ," *in Proc. of London Communication Symposium,* London, Sept 2002.

[3.7] M.R. Pakravan, M. Kavehrad, "Design considerations for broadband indoor infrared Communication systems," *International Journal of Wireless Information Networks*, Vol.2 no.4, Oct. 1995.

[3.8] G.Yun, M. Kavehrad, “Indoor Infrared Wireless Communications Using Spot Diffusing and Fly-Eye Receivers,” *Canadian Journal on Electrical & ComputerEngineering*, Vol. 18, No. 4, October 1993.

[3.9] M. Garfield et al, “Diffuse Free Space Optical MIMO Communication for Robust Indoor Local Area Network Links”, Drexel University, USA, Available: <http://www.ece.drexel.edu/faculty/dandekar/Papers/Garfield_QuantElectronics05.pdf>, Accessed: [01 April 2013].

[3.10] J. Derenick, C. Thorne, and J. Spletzer, “Hybrid Free-Space Optics/Radio in Frequency (FSO/RF) Networks For Mobile Robot Teams, Multi-Robot Systems”, *Swarms to Intelligent Automata*, Volume III, pp 263-268, 2005.

[3.11] I. I. Kim, E. Korevaar, “Availability of Free Space Optics and Hybrid FSO/RF systems” *in Proc. SPIE 4530, Optical Wireless Communications IV,* 2001.

[3.12] A. Akbulut et al, “An experimental Hybrid FSO/RF Communication System”,in *Proceeding Communication Systems and Networks,* Available :<http://morse.uml.edu/Activities.d/Summer-05/PAPERS/FSO_Paper.pdf>, Accessed: [01 April 2013].

[3.13] Z. K. Kolka, O. Wilfert, D. Biolek, “Availability Model of Free Space Optical Data Link”, *VieraBiolková Brno University of Technology Purky*, Ova 118, Brno, 612 00, Czech Republic, 2005.

[3.14] Z. Kolka, O. Wilfert, “Statistical model of free-space optical data link”, *Proc. of The International Symposium on Optical Science and Technology*, Denver, pp. 203 - 213, 2004.

[3.15] H. Moradi, M. Falahpour, H. Refai, "BER Analysis of Optical Wireless Signals through Lognormal Fading Channels with Perfect CSI", *17th International*

Conference on Communications, 2010.

[3.16]D. K. Borah, D. G. Voelz, "Estimation of laser beam pointing parameters in the presence of atmospheric turbulence", *Appl. Opt.*, vol. 46, pp. 6010–6018, Aug. 2007.

[3.17] D. K. Borah, D. G. Voelz, and S. Basu, "Maximum-likelihood estimation of a laser system pointing parameters by use of return photon counts", *Appl. Opt.*, vol. 45, pp. 2504–2509, Apr. 2006.

[3.18] S. Arnon, "Power versus stabilization for laser satellite communication", *Appl. Opt.*, vol. 38, pp. 3229–3233, May 1999.

[3.19] H. Joshi, R.J. Green, M.S. Leeson, "Multiple Sub-Carrier Optical Wireless Systems", *in Proc. of Transparent Optical Networks, 2008 (ICTON 2008)*, University of Warwick, UK, 2008.

[3.20] H. Yamaguchi, T. Ohtsuki, I. Sasase, "Multiple subcarrier modulation for infrared wireless systems using punctured convolutional codes and variable amplitude block codes", in *Proc. IEEE GLOBECOM 2002,* pp. 2031-2035, 2002.

[3.21] J. R. Barry, "Wireless Infrared Communications", *Kluwer Academic Publishers*, Boston, 1994.

[3.22] L. Diana, J. M. Kahn, "Rate-Adaptive modulation techniques for infrared wireless communications", in *Proc. of IEEE Intl. Conf. on Commun.*, Vancouver, B.C., Canada, June 6-10, 1999.

[3.23] J. Li, M. Uysal, "Optical Wireless Communications: System Model, Capacity and Coding", *in Proc. of 58th IEEE conference on Vehicular Technology Conference,* 168 - 172 Vol.1, 2003.

[3.24] M. Uysal, "Error rate performance analysis of coded free-space optical links over gamma-gamma atmospheric turbulence channels", *IEEE Transactions on wireless communications*, Vol.5, Issue: 6, Page(s): 1229-1233, 2006.

[3.25] A. Rehman, S. Mohammad, "Statistical analysis of received signal strength in fog using sliding window technique for FSO links", in *Proc. of the 8th International Conference on Frontiers of Information Technology*,ISBN: 978-1-4503-0342-2, USA, 2010.

[3.26] E. Leitgeb, T. Plank, M.S. Awan, P. Brandl, W. Popoola, Z. Ghassemlooy, F. Ozek, M. Wittig, "Analysis and evaluation of Optimum wavelengths for free-space optical transceivers", *in Proc. of 12th international conference of Transparent Optical Networks (ICTON)*, pages(1-7), July 2010.

[3.27] J. R. Barry, J. M. Kahn, W. J. Krause, E. A. Lee, and D. G. Messerschmitt, "Simulation of multipath impulse response for indoor wireless optical channels," *Selected Areas in Communications, IEEE Journal on,* vol. 11, pp. 367-379, 1993.

[3.28] D. Hash, J. Hillery,and J. White, "IR RoomNet: Model and Measurement" *inIBM Communication ITLConference*, June 1986.

[3.29] M. Shatalov, J. Zhang, A. S. Chitnis, V. Adivarahan, J. Yang, G. Simin, and M. A. Kahn, "Deep ultraviolet light emitting diodes using quaternary AlInGaNmultiple quantum wells," *IEEE J. Sel. Top. Quantum Electron, Vol.2,* **pp.** 302–309 2002.

[3.30] V. Adivarahan, Q. Fareed, S. Srivastava, T. Katona, M. Gaevski, and A. Khan, "Robust 285 nm deep UV light emitting diodes over metal organic hydride vapor phase epitaxially grown AlN/sapphire templates" *inJapan Journal of Applied Physics* 46, pp. L537– L539, 2007.

[3.31] Z. Xu, B. M. Sadler, "Ultraviolet communications: potential and state-of-the-art" *inIEEE Communication Magazine* 46(5), 67–73, 2008.

[3.32] Q. He, Z. Xu, and B. M. Sadler "Performance of short-range non-line-of-sight LED-based ultraviolet communication receivers", *Optics Express*, Vol. 18, Issue 12, pp. 12226-12238, June 2010

[3.33] G. Chen, Z. Xu, H. Ding, B. M. Sadler, "Path loss modeling and performance trade-off study for short-range non-line-of-sight ultraviolet communications" *Optics Express*, Vol. 17, Issue 5, pp. 3929-3940, 2009.

[3.34] D. J. T. Heatley, D. R. Wisely, I. Neild, and P. Cochrane, "Optical wireless: the story so far," *in IEEE Communication Magazine.*, pp. 72-74, 79-82, Dec. 1998.

[3.35] B. G. Boone, "*Signal Processing Using Optics: Fundamentals, Devices, Architectures, and Applications", Oxford University Press*, New York, 1998.

[3.36] Texas Instruments, Digital Light Processing, Available: <www.dlp.com>, Accessed: [06 May 2013].

[3.37] Y. Tanaka, S. Haruyama, and M. Makagawa, "Wireless optical transmissions with white colored LED for wireless home links", *inProc. of the IEEE International Symposiumon Personal, Indoor and Mobile Radio Communication,* volume 2, pages 1325–1329, 2000.

[3.38] S. Hranilovic, "*Wireless optical communication systems"*, Springer, New York, 2005.

[3.39] E. Bisaillon, D. F. Brosseau, T. Yamamoto, M. Mony, E. Bernier, D. Goodwill, D. V. Plant, and A. G. Kirk, "Free-space optical link with spatial redundancy for misalignment tolerance", *in IEEE Photonics Technology Letters,* 14(2):242–244, February 2002.

[3.40] G. C. Holst, "CCD Arrays, Cameras, and Displays" *in SPIE Optical Engineering Press*, Bellingham, WA, 1996.

[3.41] M. D. Higgins, R. J. Green, M. S. Leeson, Senior Member, "A Genetic Algorithm Method for Optical Wireless Channel Control", *Journal of Lightwave Technology*, Vol. 27, No.6, March 15, 2009.

[3.42] M. N. Esfahani, J.M. H. Elmirghani, "A Genetic Algorithm Method for Multi-spot Diffuse Infrared Wireless Communications", University of Leeds, *London Communications Symposium,* 2009.

[3.43] A.G. Al-Ghamdi, and J.M.H. Elmirghani, "Performance comparison of LSMS and conventional diffuse and hybrid optical wireless techniques in a real indoor environment"*Optoelectronics, IEE Proceedings*, 2005. 152(4): p. 230-238.

[3.44] S. Rajbhandari, M. Angelova, "The Bit Error Performance of Diffuse Indoor Optical Wireless Channel PPM System Employing Artificial Neural Networks for Channel Equalization", *Intelligent Modeling lab*, Northumbria University, UK.

[3.45] Z. Kolka, D. Biolek, V. Biolkova, "Simulation of Atmospheric Optical Channel with ISI", in *Proceedings of the 8th WSEAS International Conference on Circuits, Systems, Electronics, Control, and Signal Processing*, ISBN: 978-960-474-139-7, pp 198-201, 2009.

[3.46] L. R. D. Suresh, S. Sundaravadivelu, "Real Time Adaptive Nonlinear Noise Cancellation using Fuzzy Logic for Optical Wireless Communication System with Multi-scattering Channel Member", *Engineering Letters, Advance Online Publication*, November, 2006.

[3.47] Y.Zeng, R.J.Green, M.S. Leeson, "Adaptive Pulse Amplitude and Position Modulation for Optical Wireless Channel", *in proceedings of the 2nd Institution of Engineering and Technology International Conference on*, 2006.

[3.48] S. Kirkpatrick, C.D. Jr. Gerlatt, M.P. Vecchi, "Optimization by Stimulated Annealing" Science, New Series, Vol. 220, No. 4598, pp. 671-680, May 1983.

[3.49] W. K. Damon, W. & G. C. K. Chen, "Optimization of Spot Pattern in Indoor Diffuse Optical Wireless Local Area Networks" *Photonics Research Centre*, USA, 2005.

[3.50] R. J. Pratap, S. Sarkar, S. Pinel, J. Laskar, and G. S. Ma, "Modeling and Optimization of Multilayer LTCC Inductors for RF /Wireless Applications Using Neural Network and Genetic Algorithm", *in IEEE proc. of Electronic Components and Technology Conference*, 2004.

CHAPTER IV: A Genetic Algorithm-Based Selection of a Transmission Wavelength in the Outdoors LOS Optical Wireless Channel

4.1 Introduction

A genetic algorithm selection technique of appropriate transmission wavelengths in the line-of sight (LOS) optical wireless channel, under different weather conditions is described. The overall deterministic attenuations are presented in an international code of visibility, and the changes in visibility decide the wavelength control margin. However, the proposed work suggests a comprehensive method that analyses non-uniform weather conditions, and specifies a practical range in which the genetic algorithm can work. The chapter considers the fact that instantaneous attenuations are not stable and form a variable link margin that should be analytically studied for optimum wavelength selection. An application-specific genetic algorithm is discussed, and a verification methodology is proposed to check its complexity and reliability prior to use, when compared against the *MATLAB* GA toolbox, for parameter selection in the LOS OW channel modelled in chapter 5.

4.1.1 Genetic Algorithms (GAs)

Evolutionary Algorithms (EAs), inspired by biological evolution, are a subset of evolutionary computation that performs well approximating solutions to many types of problems. They have drawn researcher's attention after their great success in the fields of engineering, biology, robotics, operations research, art, social sciences, physics, chemistry and certain hybrid areas of research. They provide a more robust and efficient approach for solving complex problems [4.1]. EAs, such as genetic

algorithms (GAs) [4.1], genetic programming (GP) [4.2], evolutionary programming [4.3] and evolution strategies [4.4], have all been previously proposed for various selection and optimization problems. The genetic algorithm is a particularly well known and extensively used for search space problems. GAs have been employed for a wide variety of optimization studies, such as communication networks [4.1], [4.5], [4.6], image processing [4.7], pattern recognition [4.8] and neural networks [4.9].

GA is described by a stochastic search algorithms based on the mechanism of natural selection and natural genetics, as described by Goldberg [4.10]. The GA resolves a search space problem by following natural biological sequential events. For instance, first, a number of individuals (chromosomes) are randomly generated, and each chromosome consists of fixed number of variables. The latters are called genes in biology; the chromosomes are then applied to a mating process, where they tend to find the optimal solution according to a certain objective function. Based on the highest fitness values, the chromosomes representing a set of “fittest” solutions are chosen for survival. In this chapter, this refers to a fitness leading to lesser attenuations explained in sections 4.3 and 4.4, and in chapter 5, the parameters leading to minimal bit-error-rate BER. This process starts by initiating the genetic operators; based on a chosen selection method, applying crossover and mutation to create subsequent generations. The crossover method is applied to two selected chromosomes known as the "parents", and results in new chromosomes known as the "offspring". After several generations, the genetic algorithm converges to the best chromosome, which hopefully represents a global optimum solution to the problem. The process also allows the visualization of local optimums if it’s of importance to the researcher with a bit of code customization. There are three major advantages of

GA's that researchers target when compared to other search and optimization algorithms [4.10]:

- Flexibility: Different feature operators (selection, crossover,and mutation) in GA can be selected related to a specific problem so as to find its solution. This property provides great flexibility to make an efficient implementation for a given problem [4.10].
- Robustness: A GA is effective in performing a global search. It has been proved that a GA is more robust and more efficient in finding a feasible solution than other conventional heuristics in many applications [4.1, 4.10]. In addition, GA's reduce computational effort when optimizing the problem and leads to shorter running time, and this is one of the advantages targeted in this thesis.
- Adaptability: Most of GA features are based on probabilistic approaches. Therefore, a GA does not require substantial mathematical calculations to solve given selection problems. Thus, a GA will search for a feasible solution based on its evolutionary nature.

GAs can successfully solve any kind of optimization problem by maximizing or minimizing a suitable objective function [4.10]. The genetic algorithm is performed by applying the following consecutive steps:

1) Generate an initial population of K individuals (parameters), and set the generation index $g = 1$ to count iterations;
2) Evaluate the fitness values of each individual;
3) Select parent individuals randomly;
4) Apply crossover and mutation to generate offspring individuals from parent individuals

5) Evaluate correspondingly the fitness values of all offspring individuals;
6) Select individuals to be transferred to the next generation by using a selection method such as Tournament [4.1] or Roulette Wheel [4.11];
7) Return selected individuals to the population;
8) Increment *g,* and return to step 3,

A block diagram of a search algorithm is shown in figure 4.1.

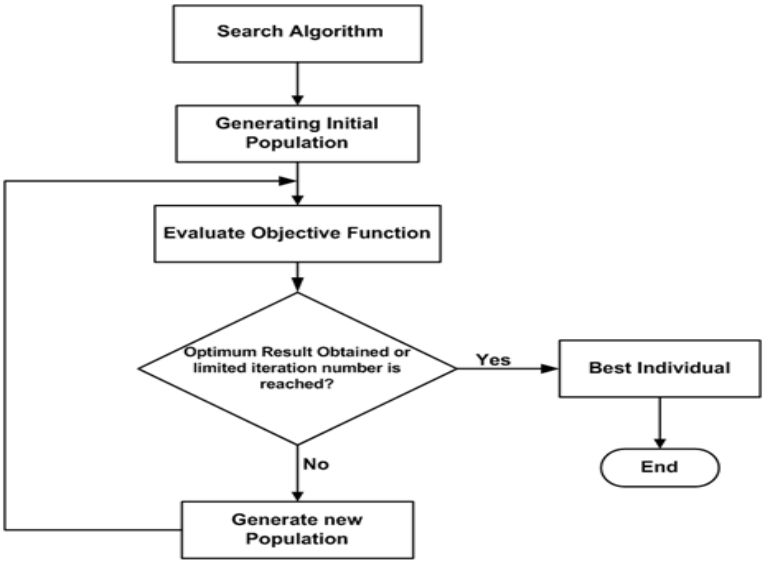

Figure 4.1 Block diagram for a Search Algorithm.

4.1.2 Why Use Genetic Algorithms

Genetic algorithms are used because of the selection power they have in compensating compilation time and the adaptability they can perform in a short period of time against traditional methods. The first experiment is a GA adaptive wavelength selection due to certain link variations. The algorithm worked efficiently, giving results near to the visibility models achieved so far, by covering a larger range of control. The genetic algorithm is able to re-allocate the costs of transmission by studying the environmental effects on each of the internal link parameters and the intended BER at the receiver photodiode.

In the coming work, different parameters will be studied by a genetic algorithm, to select the fittest ones. Random data sets along with the relations (models) will be used with a genetic algorithm. The latter is able to detect indirect relations among inputs, and recruit for better power achievement. Selecting runtime parameters is notably the most difficult part of successfully applying genetic algorithms to search and optimization problems, several investigations have discussed parameter set selection both theoretically and through experimental analyses. An attempt of generating random attenuations in the optical wireless channel was simulated in *MATLAB*2011a, giving optimal wavelength selection at runtime and increasing the control margin of link parameters. The genetic algorithm needs certain operators to function, as described below.

4.2 Genetic Operators

The crossover and mutation operators are the major operators in genetic algorithms; they need to be initialized at the beginning of the algorithm, and they are the main added features that distinguish GAs from other methods [4.1], [4.10].

4.2.1 Crossover

The crossover operator is used to exchange information between the parent chromosomes [4.12]. Crossover operates on two chromosomes and creates offspring by combining genes of both chromosomes at any iteration number. Consequently, a transfer of information or genes between the candidates happen so that the offspring created collects the beneficial information to find a better result. The idea behind crossover is that the new chromosome may be better than both of the parents, if and only if it inherits the best characteristics from each of the parents [4.1], [4.10].

In the crossover method, the most significant point is to define a proper crossover operator for the corresponding problem because it plays a major role in the GA in achieving better performance. The most known and most used crossover operators are 1-point crossover, *n*-point crossover and uniform crossover [4.10]. Thecontribution of crossover methods and their improvements to certain selection and optimization problemshave been discussed in [4.1], [4.2], [4.11], [4.12], and [4.15].

4.2.1.1 Single-Point Crossover

This is the simplest operator form in the crossover method. It starts with a random cut-point applied to two binary-coded chromosomes, which segments the parent chromosomes and generates the offspring by swapping the parts of two parents as shown in figure 4.2.

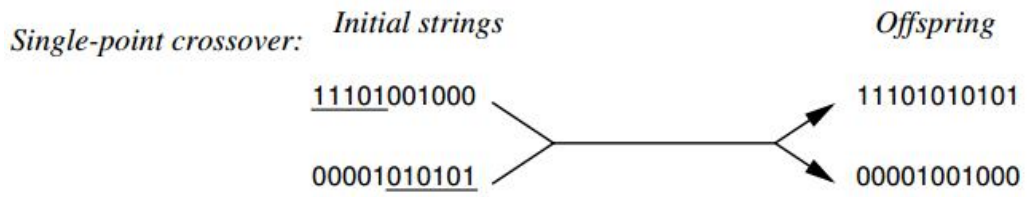

Figure4.2 Illustration of one-point crossover method applied to two binary-coded chromosomes, adapted from [4.16].

4.2.1.2 Multi-Point Crossover

In this approach, multi cut-points are first selected randomly. The regions of the chromosome between these multi cut points are called matching sections, which will be exchanged between the individuals to produce the offspring [4.13]. The production of offspring by using the multi-point crossover operator is shown in Fig. 4.3.

Two-point crossover:

Figure 4.3 Illustration of multi-point crossover method applied to the binary-coded chromosomes [4.16].

4.2.1.2 Uniform Crossover

Uniform crossover assigns certain probability to cut points; it is usually cut in half (probability usually set to 0.5), or otherwise selected randomly. As a result, the genes of the offspring will be each resembled to the genes of the parents [4.14] as shown in Figure. 4.4.

Uniform crossover:

Fig. 4.4 Illustration of uniform crossover method applied to the two binary-coded chromosomes, adapted from [4.16].

4.2.2Selection Operator

A selection operator is applied to improve the quality of a generated population in an evolutionary algorithm. It determines how individuals are selected, or in other words, it defines the criteria of selection. The produced offspring will contain combinations of the genetic information of the selected individuals; the next generation is affected by the selected individuals, and so on [4.17]. The mostly used selection operators are tournament, roulette wheel, and rank selection functions.

In Tournament selection method,two chromosomes are selected and compared to determine which one of them is the fitter for the given solution. The fitness function

and fitness assigned values of the individuals affect the selection, because fitness values affect the survival of the chromosome in the population, provided that the fitter chromosome has not been previously picked as a parent, and is therefore placed in a population pool. This process is repeated until the population pool has a sufficient number of chromosomes [4.1]. Roulette wheel selection operates by determining the selection probability or survival probability proportional to the fitness value for each chromosome. In terms of selection, each chromosome has a slice of "wheel" with the slice size dependent on the survival probability. This means that the fitter chromosomes will have a higher probability of being selected to generate the offspring. The selection process is based on spinning the wheel and selecting a single chromosome from this spinning [4.11].With Rank selection method, all individuals in the population are sorted based on their fitness values and then, each individual is assigned a rank number beginning from 1 onwards (to the population size). The weaker is the assigned number; the lower is its fitness value. For instance, the weakest individual is assigned with 1and the best will have N, which is the number of chromosomes in population. The probability that an individual is selected is proportional to its rank in this sorted list. Unlike roulette wheel selection, the rank selection might create more randomness in the generation, which would give a greater chance for the worst chromosomes to be selected for mating. Thus, the fit chromosomes may not dominate the population. This method can lead to the loss of information from the fittest chromosomes, and thus a slower convergence.However, it may also give chance to weak individuals for contributing to the solution.

4.2.3 Mutation Operator

Mutation is an operator which is responsible about creating randomness in the population. Mutation plays a crucial role in replacing the genes from a population during the selection process so that they can be tried in a new context. It could provide the algorithm with the genes that were not present in the initial population and their existence might show certain importance on the convergence process. The mutation probability rate is defined as the percentage of the total number of mutational genes in the population. It is chosen to be neither too low, nor too high. If it is too low, many genes that would have been useful are never tried out, while if it is too high, the offspring will start to lose their capacity to learn from the history of the search with an increased random perturbation. The mutation rate is chosen typically between [0.01, 0.1] for optimizing the problems [4.14]. Figure 4.5 illustrates two significant types of mutation operators that have been applied to a binary-coded chromosome with a single gene mutation and multi gene mutation.

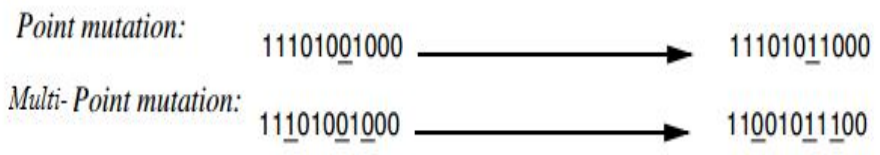

Figure 4.5 Illustration of mutation operator applied to single binary-coded chromosome showing Single and Multi gene mutation operators, adapted from [4.16].

4.2.4 Fitness Function

The quality of a represented chromosome or potential solution is estimated by a fitness function that governs the genetic algorithm. The purpose of using such a function is to map a chromosome representation into a scalar or cost value. For a specific selection or optimization problem, the fitness function estimates a cost value

for each chromosome that is close to a global optimum or not. Thus, the strong and weak candidates can be evaluated according to the fitness values and multiple offspring are produced based on them [4.16].

4.3 Visibility and Optical Attenuations

Several models describing a relationship between visibility and optical attenuation due to fog are published in the literature. Visibility, usually reported by airports, is a measure of thedistance at which light can be clearly discerned. In the field of optical wireless systems, it has been described in several models like Krus [4.17], Kim [4.18], Beer-Lambert and others. In this approach the genetic algorithm makes use of [4.17] and follows a combination of the Koschmieder and Beer-Lambert exponential, defined by:

$$\alpha_{sc} = \frac{17}{V}\left[\frac{550}{\lambda}\right]^{0.585V^{0.333}} \tag{4.1}$$

Where α_{sc} (dB/km) is the deterministic attenuations due to scattering induced by fog, mist, rain, and snow. λ is the wavelength in nanometers, and V is the visibility in Kilometers. The focus in parameter selection using a genetic algorithm will be in a 3 km visibility range, where the change in wavelengths contributes clear fluctuations in system selection. Nevertheless, one research outcome states that fog attenuations are wavelength-independent when visibility is less than 500m [4.21].

Scattering is caused by the behavior of re-radiation which depends on the wavelength, index of refraction, and isotropy. Scattering is of three types, classified according to wavelength relation with the radius of the particle as: Rayleigh, Mie, and Geometric. Light propagating through fog and haze is scattered on water droplets. As the droplet diameter is comparable to wavelength of EM radiation (Mie

theory, (4.2), [4.24]), absorption and scattering of laser photons is caused by aerosols and gaseous molecules in the atmosphere, causing spatial variations which affect the real part of the complex refractive index.

$$n(r) = ar^{\alpha} \exp(-br^{\gamma}) \tag{4.2}$$

Where a, b, α, and γ are fog modelled parameters, and r is the particle radius [4.27]. Significant efforts [4.21, 4.23]have been made to decide if atmospheric attenuations are wavelength dependent or not. Most of them agree that there's only slight wavelength dependence for attenuations caused by haze and fog particles. Mid and long-wave infrared are less sensitive due to the lower scattering effects [4.23], where Mie approximation is not applied. To avoid the discrepancy in this issue, this study is referred to as a visibility model followed by [4.21] using the standard international code of visibility [4.25].

Table 4.1 Visibility range for different weather conditions(benefited from [4.25].

Visibility (km)	**Distrib-ution Type**	**Attenuations dB/km (780 nm)**	**Attenuations dB/km (1600 nm)**	**Particle Radius (µm)**	**a**	**A**	**γ**	**b**
0.05	Dense Fog	315	272	10	.027	3	1	0.3
0.2	Thick Fog	75	60	2	607.5	6	1	3
0.5	Fog	29	21	1	341	2	0.5	4
1	fog -Haze	14	9					
2	Haze (Marine)	7	4	0.05	5.3e4	1	0.5	8.9
4	Haze (continental)	3	2	0.07	5.0e6	2	0.5	15.1
10	Clear	1	0.4	0.07	5.0e6	2	0.5	15.1
23	Very Clear	0.5	0.2					

Similarly, rain and snow affect the optical signal and cause some attenuations of minor significance compared to fog. These attenuations fall under the geometrical scattering regime and are characterized by (4.3) and (4.4) without giving major importance to the wavelength [4.22][4.23].

$$\alpha_{rain} = \frac{2.9}{V} \quad (4.3) \qquad ; \qquad \alpha_{snow} = \frac{58}{V} \quad (4.4)$$

The attenuation due to rain can be calculated as a function of rainfall rate. Its value has been approximated as 6 dB/km during heavy rain (10 mm/hr) [4.19]. Other reports indicate that the attenuation due to rain can reach values of up to 17 dB/km, while the attenuation due to snow can be as high as 60 dB/km [4.26].

4.3.1 Simulation Results

The purpose around the GA selection is to engineer an optical link such that, for a large fraction of the time, an acceptable power will be received even in the presence of heavy fog. Link engineering usually begins with the collection of fog statistics data to estimate the percentage of time the fog attenuation will be greater than a certain value. For the wavelength selected by the GA algorithm, fog attenuation is estimated and the optical wireless link is established according to Equation (4.5). The maximum link length is calculated according to:

$$Link\ Distance\ (km) = \frac{Link\ Margin\ (dB)}{Fog\ Attenuations\ (\frac{dB}{km})} \quad (4.5)$$

The deployment of locations with frequent and heavy fog is achieved at shorter allowable links for a given availability. Alternatively, a relatively fog-free site might be able to accommodate link lengths of several km using identical optical wireless equipment, and the link margin is discussed in the model of chapter 5. The genetic algorithm-based wavelength selection due to random attenuations, published in [4.28] starts with an arbitrary wavelength value. It then develops itself to understand

which wavelength leads to less attenuations, the weather conditions being determined from a visibility model [4.25] are generated in *MATLAB*, and covering up to 3Km distance between the transceivers of the optical wireless system.

4.3.1.1 Simulation Results: GA Selection for Visibility Range Up to 2000m

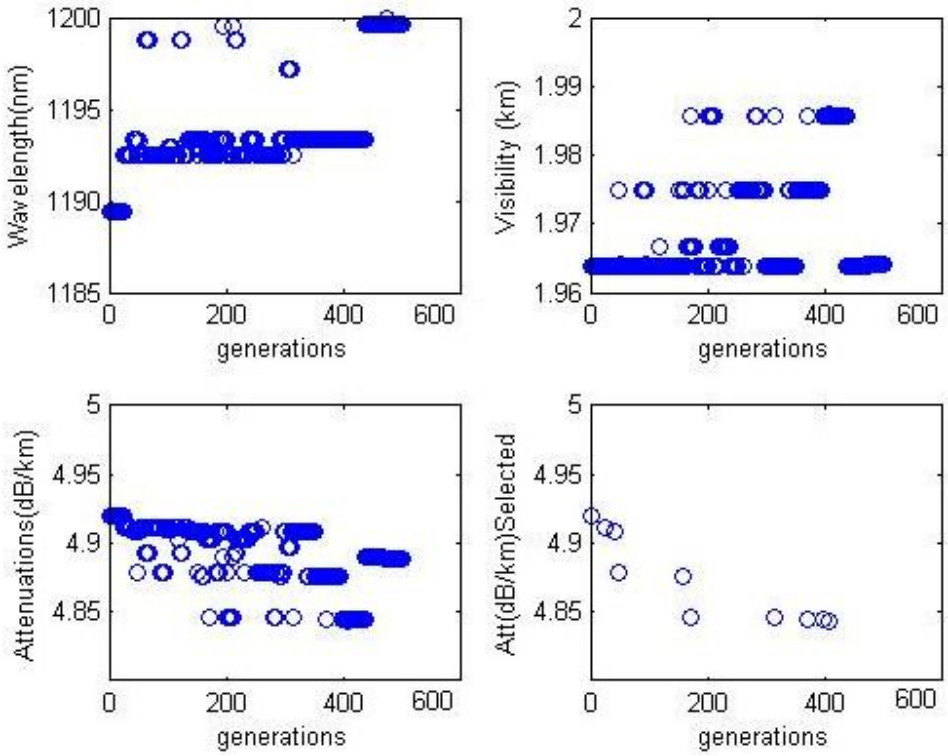

Figure 4.6 Near Infrared (NIR) Signal (V~ 2000m), Selected Wavelength=1190nm.

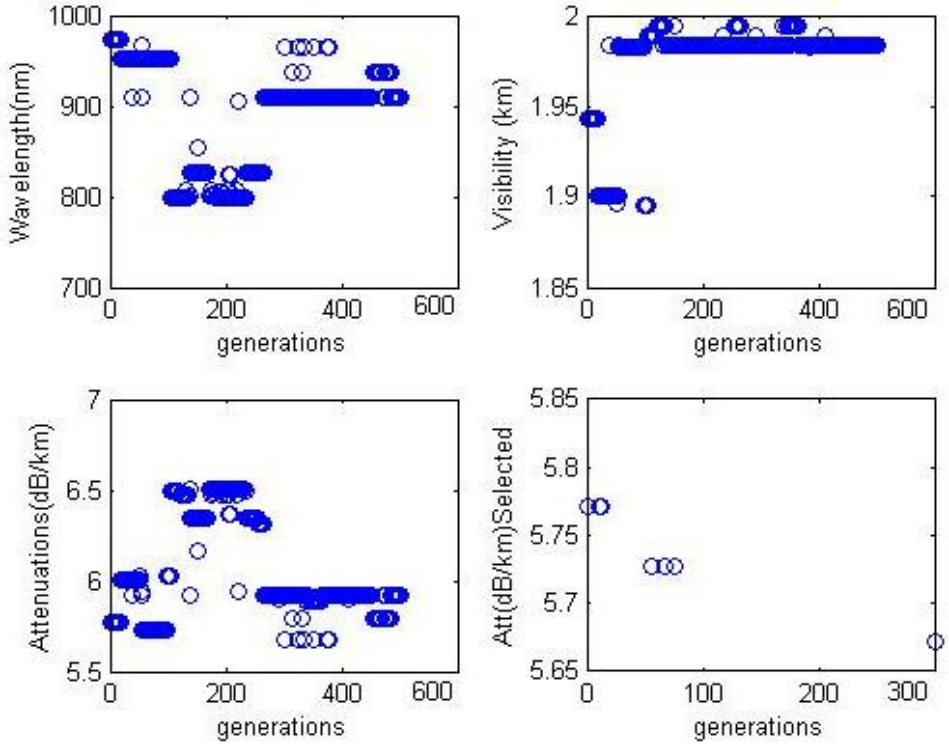

Figure 4.7 Near Infrared (NIR) Signal (V~ 2000m), Selected Wavelength=965 nm.

4.3.1.2 Simulation Results: GA Selection for Visibility Range Up to 1000m

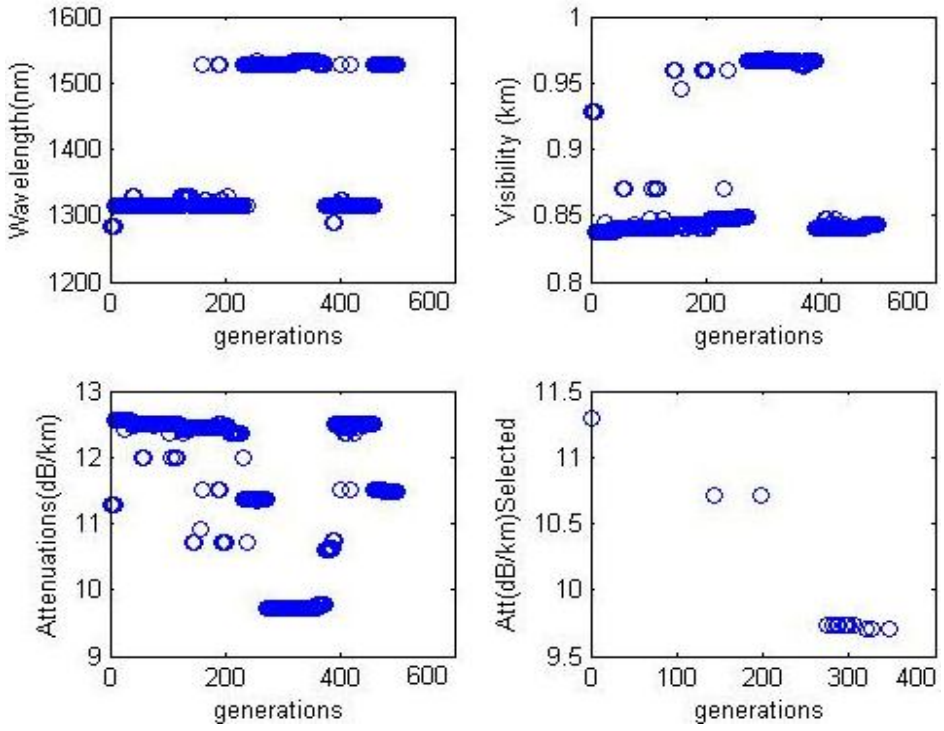

Figure 4.8 Short Infrared (SIR) Signal (V~ 980m), Selected Wavelength = 1534nm.

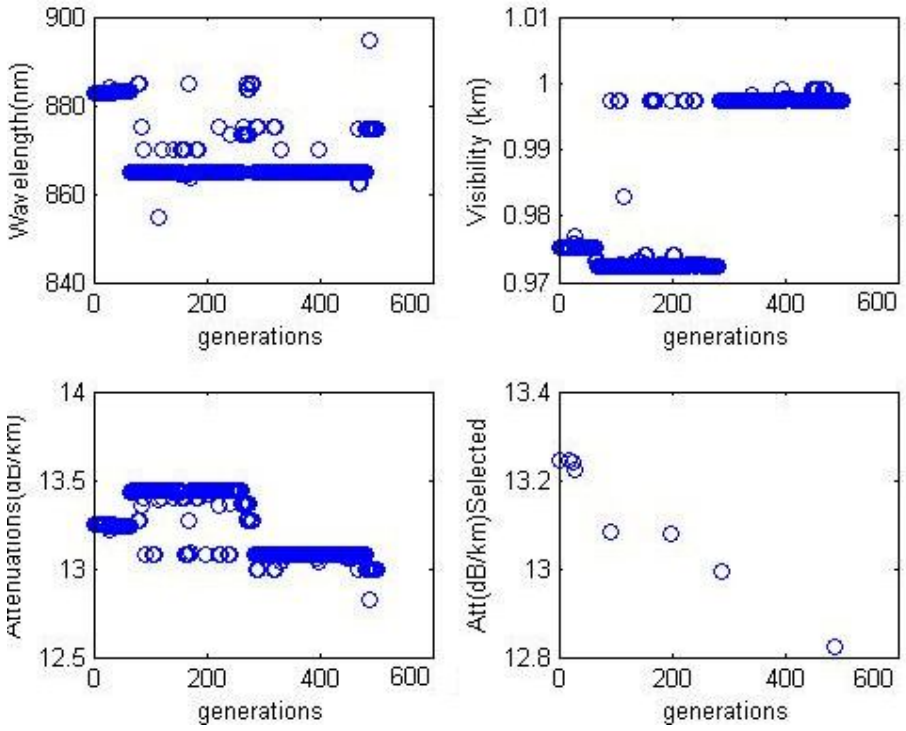

Figure 4.9 Near Infrared (NIR) Signal (V~ 980m), Selected Wavelength = 894.88 nm.

4.3.1.3 Simulation Results: GA Selection for Visibility Range Up to 100m

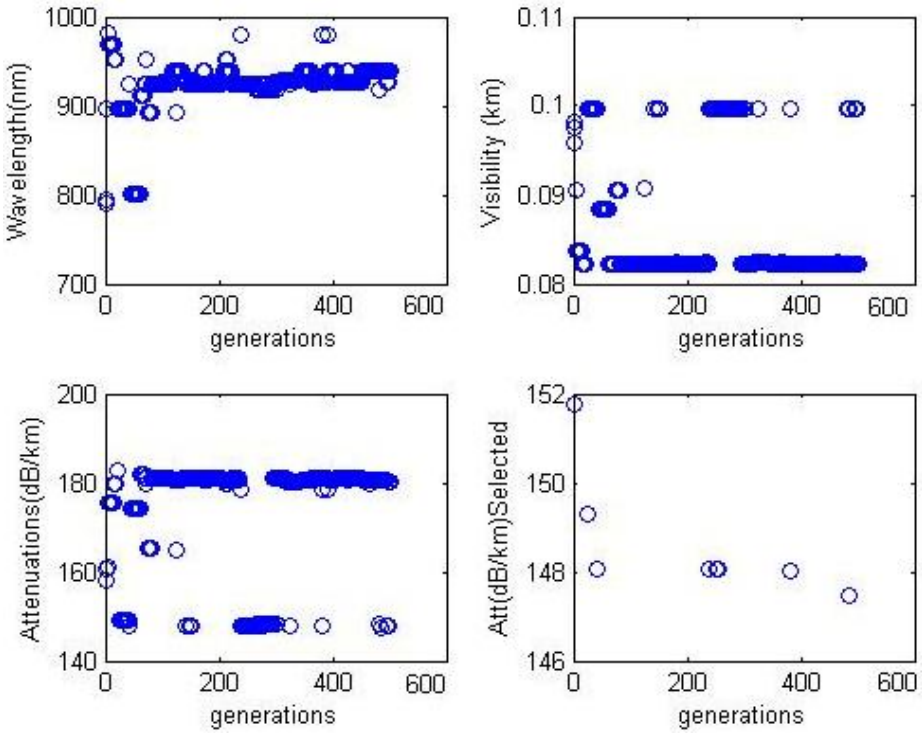

Figure 4.10 Near Infrared (NIR) Signal (V~ 100m), Selected Wavelength = 938 nm.

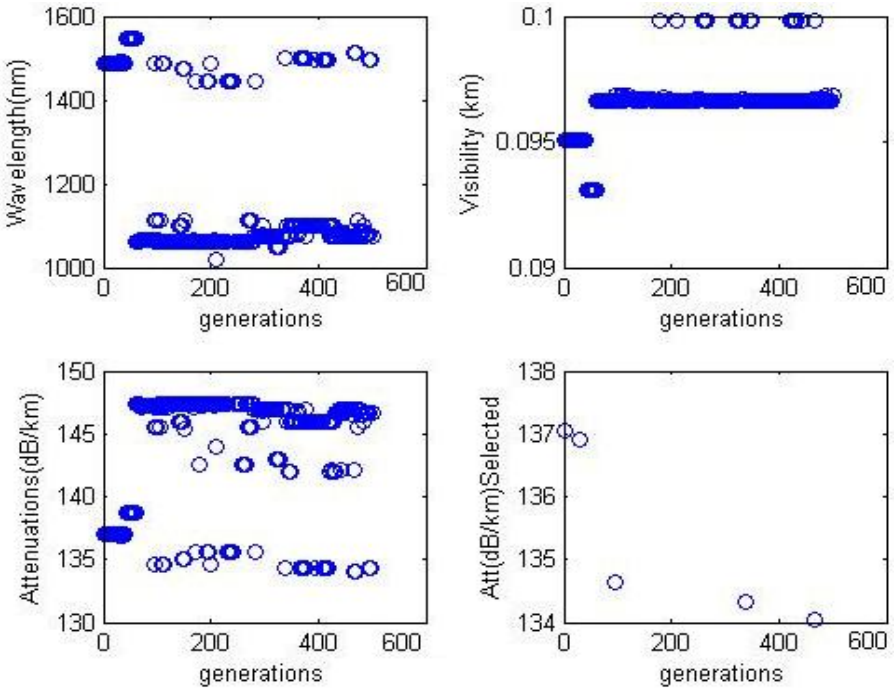

Figure 4.11 Short Infrared (SIR) Signal (V~ 100m), Selected Wavelength = 1510 nm.

4.3.2 Analysis of Results

A genetic algorithm (GA) used from the *MATLAB* 2011a Tool box, and a user defined fitness function utilising the code of visibility have been used to output figures (4.6-4.11). It is a method for solving both constrained and unconstrained optimization problems based on a natural selection process that imitates biological evolution. The algorithm repeatedly modifies a population of individual solutions of wavelength, visibility, and total attenuations. At each step, the genetic algorithm randomly selects individuals from the current population and uses them as parents to produce the children for the next generation. Over successive generations, the population "evolves" toward an optimal solution chromosome that contains 2genes; the wavelength, the visibility, and the attenuation is calculated from the fitness function of each chromosome.

Table 4.2 Compensation of Attenuation at GA-Selected Wavelengths.

Simulation	1	2	3	4	5	6
Compensation	~0.5dB	~0.5dB	~1.7dB	~0.5dB	~4dB	~4dB

The GA selection takes into consideration the selection in two categories: wavelengths near 800 nm are known as near infrared (NIR), and wavelengths near 1550 nm are known as short infrared (SIR). Laser beams at the infrared range pass through the cornea and lens and is focused onto a tiny spot on the retina (figure 4.12). Because the retina has no pain sensors, the collimated light beam entering the eye concentrated by a factor of 100,000 times when it strikes the retina, could permanently damage the eye before the victim is aware that hazardous illumination has occurred. The danger of using IR wavelengths imposes restriction on the laser power used for transmission. The GA algorithm selects the wavelength leading better link margin but adds the obligation that the link should be established at very high altitude with continuous upgradeability. Therefore, optical wireless systems allow 50 times greater intensities of wavelengths larger than 1400 than wavelengths near 800 nm.

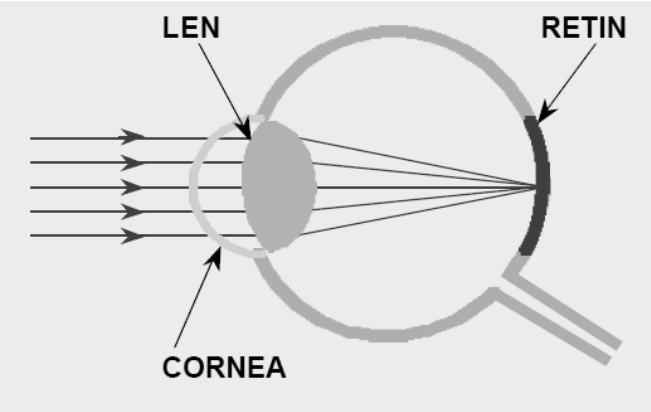

Figure 4.12 Light of $\lambda < 1400$nm focuses on eye retina.

The genetic algorithm based wavelength selection scheme has provided compensation in attenuation for real weather circumstances (Table 4.2), and for extreme foggy weather, the algorithm saves 10dB [4.28]. Such analysis agrees with the fact that light at higher wavelength is less susceptible to noise and interference in the visibility range between 0.5 and 3 kilometres, and that longer wavelengths in NIR signals escape from Mie scattering when the signal wavelength is not very comparable to the diameter of fog particles. Moreover, light at mid- and long-wave infrared suffers from less atmospheric attenuation than near visible light in all weather conditions. For hazy weather (table 4.1), the prediction of less atmospheric attenuation at larger nanometres is most likely true. In foggy weather, when visibility becomes less than 500m, [4.21] stresses that the attenuation is wavelength-independent. However, in the GA-based selection algorithm, it appears that it achieves a compensation of 10dB under foggy conditions [4.28].

The simulation resultsdid not necessarily lead to high availability but proved that the GA has achieved a good compromise for wavelength selection taking into consideration the eye safety and power legislations, which has not been coded in the GA (classes of laser discussed in section 2.4.2). Consequently, it is now worthy expansion of a multi-objective selection algorithm including all external parameters of the outdoors optical wireless channel.

4.4 Implementation of an Application-Specific-Genetic Algorithm

Genetic algorithms suffer from computational complexity and efficiency in real-time applications. Some fitness functions generate weakchromosomes and there's no guarantee that a global optimum is found. Moreover, GA real time applications are limited because of random solutions and convergence. If all the population converges

except one individual, real-time problems may happen. Thus, testing the GA approach is necessary before using it. The time complexity [4.29] [4.30] of GA selection is considered, and a GA-like algorithm that utilizes all the concepts of genetic operators to create appropriate selection, mutation and cross over functions is proposed. A task-oriented algorithm is developed, that selects suitable parameters and monitors the status of the channel at all instances, predicts the bit-error-rate, and proposes an update to the parameters for achieving a better performance.

The selection, crossover, and mutation operators are coded in separate "*m.files*" to implement the operators' tasks discussed in section 4.2. The selection function most appropriate to the model is chosen after testing, and the most appropriate during compilationwasthe tournament function; the mutation (1-point) and cross over (2-points) rates are 0.02 and 0.6 respectively. Although the *MATLAB* tool box is much more powerful, and adds more options to tackle optimization problems with various changing operators, it may impart complexity to a selection problem that depends on sensible understanding rather than on computation. An alternative implementation of a GA tackling a problem of interest is utilized for fast prototyping, showing instantaneous status of the channel, and adding the capability to include channel parameters from completely varied ranges without the constraint of having normalized data sets. Therefore, it is easier to generate random numbers, and then use the mapping function to map each variable to its lower (LB) and upper bounds (UB). The variables form a matrix X, and assigned certain fitness. The analysis shows that the proposed algorithm is reliable and might be benefited for tackling similar problems by adapting the fitness function governing the generated population.

4.4.1 Complexity Problem

Computational complexity of a genetic algorithm is the study of how complex is the algorithm in solving certain problem classes. It is related to time of convergence, rate of space growth, and reliability. Complexity analysis is a method to identify which problem instances are converging to an optimal solution. The discussion in genetic algorithms adds the effect of chromosome size, population size, and fitness function on the processing time, or speed of optimal solution convergence. In this research, the complexity of MATLAB genetic algorithm toolbox to select parameters in the optical wireless channel is considered. The ASGA is proposed to select the optimal parameters among datasets supporting various ranges without having the constraint of data normalization and feature scaling. However, a complex-similar algorithm with user-defined genetic operators for the purpose of fast prototyping at certain intended targets is proposed.

4.4.2 Verification Methodology of the ASGA

The parameters to be selected determine the value of the BER at the receiver side of the optical wireless channelcoded by Matlab2011a. Assuming the chromosome size is fixed, the steps taken for evaluating the computational complexity are as follows:

1- Run the program of the ASGA for 10 times at different total attenuations having initially started with 20 solutions, and a population size of 500.
2- Run the same program using genetic algorithm tool box of *MATLAB* 2011a.
3- Calculate the number of reliable solutions in each. Reliability is determined based on the bit-error-rate values (ideally $<= 10^{-9}$) , the lesser value obtained, the more reliable.

4- Calculate the average time needed for convergence of each when both solutions are acceptable.
5- Monitor the convergence time with the population size.
6- Complexity = Number of population reached/ number of populations used in the space * Convergence time.

4.4.3 Simulation Results on Wavelength Selection Problem

For the purpose of fast prototyping and to be able to draw a preliminary conclusion, the problem investigated in [4.28] was studied and results are compared against reliability and complexity of *MATLAB GA* Toolbox (in Chapter 5). The problem considers the selection of the most appropriate transmission wavelength of low power infrared lasers, and the international code of visibility presented in [4.25] has been adapted for channel modelling. The ASGA is able to show the channel performance at any instant, and it has the ability to monitor the percentage improvement at subsequent iterations as shown in figure 4.13 (attenuations versus generations) giving more interest at higher wavelengths (1000nm-1500nm) that are more eye-safe. Both approaches led to acceptable results, and assured that the ASGA is capable to tackle the problem with similar complexity and reliability, published in [4.28]. The algorithm is extended to include all parameters in chapter 5 and a detailed comparison of complexity and reliability appears in Table 5.5.

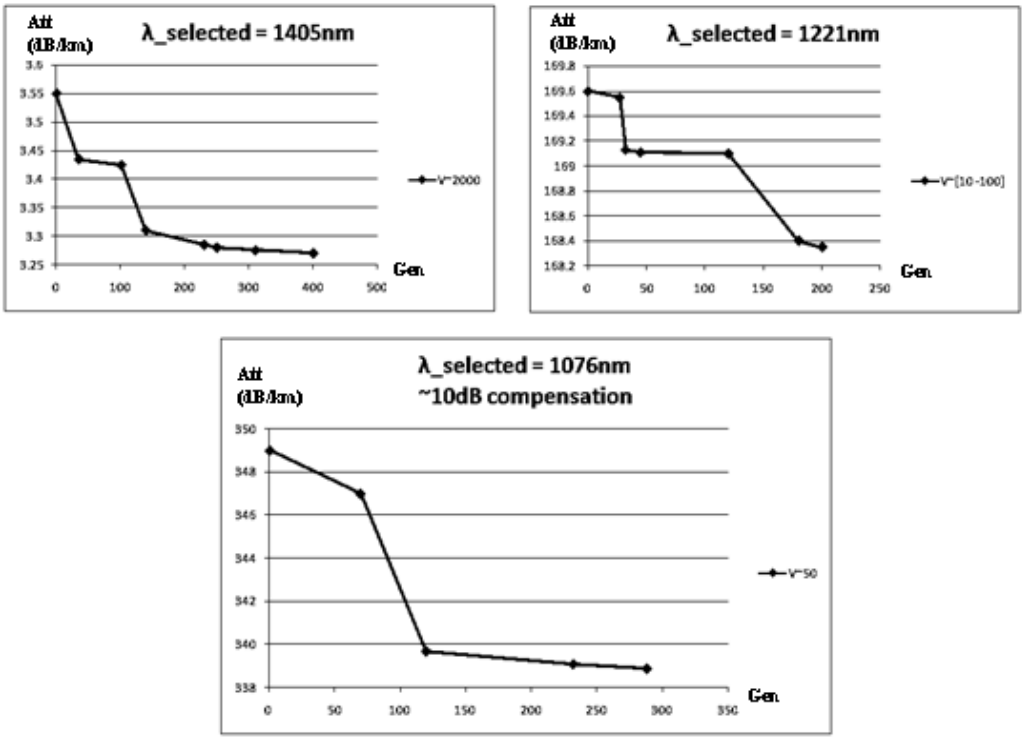

Figure 4.13 ASGA for wavelength selection of low power laser systems operating between 700nm to 1600nm in different weather conditions (Haze, Haze-Fog, and Fog).

4.5 Conclusion

This chapter has shown a new way of selecting the transmission wavelength for various weather conditions. The results achieved appear to be very realistic and it increased the confidence such that the work could be developed so that the selection algorithm can then use many other parameters. In chapter 5, the proposed application-specific genetic algorithm (ASGA) is utilized, for selecting the overall parameters of the optical wireless channel. The algorithm is built to select the optimal parameters under certain weather conditions and link characteristics that would result in a minimum fade margin and hence; larger space for control.

References:

[4.1] C. W. Ahn, R. Ramakrishna, “A genetic algorithm for shortest path routing problem and the sizing of populations”,*IEEE Transactions on Evolutionary Computation*, vol. 6, no. 6, pp. 566 – 579, Dec. 2002.

[4.2] G. Yan, “Design of qosanycast network cluster balance based on genetic algorithm”,*in Proc. International Conference on Signal Processing Systems*, pp. 610 –614, May 2009.

[4.3] J. Arabas, S. Kozdrowski, “Applying an evolutionary algorithm to telecommunication network design”,*IEEE Transactions on Evolutionary Computation*, vol. 5, no. 4, pp. 309 –322, Aug. 2001.

[4.4] S. Ullah, F. Karray, J. -M. Won, “Non-dominated sorting evolution strategy-based k-means clustering algorithm for accent classification”,*in Proc. International Conference on Pattern Recognition*, pp. 1 –4, Dec. 2008.

[4.5] S. Yang, H. Cheng, F. Wang, “Genetic algorithms with immigrants and memory schemes for dynamic shortest path routing problems in mobile ad hoc networks”, *IEEE Transactions on Systems, Man, and Cybernetics*, vol. 40, no. 1, pp. 52 –63, Jan. 2010.

[4.6] H. Sayoud, K. Takahashi, B. Vaillant, "Designing communication network topologies using steady-state genetic algorithms", *IEEE Communications Letters*, vol.5, no.3, pp.113-115, Mar. 2001.

[4.7] C.-S.Lee, S.-M.Guo, C.-Y. Hsu, "Genetic-based fuzzy image filter and its application to image processing", *IEEE Transactions on Systems, Man, and Cybernetics, Part B: Cybernetics*, vol.35, no.4, pp.694-711, Aug. 2005.

[4.8] M.M. Rizki, M.A. Zmuda, L.A. Tamburino, "Evolving pattern recognition systems", *IEEE Transactions on Evolutionary Computation*, vol. 6, no. 6, pp. 594-609, Dec. 2002.

[4.9] C. Ming, Y. Zhengwei, "Classification Techniques of Neural Networks Using Improved Genetic Algorithms", *in Proc. Second International Conference on Genetic and Evolutionary Computing (WGEC08)*, pp.115-119, 2008.

[4.10] D. E. Goldberg, "Genetic Algorithms in Search, Optimization and Maching Learning", *Addison-Wesley publishing company*, INC, 1989.

[4.11] J. Zhang, H. S.-h.Chung , W.-L. Lo , "Clustering-Based Adaptive Crossover and

Mutation Probabilities for Genetic Algorithms", *IEEE Transactions on Evolutionary Computation*, vol. 11, no.3, pp. 326-335, June 2007.

[4.12] K. Man, K. Tang, S. Kwong, "Genetic Algorithms :Concepts and Designs", *Springer*, London, 1999.

[4.13] K. De Jong, W. Spears, "A formal analysis of the role of multi-point crossover in genetic algorithms", *Annals of Mathematics and Artificial Intelligence*, vol. 5, no. 1, pp. 1–26, 1992.

[4.14] Y. Rahmat-Samii, E. Michielssen, "Electromagnetic optimization by genetic algorithms", *John Wiley&Sons*, New York, USA, 1999.

[4.15] M. Mitchell, "Review of L. D. Davis Handbook of Genetic Algorithms", *Van NostrandReinhold*, New York, 1991, Available: <http://web.cecs.pdx.edu/~mm/davis-review.pdf>, Accessed: [21st June 2012].

[4.16] T. Mitchell, "*Machine Learning"*, *McGraw Hill*, 1997.

[4.17] P. Kruse, et al., "Elements of Infrared Technology", *John Wiley & Sons*, New

York, 1962.

[4.18] Mc. B. Arthur, E. Korevaar, "Comparison of laser beam propagation at 785nm and 1550 nm in fog and haze for optical wireless communications", *in Proc. Of SPIE*, Vol. 4214, 2001, 26-37.

[4.19] P.L. Eardley, D.R. Wisely, "1 Gbit/s Optical Free Space Link Operating over 40 m Systems and Applications", *IEEE Proceedings in Optoelectronics*, 143(6), 330–333, 1996.

[4.20] M.W. Madea, et al. "The effect of four-wave mixing in fibres on optical frequency-division multiplexed systems, *Journal of Lightwave Technology*, vol. 8. pp. 1402-1408, Sept. 1990.

[4.21] I. I. Kim, B.McArthur, E. Korevaar , "Comparison of laser beam propagation at 785 nm and 1550 nm in fog and haze for optical wireless communications", *in SPIE Proceedings Vol. 4214, Optical Wireless Communications III, pp.26-37*, CA 92121, 2001.

[4.22] R.G. Smith, S.D. Personick, "Receiver design of optical fiber communications systems", in Semiconductor Device for Optical Communication, *H. Kressel, Ed., New York: Springer-Verlag*, 1980.

[4.23] D. Giggenbach, and H. Henniger, "Fading-loss assessment in atmospheric freespace optical communication links with on-off keying,",*Optical Engineering*, vol. 47, April 2008, pp. 046001-1 - 046001-6.

[4.24] S. S. Muhammad, B. Flecker, E. Leitgeb, M.Gebhart, "Characterization of fog attenuation in terrestrial free space optical links," *Optical Engineering*, vol. 46(6), June 2007, pp. 066001.

[4.25] R. R. Iniguez, S. M. Idrus, and Z. Sun, "Atmospheric transmission limitations," in Optical Wireless Communications - IR for Wireless Connectivity London: *Taylor & Francis Group*, LLC, 2008, p. 40.

[4.26]M.A.Bramson, "Infrared Radiation, A Handbook for Applications", *Plenum Press*, 1969, p.602.

[4.27] A. Rehman, S. Muhammad, "Statistical Analysis of Received Signal Strength in Fog Using Sliding Window Technique for FSO Links", *8th International Conference on Frontiers of Information Technology*, Islamabad, Pakistan, December 21-23, 2010.

[4.28] A. El. Yakzan, R.J. Green and E. L. Hines, "A Genetic Algorithm based Selection of a Transmission Wavelength in the LOS Optical Wireless Channel", *International Conference on Transparent Optical Networks*, University of Warwick, UK, July, 2012.

[4.29] F. G. Lobo, D. E. Goldberg, and M. Pelikan, **"**Time complexity of genetic algorithms on exponentially scaled problems"**,** in Darrell Whitley et al., editors, *Proceedings of the Genetic and Evolutionary Computation Conference (GECCO-2000),* pages 151-158, Las Vegas, Nevada, 2000. Morgan Kaufmann.

[4.30] B. Rylander, J. Foster, "Computational Complexity and Genetic Algorithms", *Proceedings of the World Science and Engineering Society's Conference on Soft Computing*, USA, 2001.

CHAPTER V: An Application-Specific Genetic Algorithm for Link Parameter Selection

5.1 Introduction

In this chapter, the proposed algorithm has reliability, with the ability of using defined GA operators that are customized to a specific problem so as to find its optimum solution. The system provides flexibility to make an efficient selection problem. Moreover, it is adaptable, where the program features are based on probabilistic approaches. It does not require substantial mathematical calculations but sensible parameter selection that satisfy the fitness function with global optimum under different channel characteristics. The system is robust in finding feasible solutions, and could be considered for similar applications. The ASGA has proved its ability to re-allocate the costs of transmission in the LOS optical wireless channel by studying the environmental effects on each of the internal link parameters and the intended BER required at the receiver photodiode. The system could be used at pre-installation stage, where the designer has knowledge about the channel restrictions; it can also be used at run-time if the system can be supplied with adaptive hardware that re-configures itself according to the ASGA recommendations.

5.2 The Optical Wireless channel Model

In the optical wireless environment, the received power is characterized by:

$$P_r = P_t * G_1 * \rho_1 * LR * G_2 * \rho_2 * L_{misc} \quad (5.1)$$

Where $P_r$and P_t are the peak optical powers of the received and transmitted apertures respectively. The channel is described by system and atmospheric losses. The system losses depend on the manufacturer's specifications of the transceiver designs, and the

link range. G_1andG_2 are the transmitter and receiver gains, determined by the manufacturer's data, LR is system dependent loss (absorption, scintillation), ρ_1 and ρ_2 are the efficiency of the transmitter and receiver, L_{misc}describes the atmospheric losses caused by link range, beam divergence, and scattering. The overall performance of the optical channel is affected by the distance between the transmitter and the receiver. The optical signal propagates in the field, forming a cone shape, as in figure 5.1.

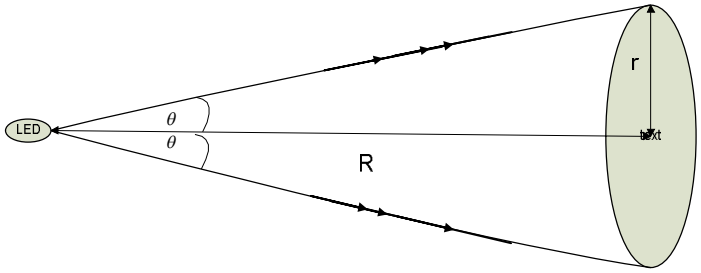

Figure 5.1 Optical signal reception.

The optical signals received form an area $A = \pi r^2$, where $r = Rtan\theta$, and $A = \pi R^2 \tan^2 \theta$. Assuming a uniform transmitted optical field, the power density is a function of the transmitted power and range R, given by: $Power\ Density = \frac{P_t}{\pi R^2 \tan^2 \theta}$ and the received power is $P_r = \frac{P_t . A_{eff(rx)}}{\pi R^2 \tan^2 \theta}$. Therefore the received beams are attenuated by a factor:

$$\alpha_R = \frac{P_r}{P_t} = \frac{A_{eff(rx)}}{\pi R^2 \tan^2 \theta} \tag{5.2}$$

For the optical wireless system to be considered, and for convenience, a square cross-section for the transmitter and also the receiver is considered (Figure 5.2), and the reception of the signal from a distributed source placed at a negligible distance (d_x from the laser diode) is then given by (5.3) [5.1]:

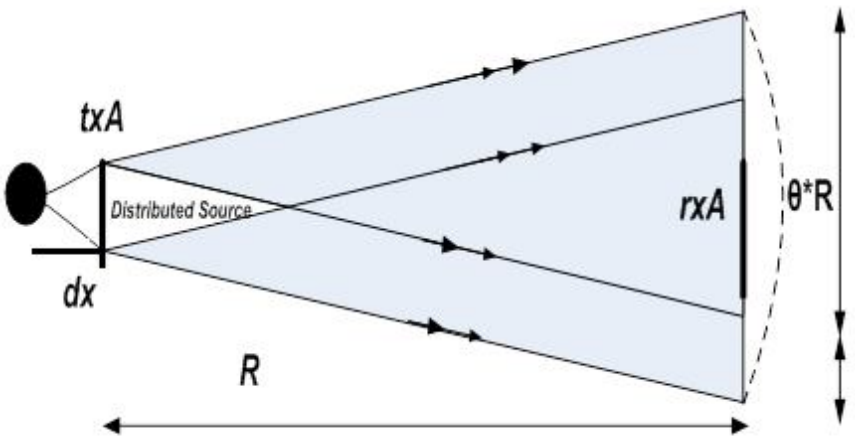

Figure 5.2 Squared Cross sectional Tx-Rx.

$$P_r = P_t \cdot \frac{r_{xA}^2}{((t_{xA} + \theta * R)^2} \cdot 10^{\left(-\alpha \frac{R}{10}\right)} \quad (5.3)$$

Where t_{xA} and r_{xA} are the transmitter and receiver apertures, α is described in (5.5), and θ is the divergence angle. Before introducing the genetic algorithm input/output functionality, the channel model used to describe the *OOK* channel is used in (5.4) starting with some of the parameters, being modeled in "m.files" for the whole practical ranges. It then extends to include several factors especially when the fading channel is introduced, where the genetic algorithm shows powerful combinatorial selections.

$$y = P_t * R_s * \alpha * h * s + n \quad (5.4)$$

Where α, is attenuation due to system loss, scattering over the range R, h is a random turbulence caused by the fading channel(explained in Section 5.4) P_t is the peak transmitted power, $R_s$is the responsivity of the receiver, s is the transmitted signal, 1 or 0, and n is the Gaussian additive noise [5.2][5.3].

The genetic algorithm takes into account the *BER* calculations of an optical channel considered under *OOK* modulation. The effect of inter-symbol interference *(ISI)* in (5.5) at the receiver is less likely to happen ($\alpha_{ISI} = 0$), assuming there's no

multipath effect. The environmental effects on the optical wireless beam are considered, according to:

$$L_{misc} = \alpha_R + \alpha_{sc} + \alpha_h + \alpha_{ISI} \quad (5.5)$$

$\alpha_R$is the effect caused by the transmitter-receiver range and beam divergence in (5.3). $\alpha_h$is a random attenuation considered in section 5.4, modeled as scintillation, presenting the dB version of h. α_{sc} is a deterministic factor caused by scattering due to fog and rain discussed in chapter 4.

The wavelength of electromagnetic wave has a theoretical relation with the responsivity of the receiver, given by [5.4]:

$$Rs\ (\lambda) = \frac{QE.q}{hc}\ .\lambda \quad (5.6)$$

Where QE is the quantum efficiency (ideally QE =1), q is the electron charge, c is the velocity of light($3x\ 10^{\ 8}\ m/s$), and h is Planck's constant (h =$6.626x\ 10^{\ -34}\ W$). However, in practical applications, this relation depends on the type of the photodiode and it is not linear. In this thesis, a look-up table is considered, which allows a general compromise when optical to electrical conversion is applied under optimum quantum efficiency.

Table 5.1 Responsivity of the Optical Receiver vs. Transmission Wavelength.

Wavelength (nm)	Responsivity (A/W)
200	0.161
300	0.242
400	0.323
500	0.403
600	0.484
700	0.565
800	0.645
900	0.726
1000	0.806
1100	0.887

The selection of different transmission wavelength by the ASGA is determined by the selected responsivity of the receiver (table 5.1), and their effect on the received power could be approximated in dB/km according to figures 5.3 and 5.4, as shown below.

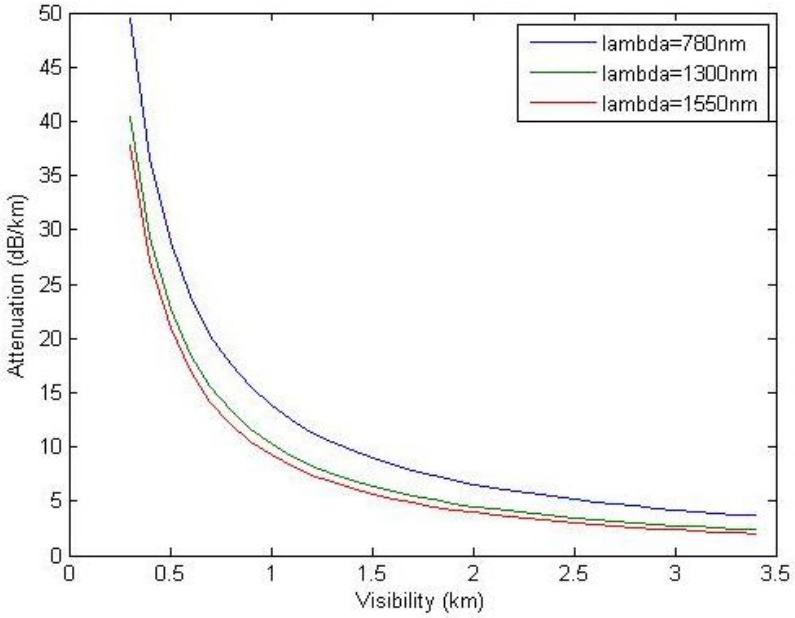

Figure 5.3 Matlab Simulation of Different Wavelength Attenuations (V<1km).

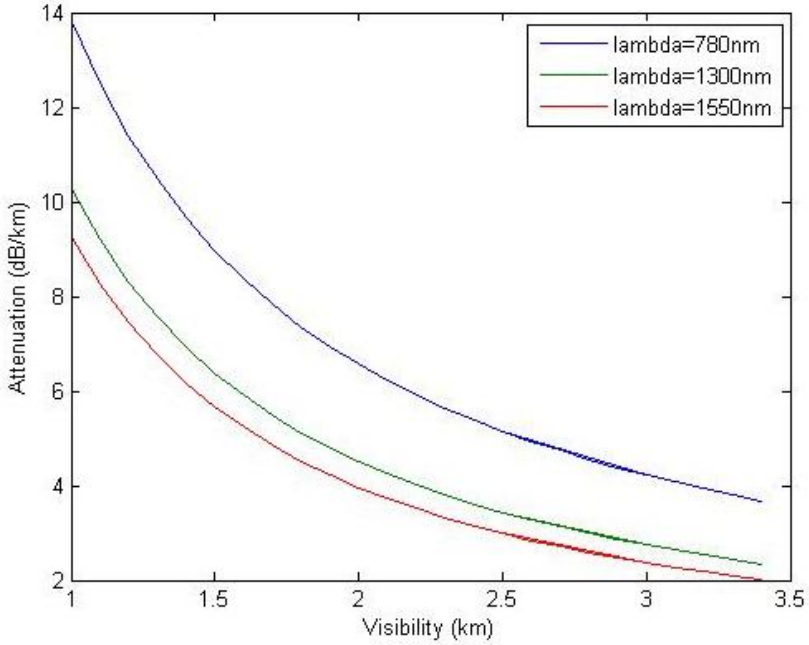

Figure 5.4 Matlab Simulation of Different Wavelength Attenuations (V>1km).

System performance will be controlled for an acceptable link margin (5.7), where a GA-based parameter selection is deployed to seek the parameters that maximize the link margin considered in Equation (4.5).

$$M[dB]_{AWGN} = P_r - P_s - \alpha_{G,R,sc} \tag{5.7}$$

$P_s$is the required peak power at the receiver to achieve a considerable *BER*, and $\alpha_{G,R,sc}$ is the system, range, and deterministic atmospheric losses.

5.3 Channel Performance under the Effect of Additive White Gaussian Noise (AWGN)

The link performance of an OOK channel during dark effects can be described by the Signal-to-noise ratio at the receiver with the effect of additive white Gaussian noise, given by:

$$SNR = \frac{i_{p1}^2 - i_{p0}^2}{\sum {\sigma_1}^2 + \sum {\sigma_0}^2} \tag{5.8}$$

Where $i_{p1} - i_{p0}$ are the photocurrents generated by OOK '1' and '0', $\sum {\sigma_1}^2 \; and \; \sum {\sigma_0}^2$are the noise variances caused by a corresponding transition (1 or 0 data). A BER calculation is performed depending on the received signal, which in turn is related to the transmitted signal, the channel attenuations, and the responsively of the receiver. A system metric called the Q factor is defined, and the corresponding BER is calculated according to:

$$BER = 0.5 \; erfc\left(\frac{Q}{\sqrt{2}}\right) \tag{5.9}$$

Where $Q = \frac{i_{p1} - i_{p0}}{\sqrt{\sigma_1^2 + \sigma_0^2}} = \sqrt{SNR}$, the received power in OOK for the low bit is considered zero, the photocurrent generated by logic zero is $I_0 = R_s P_0 = 0$; with $P_t = \frac{P1}{2}$, the signal-to-noise ratio becomes [5.5].

$$SNR_{AWGN\,(lossless)} = \frac{(R_s P_1)^2 - (R_s P_0)^2}{\sigma_1^2 + \sigma_0^2} = \frac{(2\,R_s P_t)^2}{\sigma_1^2 + \sigma_0^2} \qquad (5.10)$$

Knowing the attenuations modeled according in chapter 4 with the sets in Table 4.1, and replacing P_1 with $2P_t$, and I_1 with $2R\,P_t$, the signal-to-noise ratio in a lossy channel during darkness is represented by:

$$SNR_{AWGN} = \frac{4\,R_s{}^2 (P_t\ \alpha_{G,R,sc})^2}{\sigma_1^2 + \sigma_0^2} = \frac{4\,R_s{}^2 P_r{}_x{}^2}{\sigma_1^2 + \sigma_0^2} \qquad (5.11)$$

Where P_{rx} is the peak received power, R_s is the optical-to-electrical conversion (responsivity), $\alpha_{G,R,sc}$ is defined in (5.8), σ_1 and σ_0 depend on the noise bandwidth, and they can be expressed as the sum of two *AWGN* additive noises of shot noise and thermal noise of the photodetector[5.6], [5.7], and are further discussed in section 5.6. The bit error rate is calculated based on maximum likelihood sequence detection in due to perfect channel state information at the receiver (CSI).

$$\sigma_1 = \sqrt{2\,qB_{eq}\,I_1 + \sigma_n^2} \qquad (5.12)$$

$$\sigma_0 = \sqrt{2\,qB_{eq}\,I_0 + \sigma_n^2} \qquad (5.13)$$

I_1 and I_0 are the high and low currents of the signal, assuming no ambient light effects during dark. σ_n is the standard deviation of the Gaussian noise current due to thermal noise at the photodiode receiver and has a direct relation to the equivalent noise bandwidth, Boltzmann's constant, absolute temperature, and the resistor load at the photodetector ($i_n = \sqrt{\frac{4K_B T B_{eq}}{R}}$).

A perfect band-pass filter *(BPF)* is assumed, within this pass-band rectangular response, all the power is passed inside, and the noise density (typically in dBm/Hz) will be zero outside of the band and a fixed value within it, and it is estimated by $P_{dBm}=10\ log_{10}(K_B T B_{eq})$. Therefore, the noise equivalent bandwidth could approximate the signal bandwidth. The thermal noise power versus the selected bandwidth considered by the GA selection process, at room temperature ($T = 298K$) is revealed in Table 5.2. The bit rate has direct relation to the maximum bandwidth used in *OOK* modulation, defined as $BW = B_r/2$ for optimally shaped pulses.

$$BER = 0.5\ erfc\ (\sqrt{(SNR/2)}\ ) \qquad (5.14)$$

Table 5.2 Thermal Noise Power and Bandwidth Relation.

Thermal Noise Power (dBm)	Bandwidth (Hz)
-174	1 Hz
-164	10 Hz
-154	100 Hz
-144	1 Khz
-134	10 Khz
-124	100 Khz
-120.98	200 KHz
-114	1 MHz
-111	2 MHz
-106	6 MHz
-101	20 MHz
-98	40 MHz
-84	1GHz

5.4 Channel Performance under Dynamic Turbulence

Laser beam deformation is highly caused by the changes in the refraction index of medium in an area known as the *Fresnel zone*. It is modeled as a scintillation effect, which hinders efficient laser beam propagation, and ultimately causes fluctuation of

the receiver end signal. The attempts presented in [5.8], [5.9], [5.10] show that the scintillation index is modeled using a *gamma-gamma* or *K-distribution*. Such distribution functions are mathematically complicated, and could estimate strong channel turbulence. However, a lognormal distribution function is used in this model to describe the amplitude fading and show dynamics in the received power. In theory, if X is considered to be a positive random variable, and Y = $log_e X$ has a normal distribution, then X is lognormally distributed with density function [5.11], given by:

$$f(x;\ \mu;\ \sigma^2) \quad = \frac{1}{x\sqrt{2\pi\sigma}} \exp[-\frac{1}{2\sigma^2}(log_e\, x - \mu\ )^2] I_{(0,\infty)}(x)$$

$$where\ -\infty < \mu < \infty\ ,\ \sigma > 0 \tag{5.15}$$

If X has $m = e^{2\mu+\frac{1}{2}\sigma^2}$, and $v = e^{2\mu+2\sigma^2} - e^{2\mu+\sigma^2}$, then $E[log_e X] =$ μ and $[log_e X] = \sigma^2$. Now, h models the turbulence in the channel between the transmitter and receiver apertures. The attenuation effect caused by turbulence is considered along with (5.2), assuming perfect alignment of both ends, with the receiver underinvestigation forthe channel using Channel state information (*CSI*). The fading coefficient represents the random turbulence caused by scintillation index σ_x. These parameters are randomly modeled in Matlab2011a, $P_{rx}\ and\ I_1$ in (5.11) are affected by the fading channel *(h)*; therefore, *SNR* is now expressed in (5.17), *BER* calculation still refer to (5.14), and the link margin takes the shape of (5.18). Therefore, from (5.15) using conclusions of [5.11], it may be said that:

$$f(h) = \frac{1}{h\sqrt{2\pi\sigma}} \exp(\ -\frac{(\ln(h)-\mu)^2}{2\sigma^2}\ ) \tag{5.16}$$

$$SNR_h = \frac{4\ R_s{}^2 (P_t * \alpha_{G,R,sc} * h)^2}{\sigma_1^2+\sigma_0^2} \tag{5.17}$$

$$M[dB]_{AWGN,h} = P_{mrx} - P_s - \alpha_{G,R,sc} - \alpha_h \tag{5.18}$$

Denote by σ^2, the normalized variance of the intensity that is used to describe scintillation, the expectation value of the received value *E[H]* as a function of σ^2 becomes [5.11, 5.12]:

$$E[H] = \exp(\mu + \frac{\sigma^2}{2}) \tag{5.19}$$

$$Var[H] = \exp(2\mu + \sigma^2)\exp(\sigma^2 - 1) \tag{5.20}$$

Therefore, the so-called general scintillation index is:

$$\sigma_S^2 = \frac{Var[h]}{E[H]^2} = \exp(\sigma^2 - 1) \tag{5.21}$$

Now, if the effect of σ^2 on the received power following a lognormal distribution is to be studied, it should be substituted by the variance of the received power, and this is what is called a power scintillation index$\sigma_x{}^2$. Therefore, all received power values are normalized to the peak value P_r. The parameters of the lognormal distribution become, $\sigma^2 = \ln(\sigma_x{}^2 + 1)$ and $\mu = -\frac{\sigma^2}{2}$.

In a turbulent channel, scintillation increases with scattering effects causing the light to deflect from the main beam. As turbulence becomes stronger, it can deflect the beam light again to the main beam as shown in figure 5.5[5.12].

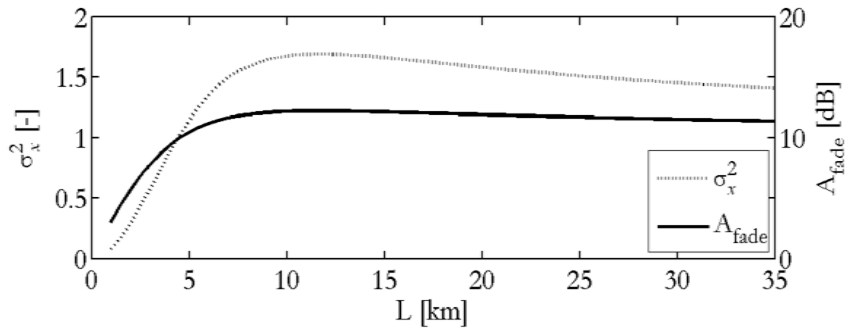

Figure 5.5 Effect of Power Scintillation Index on Fade Margin.

At this level, an analysis approached by [5.12] is utilized, where an outage probability is considered, and its parameters. The result in figure 5.5 describes a fading range as a function of scintillation due to different outage probabilities (5.22), and shows that, for moderate outage requirements (>10^{-3}) with turbulence saturation and aperture averaging, the loss will rarely exceed 13 dB. The system completely fails when there's no acceptable link margin ($M[dB]_{AWGN,h} < 0$).

$$\alpha_h = -4.343(\sqrt{2\ln({\sigma_x}^2 + 1)}.erfc^{-1}(2P_B - 1) - \frac{1}{2}\ln({\sigma_x}^2 + 1)) \qquad (5.22)$$

5.5 An ASGA for Optical Wireless Link Parameters

The optical wireless Layer in the short range LOS channel is subject to time-variant environmental challenges. There several internal and external factors that determine the overall channel performance discussed before, are considered for the channel model. In this section, single and multi-objective selection techniques are proposed, based on OOK modulation for the purpose of data survivability in the optical wireless channel, taking into consideration many variables such as: peak transmission power/laser, number of laser, transmitter beam divergence, diameters of transmit and receive apertures, the receiver sensitivity, deployment distance, the deterministic weather, effect of scattering, attenuation caused by scintillation, electrical bandwidth of the signal, its wavelength, and the bit rate. Although the approach targets one output, the terms of single and multi-objective selections are used to explain that one or many input parameters can be considered for selection, depending on the channel constraints.The parameters will be generated for a large number of combinations covering the whole ranges, some of which will be chosen to be fixed for the first stage approaches. The overall purpose is to be able to design a multi-objective selection scheme, which takes into consideration the optimum values

of all parameters, and a single-objective scheme when the channel is constrained to fix all parameters except one. The block diagram of the system appears in figure 5.6.

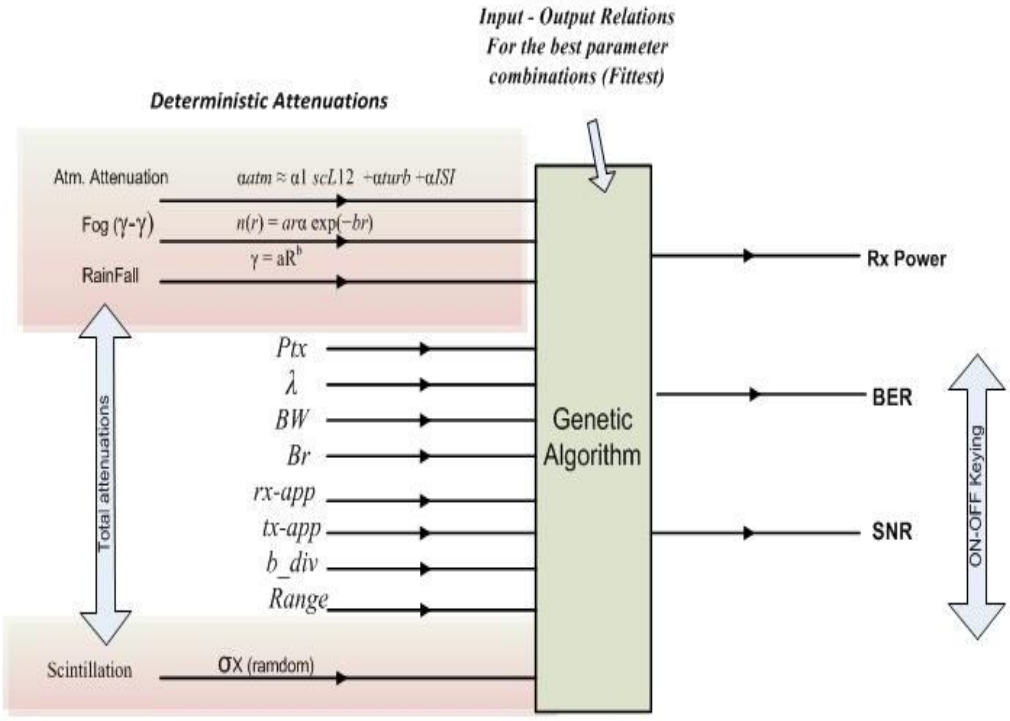

Figure 5.6 GA-based Selection Algorithm of Optical Wireless System.

An attempt with genetic algorithms to select an appropriate transmission wavelength has been published in [5.13]. Genetic algorithms, targeting the LOS optical channel, investigate all the ranges of link parameters, and seek to provide good, approximate solutions to such a combinatorial selection problem. The problem has been tried by an alternative binary search, under the same operating system specs, and has taken about 29 minutes of compilation in Matlab2011a, to select out the needed parameters. However, a code utilizing the idea of genetic algorithms, takes few seconds to do the intended purpose. Based on the characteristics of Darwinian evolution and the different models discussed before, the GA uses all the combinations of link parameters to predict the performance of the optical channel.

The GA fitness function targets different attenuations in *AWGN* (darkness) and fading channels (day light), then proposes a minimum cost of inputs that will optimize the overall channel performance and still produce an acceptable bit rate. The program uses 20 solution sets, each parameter constitute a gene of a chromosome.

5.5.1 System Flowchart and Methodology

The system flow chart appears in figure 5.7. It starts by generating an initial population that consists of *20* individual solutions; it then evaluates the fitness value of each individual by calculating *SNR* at the receiver, and then the *BER* using the error complementary function. The parameters are selected so that they comply with their industrial ranges [5.14]; and they consequently form different genetic material of a chromosome. Cross over and mutation functions are applied, and then the fitness function of each offspring is evaluated. ASGA selects the chromosomes leading highest SNR, or lowest BER, and transfers to the next generation by using a user-defined selection method (adapted from Tournament [5.15]). Finally, the selected individuals (parameters) are returned to the population and the generation is incremented, looping back to the parameter selection.

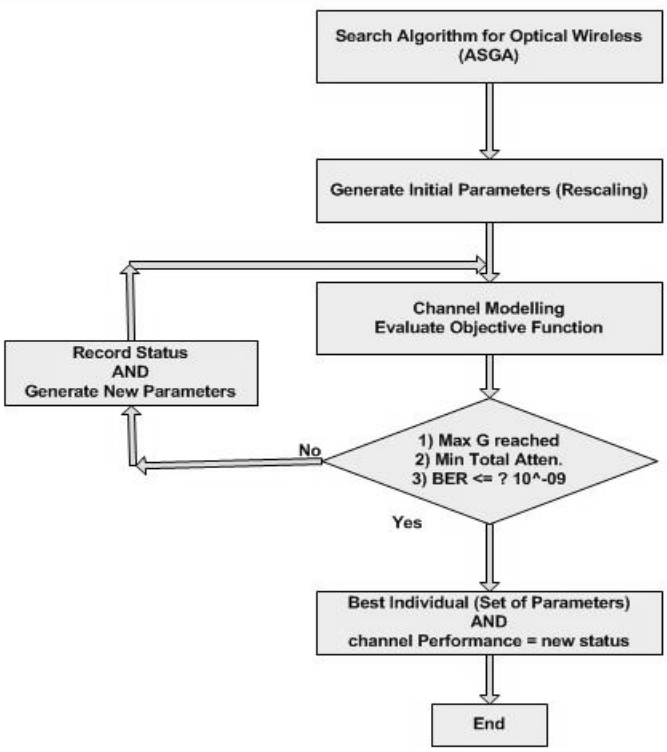

Figure 5.7 The ASGA Flow Chart.

The ASGA is targeted to select the optimal parameters of the optical wireless system of variable lower and upper bounds such as: transmitter aperture *(tx_app)*, beam divergence *(b_div)*, receiver (aperture), transmitted power *(Pt)*, responsivity of the receiver(*Rs*), wavelength *(λ)*, total attenuations (*α_sc*), Range (R), electrical bandwidth *(BW)*, and FVAL*(BER)*. The generated noises considered by the ASGA at the receiver photodiode are discussed in section 5.6. The steps followed in the methodology of the ASGA are:

1) Generate random population of 20 chromosomes random solutions (N=20)
2) calculate the fitness of each solution
3) error = FunGen(X), this calculates the BERfor 20 solutions.

$$Min\ \mathrm{P}\ [Selection(\ 0.5\ erfc\ (\ \sqrt{\frac{SNR}{2}}\ )\ ]$$

4) select the solution of parameters with lowest error, Min P [Selection]
5) check the lowest error with the GLOBAL lowest error (FVAL, BER)
6) if current error < (FVAL, BER): GLOBAL SOLUTION = current solution
7) step5: if termination condition has been reached (reached the maximum number of generations or FVAL< Intended BER);

Otherwise: do,

a) selection: to choose the new parents.
b) crossover: to reproduce new offspring , hopefully offspring should have better solutions than their parents.
c) mutation : percentage based -in order to diversify the solutions.
d) Repeat from step2, until Termination condition satisfied or G = 500, STOP

5.5.2 Simulation Results

Simulations of the genetic algorithm based approach were tested during night by varying the amount of attenuation assuming no scintillation and moonlight effects, leaving the choice open for the GA to setup the best parameters at pre-installation stage. It selected optimum parameters by choosing the fittest chromosomes contributing to minimal BER. Another simulation was carried during day light, which emphasized on the scintillation effect in terms of dB/km attenuation.

5.5.2.1 ASGA-Simulation Results during Darkness

Table 5.3 ASGA Simulation during Darkness ($\alpha = 1, 5, 10, 20, 30, 40$).

tx_app (m)	rx_app (m)	b_div (mrad)	tx_P (mW)	Rs (A/W)	α_{sc} (dB/km)	Range(km)	BW (mhz)	α_n^2	G	FVAL (BER)
0.0548	0.2370	1.1242	0.0018	0.4994	1.0497	0.6242	100.25	JOHNSON NOISE LMTD		0.0046
0.1568	0.3926	1.2387	0.0020	0.7909	1.1955	0.9887	100.98			3.8561e-04
0.0749	0.3649	1.1960	0.0018	0.5568	1.0784	0.6960	100.39			8.4986e-07
0.1490	0.3745	1.2108	0.0034	0.7686	1.1843	0.9608	100.92			1.0291e-08
0.1244	**0.3173**	**1.3728**	**0.0030**	**0.6982**	**1.1491**	**0.6228**	**100.75**		**320**	**2.7338e-11**
0.0333	0.2684	1.0475	0.0019	0.4380	4.9285	0.5475	100.10			0.0014
0.1063	0.2753	1.3082	0.0028	0.6465	5.0849	0.5582	100.62			1.8925e-04
0.1412	0.3564	1.4329	0.0033	0.7463	5.1598	0.6829	100.87			7.3632e-05
0.0816	0.3804	1.2199	0.0032	0.5759	5.0319	0.7199	100.44			8.4250e-06
0.0837	0.3855	1.2277	0.0037	0.5821	5.0366	0.7277	100.46			3.6781e-07
0.1474	**0.3709**	**1.4552**	**0.0056**	**0.7641**	**5.1731**	**0.7052**	**100.91**		**364**	**7.3467e-11**
0.0804	0.2152	1.7157	0.0282	0.5726	9.9863	0.9270	100.43			0.1348
0.1293	0.3286	1.8902	0.0472	0.7121	10.0561	0.9963	100.78			9.7681e-04
0.1162	0.2984	1.8437	0.0562	0.6750	10.0375	0.9312	100.69			2.4677e-05
0.0495	0.3572	1.6842	0.0762	0.5474	9.9737	1.0579	100.37			5.8541e-07
0.0639	0.2534	1.7744	0.0732	0.6196	10.0098	0.8342	100.55			2.9309e-10

Table 5.3 ASGA Simulation during Darkness ($\alpha = 1, 5, 10, 20, 30, 40$).

tx_app (m)	rx_app (m)	b_div (mrad)	tx_P (mW)	Rs (A/W)	α_{sc} (dB/km)	Range(km)	BW (mhz)	α_n^2	G	FVAL (BER)
0.0776	**0.3091**	**1.8602**	**0.0948**	**0.6882**	**10.0441**	**0.9543**	**100.72**		**390**	**2.1496e-12**
0.1090	0.2817	2.2452	0.4467	0.6544	19.9908	0.8952	100.64			0.0018
0.1229	0.3139	2.3146	0.7362	0.6941	20.0206	0.9646	100.74			1.1212e-04
0.0940	0.2467	2.1698	0.5301	0.6113	19.9585	0.8198	100.53			3.1778e-06
0.1311	0.3328	2.3553	1.2726	0.7173	20.0380	1.0053	100.79			2.7816e-08
0.1211	**0.3096**	**2.3053**	**1.1940**	**0.6887**	**20.0165**	**0.9553**	**100.72**		**365**	**2.8113e-10**
0.1011	0.1474	2.2056	6.2145	0.7579	29.9738	0.8556	100.58			0.0071
0.0952	0.2495	2.1758	3.0369	0.6148	29.9611	0.8258	100.54			7.7224e-05
0.1247	0.3180	2.3235	7.7301	0.7748	30.0243	0.9735	100.75			5.1936e-06
0.0966	0.1981	2.1831	5.9259	0.7547	29.9642	0.8331	100.55			5.8255e-08
0.1135	0.2920	2.2674	7.0091	0.7668	30.0003	0.9174	100.67			2.5064e-09
0.0950	**0.2491**	**2.1751**	**5.8226**	**0.6143**	**29.9608**	**0.8251**	**100.54**		**402**	**1.6921e-13**
0.0626	0.1435	2.0130	3.7386	0.7304	40.1956	0.8380	100.30			0.3922
0.0941	0.2588	2.5588	17.6473	0.6118	40.4883	0.8206	100.53			0.0065
0.0284	0.2679	1.8418	10.1194	0.7060	39.8776	0.8418	100.06			8.1466e-04
0.1060	0.2798	2.4298	31.9855	0.4397	39.9291	0.8199	100.10			1.7717e-06
0.0209	0.3006	2.1019	19.0012	0.4025	39.8081	0.8012	100.01			4.4095e-08
0.0925	**0.3518**	**2.2553**	**15.1035**	**0.6070**	**40.4728**	**0.8035**	**100.52**		**411**	**6.1029e-10**

JOHNSON NOISE LMTD

5.5.2.2 ASGA-Simulation Results during Day Light

Table 5.4: GA Simulation during Daylight ($\alpha = 10, 20, 30, 40$).

tx_app (m)	rx_app (m)	b_div (mrad)	tx_P (mW)	Rs (A/W)	α_{sc} (dB/km)	Range(km)	BW (mhz)	SN	σ_x	G	FVAL (BER)
0.0449	0.1327	3.3550	2.5976	0.4710	10.0178	1.3550	100. 18	SHOT NOISE LMTD	**2 ~ 6 dB/ Km**	**320**	0.3528
0.0727	0.3597	3.7521	4.3847	0.5504	10.0376	1.7521	100. 38				0.1679
0.1228	0.3136	4.4685	7.6083	0.6937	10.0734	1.4685	100. 73				1.5059e-04
0.1140	0.2933	4.3435	7.0459	0.6687	10.0672	1.3436	100. 67				1.1525e-07
0.0265	0.2526	4.0046	5.2323	0.4186	10.0046	1.0929	100. 05				4.0318e-08
0.1069	**0.2768**	**4.0621**	**8.1045**	**0.6484**	**10.0621**	**1.2418**	**100.00**				**3.5986e-10**
0.0902	0.2381	3.8011	19.508	0.6007	20.0502	1.0036	100. 50				7.6049e-04
0.0910	0.2398	3.8043	25.071	0.6029	20.0507	1.0143	100. 51				5.8347e-05
0.0202	0.2380	3.5010	29.117	0.4007	20.0002	1.0033	100. 00				1.0744e-06
0.1021	0.2655	3.8517	70.614	0.6344	20.0586	1.1722	100. 59				3.6256e-08
0.0996	0.2598	3.8412	69.369	0.6274	20.0569	1.1372	100. 57				7.9808e-09

Table 5.4: GA Simulation during Daylight ($\alpha = 10, 20, 30, 40$).

tx_app (m)	rx_app (m)	b_div (mrad)	tx_P (mW)	Rs (A/W)	α_{sc} (dB/km)	Range(km)	BW (mhz)	SN	σ_x	G	FVAL (BER)
0.0967	**0.2531**	**3.8288**	**67.911**	**0.6192**	**20.0548**	**1.0961**	**100. 55**	SHOT NOISE	**2 ~ 6 dB/ Km**	**364**	**4.2179e-12**
0.0219	0.0794	3.5082	29.965	0.4054	30.0014	1.0272	100. 01				0.482
0.0929	0.2442	2.5207	110.26	0.6083	30.0521	1.0414	100. 52				0.0014
0.0925	0.2433	2.5179	135.53	0.6071	30.0518	1.0018	100. 52				1.11e-07
0.1559	0.3905	2.7207	149.1197	0.7883	30.0971	1.0971	100. 97				1..37e-9
0.1181	**0.3840**	**2.7009**	**141.0277**	**0.6804**	**30.0701**	**1.0701**	**100. 70**			**377**	**1.246e-11**
0.1500	0.3768	2.9286	147.8573	0.7714	40.0929	1.0929	100. 93				0.3456
0.0457	0.2972	1.0918	191.83	0.4734	40.0184	1.0184	100. 18				1.194e-05
0.0820	0.3814	1.2213	222.1330	0.5771	40.0443	1.0443	100. 44				1.8512e-07
0.0258	0.2511	1.0209	270.8348	0.4167	40.0042	1.0042	100. 04				1.6781e-08
0.0694	0.3521	1.1763	277.0532	0.5411	40.0353	1.0353	100. 35				1.2302e-10
0.0780	**0.372**	**1.207**	**278.282**	**0.565**	**40.041**	**1.041**	**100. 4**			**402**	**9.3283e-11**

5.6 Noise Analysis

The term “noise” describes the unwanted random components of an electrical signal that tend to disturb the transmission and processing of the signal; in other words, it refers to any signal present in the receiver other than the desired signal. An understanding of the origins of noise helps to characterize the performance of optical wireless photodetector and defines its sensitivity. The optical signal at the end of an optical link is often highly attenuated, and so any optical detector noise should be as small as possible, to prevent any degradation of the signal quality and put a lower limit on the receiver sensitivity. There are many types of noise source in photodetection referred to as quantum shot noise, dark current, optical background noise, and electronic thermal noise. The major noise sources which can significantly affect the system sensitivity are shot noise, dark noise and thermal noise, as other noise sources are considerably negligible when compared to these. A review analysis of noise sources, especially in semiconductor photodetectors, can be found in [5.16][5.17]. The experimental work makes use of a radiometer at the communications lab of University of Warwick to measure the intensity of ambient light at different day and night times, and analyses the change in noise values under an ultimate performance obtained by using an ASGA [5.18]. The ASGA doesn’t improve the noise effect, but alternatively the overall channel performance. An increase in shot noise doesn’t always mean decay in signal-to-noise ratio at the receiver photodiode if a best fit of link parameters is chosen for the optical wireless channel.

5.6.1 Performance of Johnson and Shot Noises

The performance of Johnson and shot noises in the Line-Of-Sight (LOS) optical wireless channels has been monitored under the supervision of an ASGA. The ASGA achieved

sensible selection requirements of link parameters in different weather conditions and link characteristics, and the changes in thermal and shot noises are recorded correspondingly. A Johnson-noise limited channel is considered during darkness, where the ambient light effect is minimal, and a shot-noise limited channel during daylight.

Noise in the optical receiver is primarily due to shot noise in the photodiode, but there is also noise which is related to dark current, and any other currents flowing through the junction, such as bias current. The random nature of the generation of carriers in the junction yields also a current fluctuation that makes up the shot noise, which result from the random arrival rate of photons from the source of radiant energy under measurement and ambient background illumination (i.e. shot noise is far smaller for optical fibre than for OW). The effect of this process can be represented as a noise source, and can be expressed either as a voltage source or a current source [5.19]. The mean-square value of the shot current for a *pin* photodiode is given by:

$$< i_{sh}^2 > = 2q\big(I_p + I_d\big)B \quad (A^2) \tag{5.23}$$

Where q is the electron charge, I_p is the photo-generated current, I_d is the dark current, and B is the noise measurement bandwidth. Thermal noise, also known as Johnson noise, is a result of thermally induced random fluctuations in the charge carriers in a resistance. These carriers are in random motion in all resistance at a temperature higher than zero. The shunt resistance and the bulk resistance and the load resistance in a photo detector have Johnson noise associated with it. The mean square value of the thermal current for *pin* photodiode is given by:

$$< i_{th}^2 > = 4KTB/\,R \quad (A^2) \tag{5.24}$$

Where $k_B$is Boltzmann's constant, T temperature, in degrees Kelvin (~298K, IEEE standard) and R resistance in ohms. The total noise current generated in a photodetector is given by:

$$< i_n^2 > = B\left(2q\left(I_p + I_d\right) + \frac{4k_B T}{R}\right) \quad (A^2) \tag{5.25}$$

5.6.2 Simulation Results: BER decay using an ASGA for parameter selection

Before thermal and Johnson noises are analyzed at the receiver photodiode, the BER performance is monitored under the supervision of the ASGA. Figure 5.8 shows a logarithmic scale of the BER improvement at subsequent generations of the genetic algorithm to attain a target of 1×10^{-9}. The BER performance refers to a 1 km transmitter to receiver range, with 100 MHz electrical bandwidth in adverse weather conditions with total attenuations ranging between [30 - 40] dB/km. In practice, the incident optical power that represents the ambient light was evaluated using an Ealingradiometer device (IL700A) with sensitivity factor set to equal 1.776E-2 (cm^2/W) at Warwick University. The noises generated at the receiver photodiode are calculated according to the code below:

```
%Code for calculating Johnson and shotnoises at the receiver of the optical wireless system.

T = 298; % Room Temperature (K)
R = 1000; % Load resistance (Ohms)
Kb = 1.38 * 10^-23; % Boltzmann's constant (J/K)
q = 1.6 * 10^-19; % Electron Charge
amb_light = 0.032;  % in W, the lab Measurement indicated
3.2mw/cm^2
Photo_diode_Area = 0.05; % 5 mm^2,
amb_light_power = amb_light * Photo_diode_Area;
Sigma1= sqrt (2 * q * X(8,val)*10^8* 2 * X(5,val)* (Pr+amb_light_power) + (4 *
Kb*T*X(8,val)*10^8/R) );
Sigma0= sqrt ( 2 * q * X(8,val)*10^8* 2 * X(5,val)* 0.1*(Pr+amb_light_power) +(4 *
Kb*T*X(8,val)*10^8/R) );
```

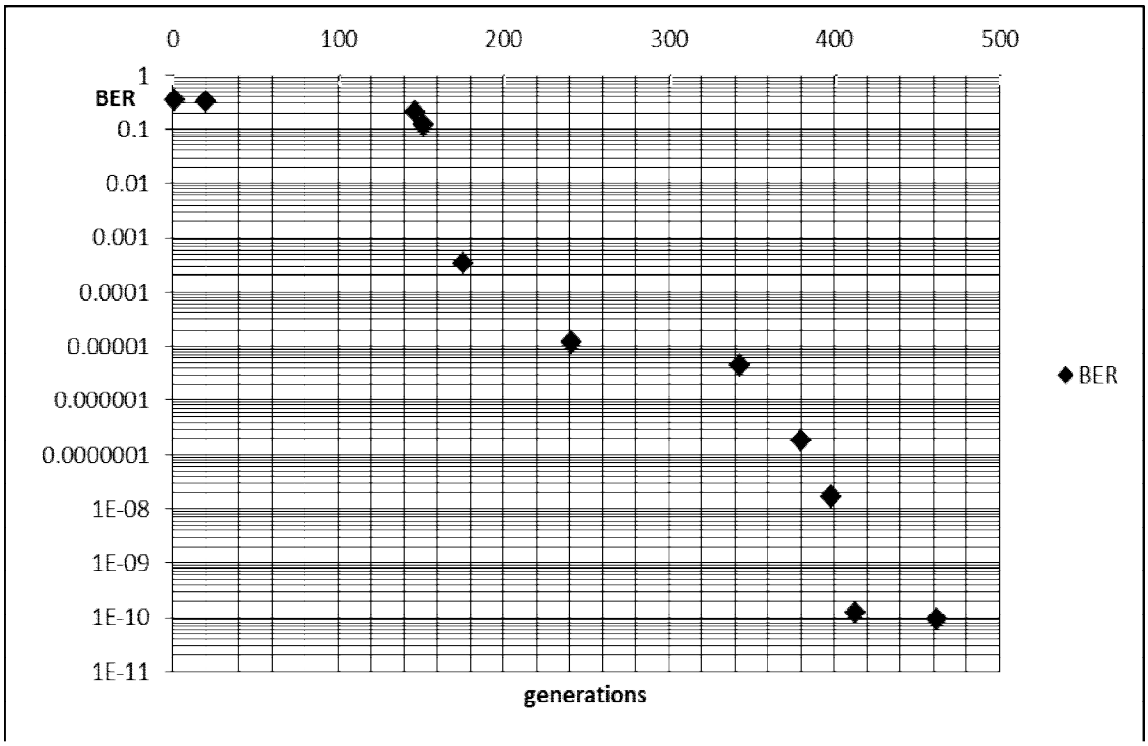

Figure 5.8 BER improvement with ASGA for parameter selection, B = 100MHz, R = 1Km, α = 30-40dB/km.

5.6.3 Simulation Results: ASGA Performance Targeting Change in Transmitted Power

The effect of ambient light was added to the noise but the SNR remains limited only by the received light and to the adaptive configurations proposed by the ASGA, and the data sets corresponding to each generation are shown in the Appendix. Ambient light is considered to be negligible during night by ignoring star and moonlight effects. The area of the photodiode used for analysis is $5\,mm^2$, and the light captured by the receiver aperture is assumed to be passed without loss to the receiver photodiode.

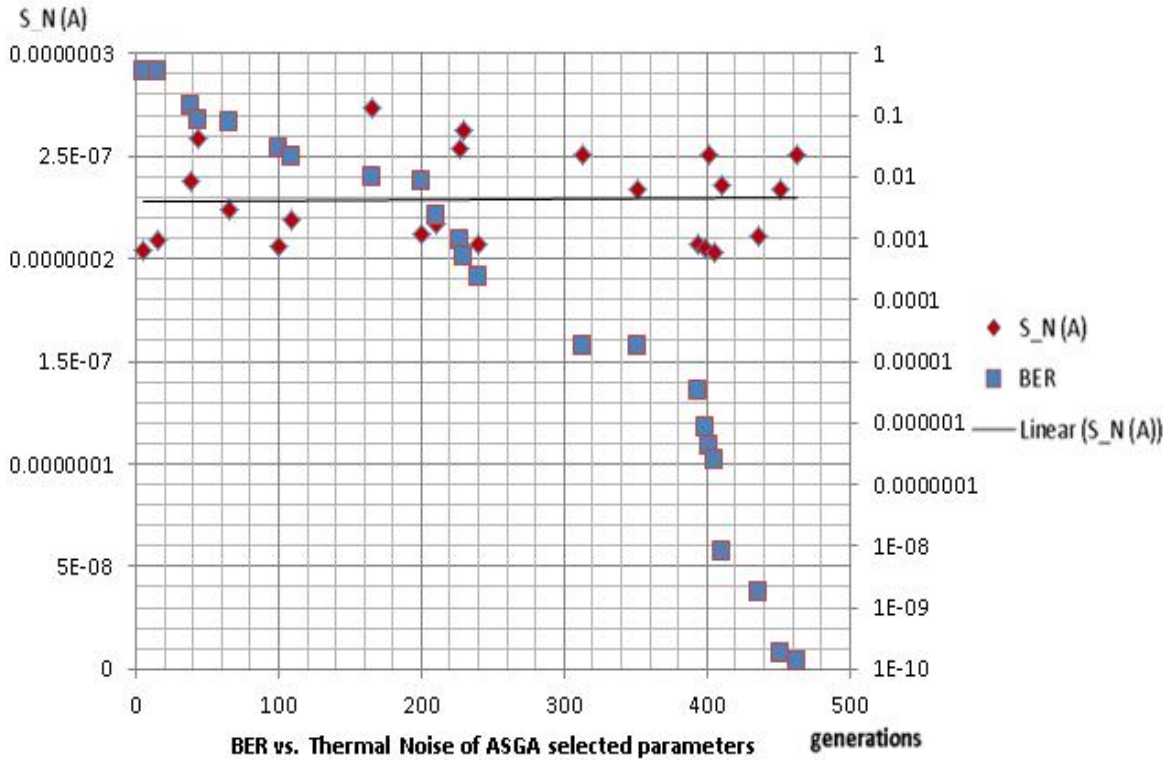

Figure 5.9ASGA performance targeting change in transmitted power, B = 500 MHz, R = 1Km, α = 30-40dB/km, shot noise fluctuates around $4.88\text{x}10^{-7}$A, Johnson noise = $1.28\text{x}10^{-7}$A, Ambient_light = 3.2mW/cm^2.

Figure 5.9 shows that the thermal noise is minimally affected by the change in transmitted power being monitored at $17.455 - 251.76\ mW$ (Figure 5.12). There's no obvious variation in thermal noise during ASGA selection, although the increase in the transmitted power clearly causes the thermal noise to increase; however, it remains within a range averaged by (*linear S_N*). This fact implies that, when the received power is improved, it doesn't mainly affect the thermal noise if the weather conditions at the two instants remained constant. Consequently, the effect of ambient light is studied in figure 5.10.

5.6.4 Simulation Results: Effect of Ambient Light on noises and BER under the supervision of ASGA

The intensity of the ambient light is varied in the simulation software to check the ability of the ASGA to compromise the performance. Ambient light was varied up from $3.2mW/cm^2$ to $0.1w/cm^2$, and the total effect of ambient light is depending on the effective area of the receiver photodiode. The change in ambient light has led todirect change in the shot noise during daylight simulation, but kept the Johnson noise unchanged. The figure below shows the simulation results at 500 MHz electrical bandwidth with attenuation levels reaching 40dB/km.

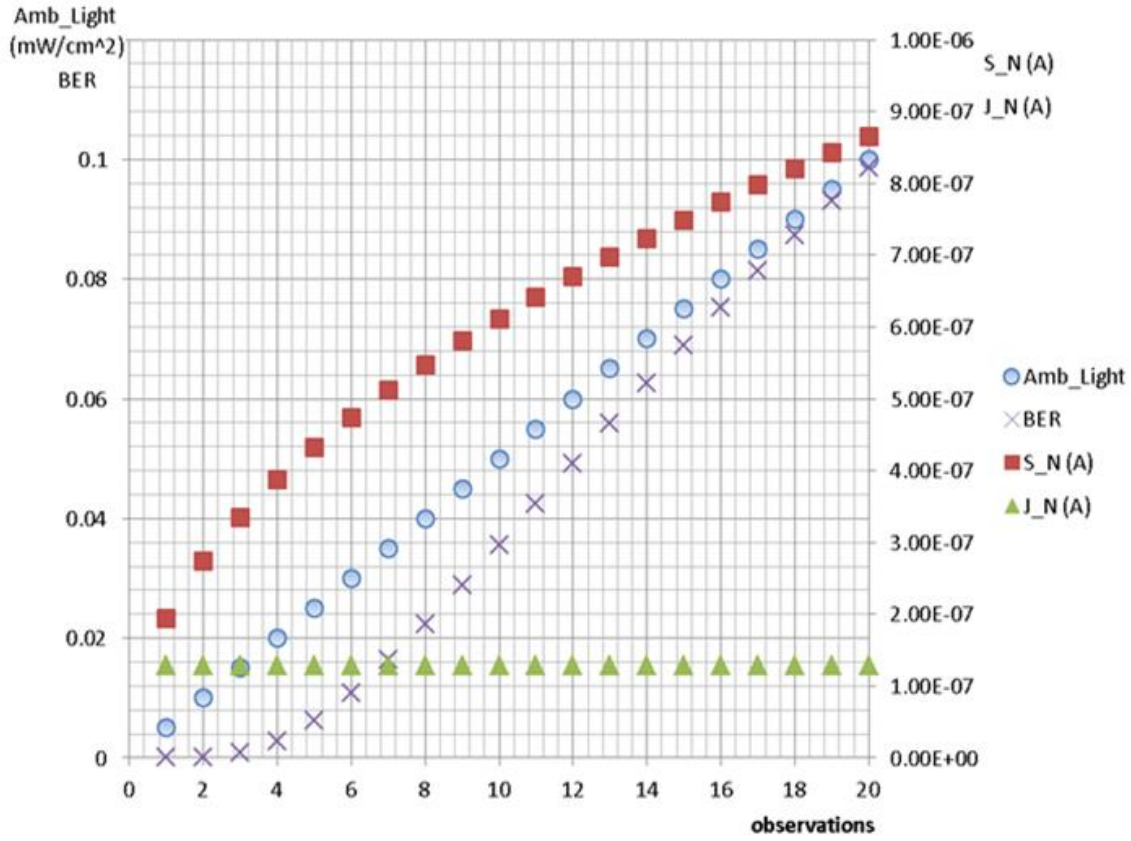

Figure 5.10 Effect of ambient light on shot noise and BER as observed by ASGA, B fixed to 500Mhz, R = 1km,α =30-40dB/km, at room temperature (290K).

5.6.5 Simulation Results: Effect of Electrical Bandwidth on Shot and Johnson Noises

The electrical bandwidth is changed from 100MHz to 500MHz, at optimally shaped pulses of OOK modulation, which means that the maximum allowed bit rate is 1Gbps. Both noises are affected, and the simulation is shown in figure 5.11.

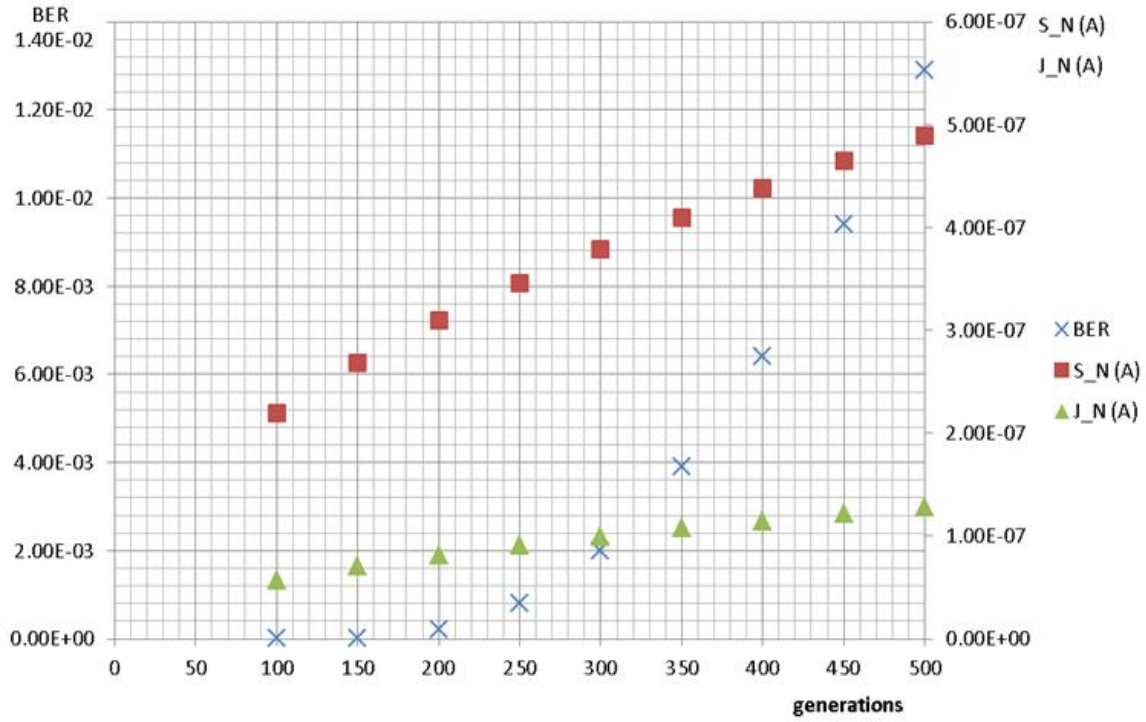

Figure 5.11 Decay in performance, increase of thermal & Johnson noises with change in Bandwidth, up to 500MHz,R = 1Km, α = 30-40dB/km.

Having more power emerging from the transmitter aperture doesn't mean that a better performance is expected at all times; consequently, the ASGA proves that increasing the transmitted power should not always be the channel cost, the link is optimized with a relatively low transmitted power of *67.8 mW*, and also it shows it could have a good

performance (*low BER*) even if it the transmitted power is compensated to *17.8mW* (Figure 5.12, G=451) by adjusting all other channel parameters, which therefore maximize the channel link margin. The intensity of the ambient light was varied up to $0.1w/cm^2$ in the simulation software (Matlab 2011a) to check the ability of the ASGA to compromise for the performance; and the result is depicted in Figure 5.10. The change in ambient light has led directly to a change in shot noise, but kept Johnson noise unaffected. It is realized that shot and Johnson noises behave likewise in Figure 5.11 when more electrical bandwidth is used in the channel but with different significance. This shows that ASGA also verifies the fact that the optical wireless channel during daylight is shot-noise limited, where the Johnson noise could rather be more deterministic.

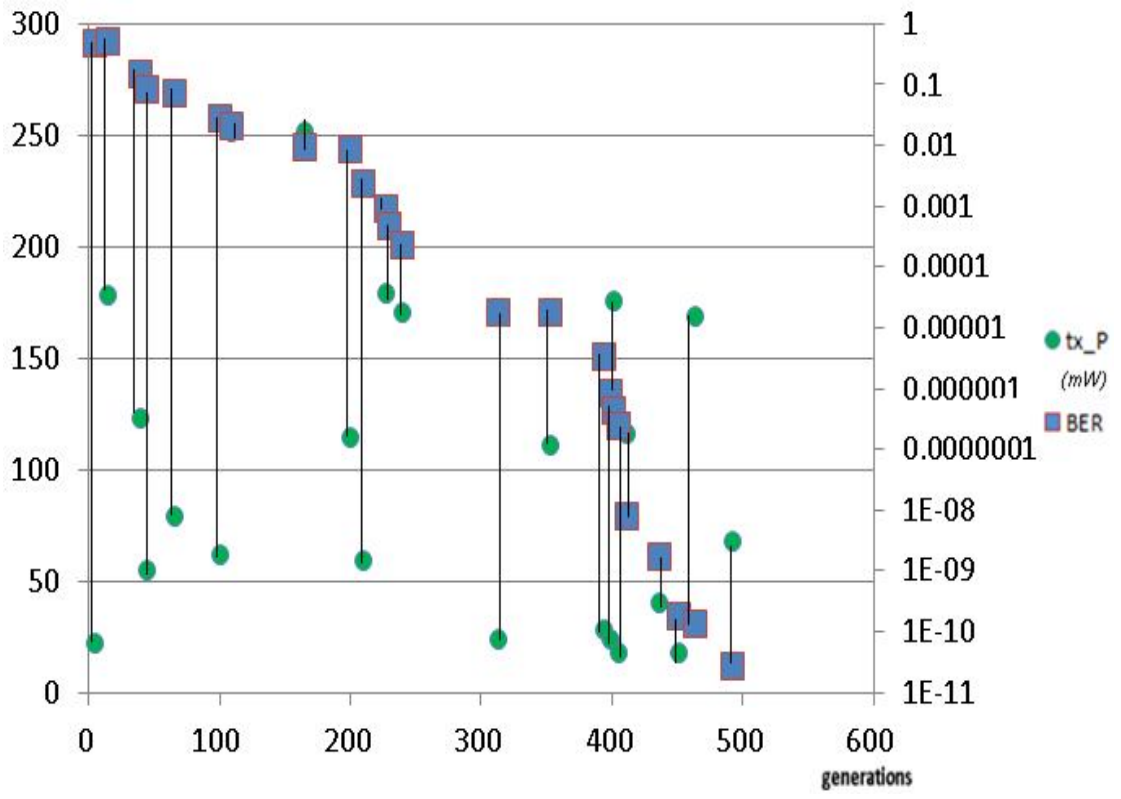

Figure 5.12.A generation-based variation of transmission power, R = 1Km, α = 30- 40dB/km, B = 500Mhz, at room temperature, final BER = 2.69E-11.

5.6.6 Analysis of Results

Shot and thermal noises have been evaluated and monitored at different successive generations of a genetic algorithm. The ASGA is powerful when the channel needs to set up link parameters especially at a pre-installation stage where it has restrictions on certain variables. The objective is not to minimize the noise but the BER, and record how various parameters affect the noise. In other words, the noise depends on the received power (signal + ambient) and the electrical bandwidth used in transmission, but the received power could be adjusted by using different link parameters. However, if all parameters are fixed and only the transmitted power is controlled, the BER will have a direct relation with the noise, and minimizing the noise maximizes the channel performance. To achieve an acceptable BER at the receiver photodiode, it is possible to maximize the channel link control margin by using an Application- Specific Genetic Algorithm (ASGA). The analysis shows that the transmitted power is not the only penalty, and minimum noise at the receiver photodiode does not always mean a better performance.

5.7 Simulation Results: Complexity of ASGA against Matlab Toolbox

The ASGA tackled the problem by adapting the variables of figure 5.6 to their lower (LB) and upper bounds (UB) to form a Matrix X (random solutions) of certain fitness value. The ASGA makes rescaling and selection of parameters and uses them as parents to produce the children for the next generation. Over successive generations, the optical wireless channel "evolved" toward an optimal solution as shown in 4 simulations at different total attenuations (figure 5.13).

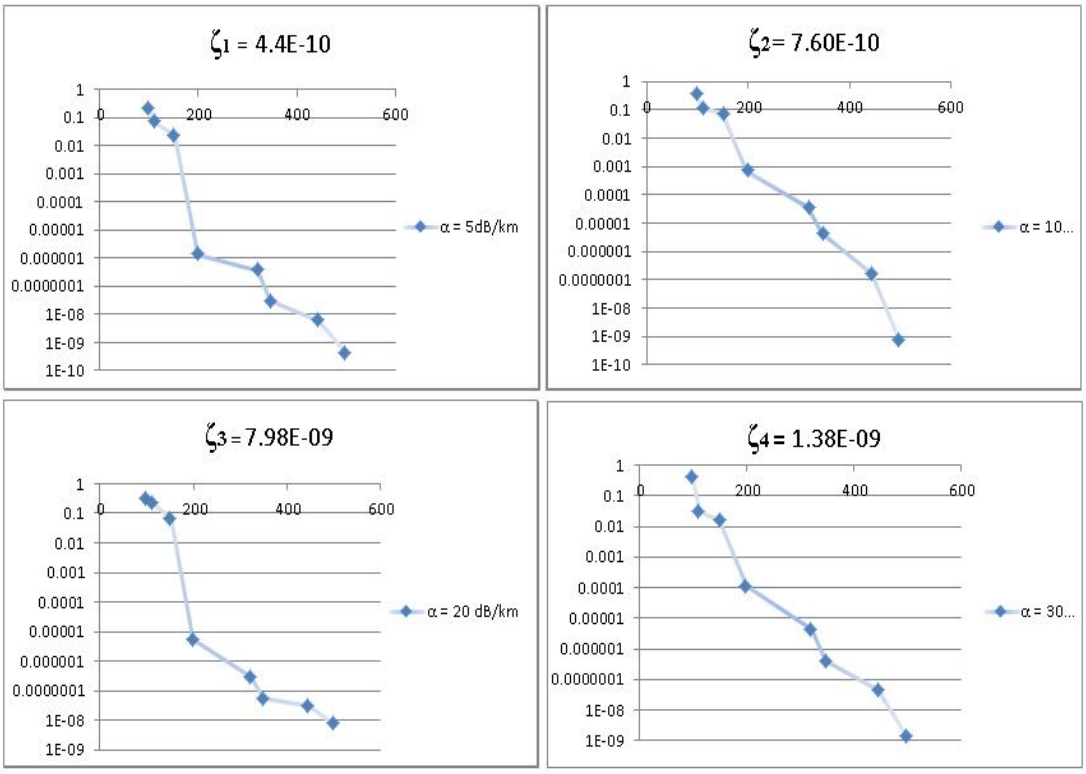

Figure 5.13: BER improvement using ASGA for 8-parameter selection.

The methodology discussed in section 4.4.2 is implemented to verify the use of the ASGA against the GA tool box offered by Matlab2011a. The channel model built on OOK modulation is used to build their fitness functions; the two systems are simulated 10 times, the first 5 simulations are used for a brief verification, and results are shown in Table 5.5.

Table 5.5: Channel Performance using GA and ASGA for parameter selection at the best five simulations results leading high reliability.

Application-Specific-Genetic Algorithm					
	1	2	3	4	5
Reliability	6.28E-09	4.40E-10	7.60E-10	7.87E-09	5.57E-07
Complexity	4.457	5.631	8.878	11.159	14.492
Matlab Genetic Algorithm Tool Box					
	1	2	3	4	5
Reliability	2.89E-08	6.52E-11	7.59E-10	6.77E-09	1.62E-10
Complexity	3.999	6.231	8.496	11.988	14.321

The ASGA experienced the whole range of parameter combinations and enables the system to check out performance at all instances (generations). The simulation targeted different attenuation levels, expressed in dB/km. The selected generations depicted in table 5.5 are presented at the last point of conversion in channel performance. The ASGA and GA Tool box make use of 0.02 and 0.6 mutation- and crossover rates, respectively. Both selection algorithms have shown reliability with an accepted BER approaching ξ= (1.00E-09) at the receiver with high reliability and average complexity of 8.923 and 9.007 for the ASGA and GA Tool Box, respectively. However, the ASGA can support variables without the need of normalization and could be easily adjusted to meet specific targets and upgradeability requirements. Consequently, the ASGA could be reliable in selection problems of specific purposes where the need of tackling convergence instances in system performance is of particular interest.

The ASGA has shown that the transmission power could be well compensated during darkness in μW (Table 5.3) and designed a set of systems up to a user defined transmitted power limitation during day light at 278mW (Table 5.4). In fact, there is no possibility of drawing one general conclusion regarding different effects on BER unless all parameters are fixed against the targeted values. The logical reasoning that is obeyed here stresses the importance of all mentioned parameters; even a small change in one of them, could affect the channel performance. The several combinations are significant to meet various channel characteristics and link requirements at pre-installation stages. For instance, the system can offer a set of solutions based on sensible selection criteria. However, it's worth studying the effect of one parameter on the BER throughout consecutive generations in the perspective of this intelligent system.

5.8 Conclusion

The developed system has been used for the necessity of sensible selection requirements and design advice at pre-installation. A traditional search algorithm has been used to select parameters of the proposed system; it took 29 minutes to try all possible combinations. The iterations should cover all variables since the data is not able to be sorted in order, and thus, there's no way for an improvement using methods like binary search, recursion, forward addition, backward elimination, or others. The genetic algorithm technique achieved the approach in an average time of 9.62 seconds, which is an improvement of a factor of (29*60/average simulation time). The power of genetic algorithms in selection techniques has been well-established before, and the achievement in optical wireless communication would help designers get an estimation of the channel performance. The objective measures the "goodness of fit", and after several

generations, learns fitness. The algorithm, according to certain link characteristics, can be utilized at run-time and produce corresponding parameter updates given that the channel is equipped with a reconfigurable hardware that adjusts according to the advised selections. Moreover, the genetic algorithm is easy for upgradeability to include any extra parameters that are significant to be considered for further consideration.

References:

[5.1] Cablefree Solutions Limited, Available: <http://www.cablefreesolutions.com/>, Accessed [23rd June 2012].

[5.2] R. M.Gagliardi, and S. Karp, "Optical Communications", 2nd edition, *John Wiley & Sons, Inc.* 1995.

[5.3] S. Karp, E. L. O'neill, and R. M. Gagliardi, "Communication theory for the free-space optical channel," *in Proc. IEEE, vol. 58, pp. 1611 –1626*, Oct. 1970

[5.4] C. DeCusatis, Handbook of Fiber Optic Data Communication: "A Practical Guide to Optical Networking" 3rd Edition, *Elsevier*, ISBN: 978-0-12-374216-2, 2008.

[5.5] J. R. Barry, "Wireless Infrared communications", *Kluwer Academic*, Boston, 1994.

[5.6] H. Moradi, M. Falahpour, H. H. Refai, P. G. LoPresti, M. Atiquzzaman, "An Estimation-Based Optimum Receiver for FreeSpace Optics Using Pilot-Aided Modulation", *in SPIE Photonic West Conference,* Jan. 2010.

[5.7] S. Karp, R. M. Gagliardi, S. E. Moran, and L. B. Stotts, "in Optical Channels: Fibers, Clouds, Water, and the Atmosphere", *Plenum Press*, 1988

[5.8] F. S. Vetelino, C. Young, L. Andrews, " Fade statistics and aperture averaging for Gaussian beam waves in moderate to strong turbulence", *Applied Optics*, vol. 46, no. 18, p. 3780 – 3789, 2007.

[5.9] M. Al-Habash, L. Andrews, R. Philips, "Mathematical model for the irradiance probability density function of a laser beam propagating through turbulent media", *Optical Engineering*, vol. 40, p. 1554 – 1562, 2001.

[5.10] H. Sandalidis, T. Tsiftsis, "Outage probability and ergodic capacity of free-space optical links over strong turbulence".*Electronics Letters*, vol. 44, no. 1, p. 46 – 47, 2008.

[5.11] M. A. Mood, F.A. Graybill, D. C. Boes, "Introduction to the theory of statistics", *McGraw-Hill*, 3rd Edition, pp 171, 1974.

[5.12] H. Henniger, O. Wilfert, "An Introduction to free space optical communication", *Radio Engineering*, VOL. 19, NO. 2, pp. 203, June 2010

[5.13] A. El. Yakzan, R.J. Green, and E. L. Hines, "A Genetic Algorithm based Selection of a Transmission Wavelength in the LOS Optical Wireless Channel", *inInternational Conference on Transparent Optical Networks*, Warwick, UK, July, 2012.

[5.14] A. El. Yakzan, R.J. Green, E.L. Hines and M. Ali, "An Intelligent Approach to Link Parameter Estimation for Outdoor Optical Wireless Channels", *in Proc. Of IEEE Conference Mediterranean Conference on Embedded Computing,* Montenegro, 2012.

[5.15] C. W. Ahn, R. Ramakrishna, "A genetic algorithm for shortest path routing problem and the sizing of populations", *in IEEE Transactions on Evolutionary Computation*, vol. 6, no. 6, pp. 566 – 579, Dec. 2002.

[5.16] S. B. Alexander, "Optical communication receiver design", *SPIE International Society for Optical Engineering,* 1997.

[5.17] N. B. Lukyanchikova, “Noise research in semiconductor physics”*Gordon and Breach Science publishers,* Amesterdam,1996.

[5.18] A.El.Yakzan, R.J. Green and E. L. Hines, “Application-Specific Genetic Algorithm Targeting the Complexity of Parameter Selection in LOS Outdoors Optical Wireless Channel”, *UKSim 15th International Conference on Mathematical/Analytical Modelling and Computer Simulation,* Cambridge, UK, 2013

[5.19]H.A.Alhagagi, “Theory and Optimisation of Double Conversion Heterodyne Photoparametric Amplifier”, *PhD Thesis,* Warwick, UK, 2012.

CHAPTER VI: Effects of Parameters on Channel Performance Using Multivariate Statistical Analysis

6.1 Introduction

This chapter considers studying the effects of parameters on channel performance using two types of studies: testing based on one parameter change, and a multivariate statistical analysis that studies the correlations among inputs in data samples.

6.2 Parameter Effects on Channel Performance

In this approach, all variables were tested separately by incrementing the value of the concerned parameter against all other fixed parameters, and the change in BER was recorded for a number of observations at each parameter. Unlike chapter 5, the variables are not monitored at the surveillance of the ASGA, which means that they are fixed, and only one parameter varies against all others to monitor its effect. The actual value of the BER at the beginning is not of high importance, but the change which each parameter variation imparts on channel performance.

6.2.1 Simulation Result: Effect of Transmitter Aperture on Channel Performance

Table 6.1 Effect of Transmitter Aperture on Channel Performance.

Observations of Parameters' Effects on Bit Error Rate at Optimal GA-Selected Values										
Observations	1	2	3	4	5	6	7	8	9	10
TX-AP	0.02 / 1.639 e-12	0.03 / 3.50 e-12	0.04 / 7.28 e-12	0.05 / 1.472 e-11	0.06 / 2.901 e-11	0.07 / 5.575 e-11	0.08 / 1.046 e-10	0.09 / 1.919 e-10	0.1 / 3.446 e-10	0.11 / 6.059 2e-10

P (m)	11	12	13	14	15	
	0.12 / 1.044 e-09	0.13 / 1.76 e-09	0.14 / 2.933 e-09	0.15 / 4.787 e-09	0.16 / 7.682 e-09	

6.2.2 Simulation Result: Effect of Receiver Aperture on Channel Performance

Table 6.2 Effect of Receiver Aperture on Channel Performance.

RX-AP	1	2	3	4	5	6	7	8	9	10
	0.075 / 0.397	0.091 / 0.350	0.107 / 0.297	0.123 / 0.24	0.140 / 0.183	0.156 / 0.130	0.172 / 0.085	0.188 / 0.505	0.205 / 0.026	0.221 / 0.012
P (m)	11	12	13	14	15	16	17	18	19	20
	0.237 / 0.004	0.253 / 0.001	0.270 / 3.948 e-04	0.286 / 8.08 e-05	0.302 / 1.26 e-05	0.335 / 1.193 e-07	0.351 / 6.751 e-09	0.367 / 2.535 e-10	0.383 / 6.068 2e-12	0.4 / 8.889 e-14

6.2.3 Simulation Result: Effect of Beam Divergence on Channel Performance

Table 6.3 Effect of Beam Divergence on Channel Performance.

B-DIV (mrad)	1	2	3	4	5	6	7	8	9	10
	1.175 / 1.081 e-011	1.40 / 7.32 e-07	1.625 / 1.44 e-04	1.85 / 0.002	2.075 / 0.011	2.3 / 0.031	2.525 / 0.060	2.750 / 0.094	3.425 / 0.196	3.65 / 0.225
	11	12	13	14	15	16				
	3.875 / 0.250	4.10 / 0.273	4.325 / 0.312	4.55 / 0.031	4.77 / 0.328	5.00 / 0.342				

6.2.4 Simulation Result: Effect of Transmitted Power on Channel Performance

Table 6.4 Effect of Transmitted Power on Channel Performance.

TX-P (mW)	1	2	3	4	5	6	7	8	9	10
	15 / 0.365	30 / 0.245	45 / 0.151	60 / 0.084	75 / 0.042	90 / 0.019	105 / 0.008	120 / 0.003	135 / 9.92 e-04	150 / 2.95 e-04
	11	12	13	14	15	16	17	18	19	20
	165 / 7.85 e-05	180 / 1.86 e-05	195 / 3.973 e-06	210 / 7.543 e-07	225 / 1.278 e-07	240 / 1.931 e-08	255 / 2.603 e-09	270 / 3.128 e-10		

6.2.5 Simulation Result: Effect of Responsivity of the Receiver on Channel Performance

Table 6.5 Simulation Result: Effect of Responsivity of the Receiver on Channel Performance.

R_s (A/W)	1	2	3	4	5	6	7	8	9	10
	0.4 / 5.61e-08	0.44 / 1.18 e-08	0.46 / 5.48 e-09	0.48 / 2.528 e-09	0.50 / 1.166 e-09	0.52 / 5.389 e-10	0.54 / 2.4903e-10	0.56 / 1.1514e-10	0.58 / 5.326 e-11	0.62 / 1.14 e-11
	11	12	13	14	15	16	17	18	19	20
	0.64/ 5.28e-12	0.66 / 2.450e-12	0.68 / 1.135 e-12	0.70 / 5.268 e-13	0.72 / 1.134 e-13	0.76 / 5.264 e-14	0.78 / 2.444 e-14			

It is now intended to worsen the weather conditions by increasing the effects of rain, snow, fog, mist, and scintillation; the attenuations' effect, where turbulence accounts as part of fixed losses, on bit error rate (BER) appears below:

6.2.6 Simulation Result: Effect of Total Attenuation on Channel Performance

Table 6.6 Effect of Total Attenuation on Channel Performance.

α_{Tot} (dB/Km)	1	2	3	4	5	6	7	8	9	10
	41 / 2.04e-07	42 / 3.36 e-05	43 / 8.56 e-04	44 / 0.0068	45 / 0.026	46 / 0.063	47 / 0.1147	48 / 0.172	49 / 0.228	50 / 0.279
	11	12	13	14	15	16	17	18	19	20
	51 / 0.322	52 / 0.358	53 / 0.387	54 / 0.411	55 / 0.429	60 / 0.478				

6.2.7 Simulation Results: Effect of Electrical Bandwidth on Channel Performance

Table 6.7 Effect of Electrical Bandwidth on Channel Performance.

BW (MHz)	1	2	3	4	5	6	7	8	9	10
	100 / 8.50 e-11	115 / 1.29 e-09	130 / 1.065 e-08	155 / 1.452 e-07	200 / 3.155 e-06	350 / 3.20 e-04	500 / 0.0021	650 / 0.006	800 / 0.012	950 / 0.0191

6.2.8 Analysis of Results

Extreme cases for the total attenuations-range relationship are built where the channel fails to achieve an acceptable BER areshown in Table 6.8.

Table 6.8 Extreme relations between Link Range and attenuations.

Link Range:R(km)	Total attenuations-: (dB/km)	Bit Error Rate (BER)
1.1000	41	0.0043
1.3000	36	0.0978
1.3000	31	3.7717e-009
1.5000	36	0.4256
1.5000	26	1.5209e-009
1.5000	46	0.4976
3.000	12	6.8167e-009

The results of the ASGA simulation have been analysed in order to establish input-input and input-output relationships. The distance between the transmitter and the receiver does not have a great influence on the bit error rate unless it is linked to the total link attenuations affecting the transmission. The GA experiences difficulties in selection when the distance increases more than 3Km and attenuation becomes more than 12dB/km, where the GA best achievement lies around a BER of 6.8167e-009. A range-attenuation relationship is presented below, investigating channel performance at 100MHz bandwidth, and a guaranteed margin is proposed within 3Km distance under which the channel tends to achieve 100% availability. As a conclusion, from using Table 6.2.8 and applying many parameter combinations (Table 5.4), the GA controlled channel achieves an acceptable bit error rate (BER<10^{-9}) if the link range-attenuation(R, α) satisfies:

$$(R, \alpha) \rightarrow \quad \forall\, R \in \{0 \leq R \leq 2.9\}, \qquad \alpha \leq 12$$

$$\forall\, R \in \{0 \leq R \leq 1.3\}, \qquad \alpha \leq 31$$

$$\forall\, R \in \{0.5 \leq R \leq 1\}, \qquad \alpha \leq 46$$

$$\forall\, R \in \{R \leq 0.5\}, \qquad \alpha \leq 96$$

$$\forall\, \alpha > 96, \qquad Link\ Failure.$$

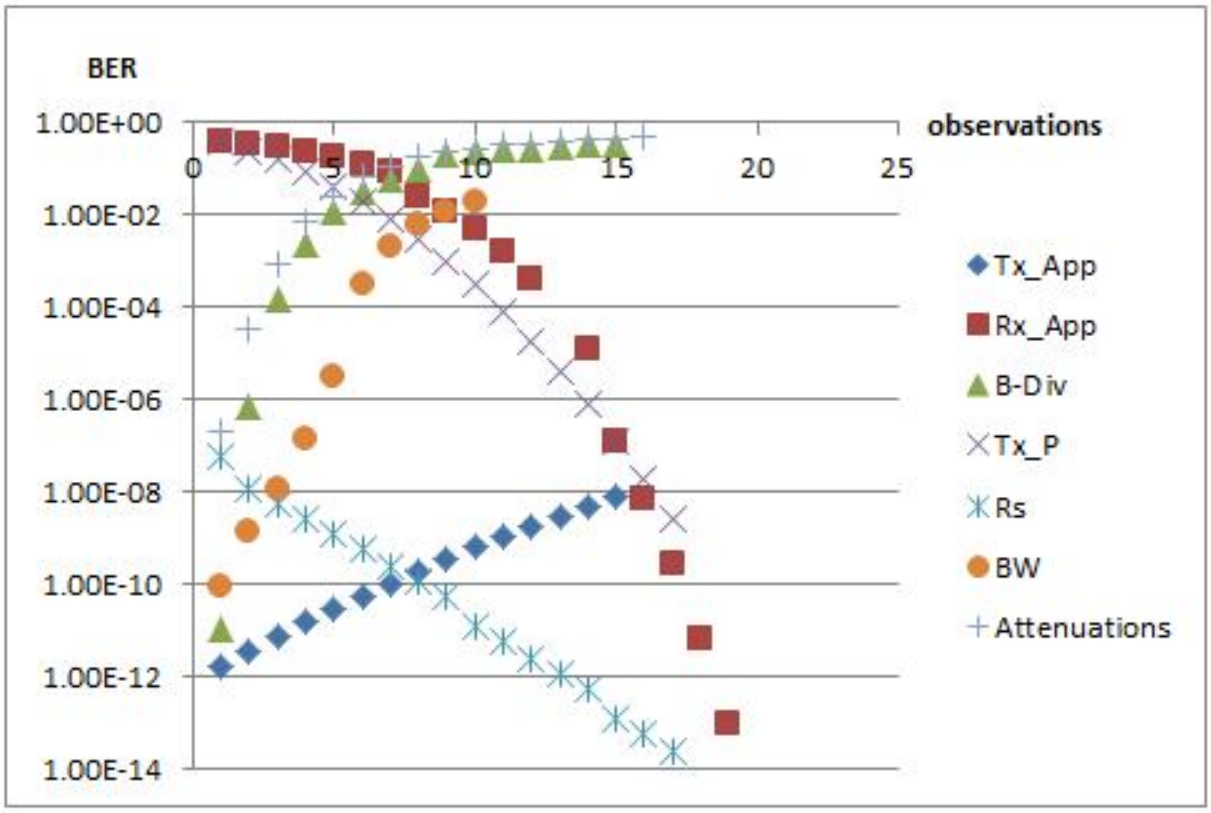

Figure 6.1 Scatter-Plot of Different Parameters' Effects on GA-Achieved BER.

The influence of different parameters on bit-error-rate (BER) in the optical wireless channel has been analyzed in Figure 6.1. The scatter-graph with markers separate measurements of different observations. The second study incorporates the use of multivariate statistical where the effect of parameters on BER will be studied using statistical analysis, and limited to the combinations that lead a low BER at the receiver photodiode. The ASGA produced combinations of variables are selected so that the channel achieves a BER not more than 10^{-6}. The analysis aims at studying the correlation amongst sets that assure this achievement, and shows the percentage contribution that each input exhibits on other parameters, which implies the priority considerations of designers at channel installation.

6.3 Multivariate Statistical Analysis

Multivariate statistical analysis encompasses the simultaneous observation and analysis of variables in a dataset. It involves several types of univariate and multivariate analyses that aim at understanding the relationships between variables and their relevance to the actual problem. There are many types of multivariate models such as: Principal Component Analysis (PCA), Canonical Correlation Analysis (CCA), Redundancy Analysis, and Correspondence Analysis, Clustering, and Artificial Neural Networks. In this chapter, the data sets produced by the genetic algorithm are studied using Principal Component Analysis to investigate the relationships among different variables of possible link importance [6.1].

6.3.1 Principal Component Analysis (PCA)

PCA is a mathematical procedure used for transforming a high-dimensional data, by studying the dependencies among variables, to a lower-dimensional form without losing too much information. PCA, also known as Karhunen-Loeve transformation, is a technique that transforms a number of correlated variables into a reduced number of uncorrelated (orthogonal) variables called principal components [6.2]. Although the problem addressed by this chapter doesn't require dimension reduction; then, PCA was used to extract correlations among variables, and the way they should change for achieving a low BER. The components are determined in a way that satisfies the maximum variability in the data set, which means that the first component accounts for as much of the variability in the data as possible, and the second accounts as such for the

remaining datasets. PCA detects dominant patterns in the matrix in terms of a complementary set of score-and loading plots [6.3].

6.3.2 Mathematics of the PCA

The general objective of PCA is to obtain another basis that is a linear representation of the original basis and that re-expresses a certain data in an optimal way. The samples considered by this study is represented by a matrix X= [8x165], the rows $m = 8$ represent the number of variables, and the columns $n = 165$ represent the number of samples. The intention here is to find a transformation matrix P[$8x8$] that is able to transform X[$8x165$] from the original basis to Y[$8x165$] in the new basis, such that [6.6]:

$$Y = P X \tag{6.1}$$

Where the rows of P are $\{p_1, p_2, \dots, p_m\}$, Y is therefore represented as:

$$Y = PX = \begin{pmatrix} p_1.x_1 & p_1.x_2 & \cdots & p_1.x_n \\ p_2.x_1 & p_2.x_2 & \cdots & p_2.x_n \\ \vdots & \vdots & \ddots & \vdots \\ p_m.x_1 & p_m.x_2 & \cdots & p_m.x_n \end{pmatrix} \tag{6.2}$$

Where $p_i.x_j$ is a dot product and both p_i and $x_j \in \mathbb{R}^m$, and the rows of P make a new basis for representing the columns of X. To make a decision of what basis (principal components) is mostly fitting to describe the data presented in X, the variance of the original data is to be studied. The original data is de-correlated by finding the directions for which the variance is maximized, and those directions are used to define the new basis. Therefore, the principal components are used so that they express the maximum

variability with minimum data loss (Figure 6.2), and then factors are rotated to find out other components with less variability, and so on, with a constraint that they should all be orthogonal.

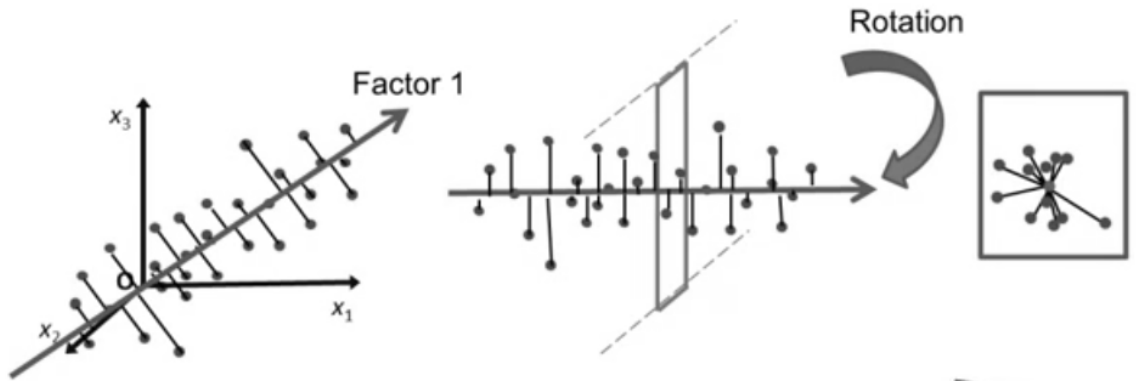

Figure 6.2: Concept of Principal Components.

The variance of a random variable (Z) is:

$$\sigma_Z^2 = E[(Z - \mu)^2] \tag{6.3}$$

If the variables used do not have same units of measure, which is the case with the parameters produced by the genetic algorithm (meter, milliwatts, ampere per watt, milliradians, Megahertz, kilometres, and decibel), it is important to subtract the mean for all the measurements for having a standardized data. The variance of any vector $r = (r_1, r_2, \ldots, r_n)$ is given by [6.7]:

$$\sigma_r^2 = \frac{1}{n} rr^T \tag{6.4}$$

Now if a variance of two variables together is to be considered, it is called covariance, and it aims on calculating how both variables change together. It is divided by (n-1) instead of n for some analysis in [6.6], and the covariance of vectors r and s is given by:

$$\sigma_{rs}^2 = \frac{1}{n-1}\, rs^T \tag{6.5}$$

Since the matrix X represents m row vectors of length n , it becomes important to study the covariance between all vectors inside matrix X, which forms a covariance matrix $\mathbf{C_X}$ with diagonal entries representing the variances, and off-diagonal entries representing the covariances. Thus, $\mathbf{C_X}$ contains all covariance pairs between m variables and is defined by[6.7]:

$$\mathbf{C_X} = \frac{1}{n-1}\mathbf{X}\mathbf{X}^T = \frac{1}{n-1}\begin{pmatrix} \mathbf{x_1}\mathbf{x_1}^T & \mathbf{x_1}\mathbf{x_2}^T & \cdots & \mathbf{x_1}\mathbf{x_m}^T \\ \mathbf{x_2}\mathbf{x_1}^T & \mathbf{x_2}\mathbf{x_2}^T & \cdots & \mathbf{x_2}\mathbf{x_m}^T \\ \vdots & \vdots & \ddots & \vdots \\ \mathbf{x_m}\mathbf{x_1}^T & \mathbf{x_m}\mathbf{x_2}^T & \cdots & \mathbf{x_m}\mathbf{x_m}^T \end{pmatrix} \in \mathbb{R}^{m\times m} \tag{6.6}$$

This covariance matrix is represented in the original basis, and now the interest is to define the features that a transformed matrix Y will exhibit, and correspondingly relate it to the covariance matrix C_Y. This is achieved by two major requirements: maximizing the variance (diagonal entries), and minimizing the covariance between variables (off-diagonal entries); therefore the objective is met if a transformation matrix P could be defined such that C_Y is diagonal. Knowing that all vectors of P should be orthogonal, with the tool of linear algebra, and interpretation of P, X, and Y could be constructed such that [6.7]:

$$C_Y = \frac{1}{n-1}\, YY^T = \frac{1}{n-1}\, PX(PX)^T = \frac{1}{n-1}(PX)(X^T P^T)$$

$$= \frac{1}{n-1}P(XX^T)P^T = \frac{1}{n-1} = PSP^T \tag{6.7}$$

where S is an $[mxm]$ symmetric matrix, such that $S = XX^T$. A known theorem of linear algebra is that every symmetric matrix is orthogonally diagonalizable, therefore$S = EDE^T$, where E is an $[m\,x\,m]$ orthogonal matrix whose columns are orthogonal eigenvectors of S, and D is a diagonal matrix which constitutes the eigenvalues of S as its diagonal entries.

The decision of the transformation matrix is now done by choosing the rows of P to be the eigenvectors of S, and $P = E^T$; therefore by substituting P in 6.6, the covariance matrix of Y is expressed by [6.7]:

$$C_Y = \frac{1}{n-1}\, PSP^T = \frac{1}{n-1} E^T(EDE^T)E = \frac{1}{n-1}\, D \qquad (6.8)$$

This is because $EE^T = I\ (identity\ matrix)$.Now, the first principal component refers to the largest variance, the second largest make the second principal component and so on. The diagonalisation stage takes place once the eigenvalues and eigenvectors of $S = XX^T$ are obtained. The eigenvalues are placed in descending order on the diagonal of D. Similarly the eigenvectors are placed in the same order to form the columns of E. Finally, the principal components or the rows of P are now obtained from the eigenvectors of the covariance matrixXX^T, and the rows are in order of importance.

Although the purpose of using PCA is finding a correlation amongst the inputs when a BER of 10^{-6} is targeted as a purpose, it is an additional analysis to know if the ASGA generated data behave similarly and could be mostly presented even after dimension reduction.

6.3.3 Results of Statistical Data Analysis

Matlab2011a is used to program the code for PCA. The *princomp*command is used to calculate the coefficients, scores, variances, and eigenvectors. The data sets selected using the ASGA are shown in a scatter plot of Figure 6.5, and the statistics are calculated below. 106 Data sets are produced by the GA covering all possible values of parameters as they may exist in the optical wireless channel [6.5]. The statistics of the original and standardized data is shown in tables 6.9 and 6.10 respectively.

Table 6.9 Statistics of Original Data.

Variable	Observations	Obs. with missing data	Obs. without missing data	Minimum	Maximum	Mean	Std. deviation
Tx_APP (m)	106	0	106	0.020	0.160	0.099	0.050
Rx_App (m)	106	0	106	0.090	0.400	0.320	0.075
B_Div (mrad)	106	0	106	0.522	4.178	1.910	0.795
Tx_P (mW)	106	0	106	1.695	298.458	183.445	103.618
Rs (A/W)	106	0	106	0.401	0.800	0.533	0.118
α_tot (dB/km)	106	0	106	1.695	35.231	16.194	7.376
R (km)	106	0	106	0.678	3.100	1.909	0.714
Bw(MHz*100)	106	0	106	1.000	5.000	3.269	1.413

Table 6.10 Statistics of Standardized Data.

Variable	Observations	Obs. without missing data	Minimum	Maximum	Mean	Std. deviation
Tx_APP	106	106	0.407	3.225	1.995	1.000
Rx_App	106	106	1.205	5.354	4.288	1.000
B_Div	106	106	0.656	5.253	2.402	1.000
Tx_P	106	106	0.016	2.880	1.770	1.000
Rs	106	106	3.398	6.781	4.517	1.000
α_tot	106	106	0.230	4.777	2.196	1.000
R	106	106	0.950	4.343	2.674	1.000
Bw	106	106	0.708	3.538	2.313	1.000

6.3.3.1 Principal Components and Correlations between Variables Using Standardized Data

The data generated by Matlab shows that 64.5% of the data could be presented by F1 and F2 (Cumulative variability in Table 6.11 and Figure 6.3) which will be mainly used for the analysis in this section. The statistical analysis carried out for the work is shown below:

Table 6.11 Eigen Values of Principal Components.

	F1	F2	F3	F4	F5	F6	F7	F8
Eigenvalue	2.998	2.159	1.100	0.746	0.534	0.259	0.163	0.041
Variability (%)	37.47	26.989	13.755	9.328	6.669	3.235	2.034	0.519
Cumulative %	37.47	64.460	78.216	87.543	94.213	97.448	99.481	100

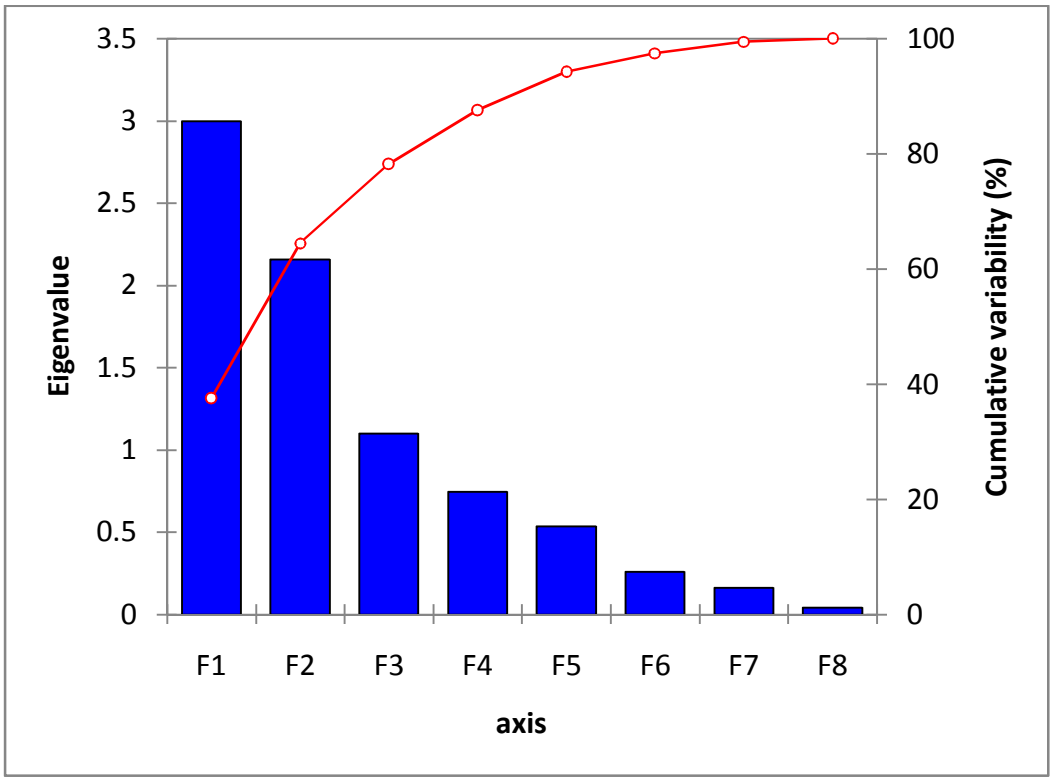

Figure 6.3 Scree Plot of Principal Component Analysis.

The parameters are correlated with the principal components, and their contributions to each factor are shown below:

Table 6.12 Correlation between Variables and Factors.

	F1	F2	F3	F4	F5
Tx_APP	16.329	13.549	2.621	9.872	0.883
Rx_App	11.872	18.759	0.010	0.467	22.626
B_Div	5.707	15.915	20.675	27.425	2.767
Tx_P	21.760	4.422	9.817	4.848	0.033
Rs	3.700	5.622	47.458	12.232	27.934
α_tot	22.138	4.263	11.688	3.222	9.915
R	15.155	19.438	1.551	5.277	6.492
Bw	3.338	18.034	6.179	36.657	29.351

Table 6.13 Correlations between Variables.

Variables	Tx_APP	Rx_App	B_Div	Tx_P	Rs	α_tot	R	Bw
Tx_APP	**1**	0.716	0.146	0.628	0.413	0.263	-0.147	0.150
Rx_App	0.716	**1**	-0.053	0.597	0.298	0.245	0.043	0.124
B_Div	0.146	-0.053	**1**	-0.045	0.099	0.245	-0.634	-0.417
Tx_P	0.628	0.597	-0.045	**1**	0.185	0.663	-0.312	-0.078
Rs	0.413	0.298	0.099	0.185	**1**	0.048	0.081	-0.075
α_tot	0.263	0.245	0.245	0.663	0.048	**1**	-0.799	-0.336
R	-0.147	0.043	-0.634	-0.312	0.081	-0.799	**1**	0.412
Bw	0.150	0.124	-0.417	-0.078	-0.075	-0.336	0.412	**1**

6.3.3.2 Behaviour of Parameters inside Principal Components

The parameters being studied present their behaviour as shown in the figure below, and a relation between two parameters is evaluated according to the magnitude of each parameter and their corresponding angle.

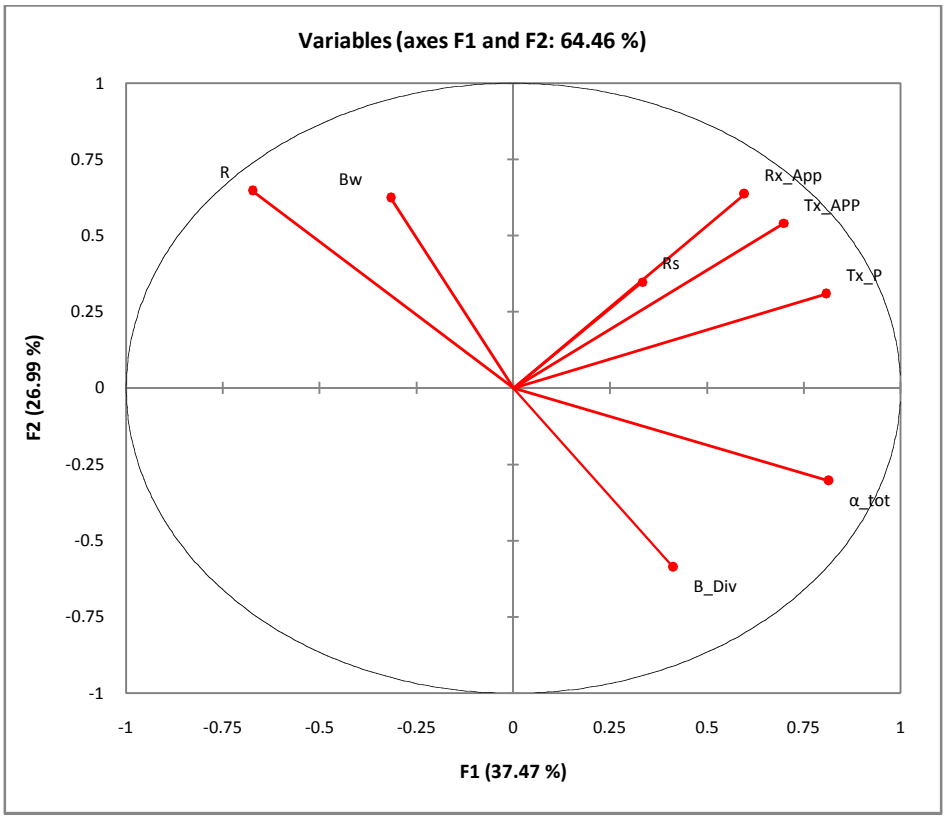

Figure 6.4 Behavior of Parameters Inside principal Components.

The selected data are separated into three categories: A, B, C. Each category corresponds to the dataset combinations that lead a certain BER. The data sets that make up factors F1 and F2 are depicted in Figure 6.5. F1 and F2 are the principal components that included the majority of samples obtained from the combinations of parameters in Table 6.10. correlation between variables and factors shown in Table 6.14 describes the 106 sets when being projected on the principal components of the new defined basis.

Table 6.14 Categories of Data Sets.

Category	BER Range	F1	F2	F3	F4	F5
A	$[1x10^{-10}$- $1x10^{-09}]$	1.061	0.708	0.806	0.975	1.132
B	$[1x10^{-09}$- $1x10^{-08}]$	0.99	1.344	0.94	1	0.934
C	$[1x10^{-08}$- $1x10^{-06}]$	0.426	1.048	1.384	0.694	0.292

The new basis doesn't highly favor the case here since the problem does not aim at dimension reduction; however, throughout the process of PCA, the correlation matrix is built in 6.13 giving considerations to all factors and correlating the parameters of link importance. Nevertheless, if only factors 1 and 2 (F1, F2) are to be considered, the samples cover about %65 (Figure 6.5) of the overall population. Limiting the analysis on the majority of samples and not all of them, simplifies the analysis and correlates variables with at least %65 accuracy depending on the problem considered.

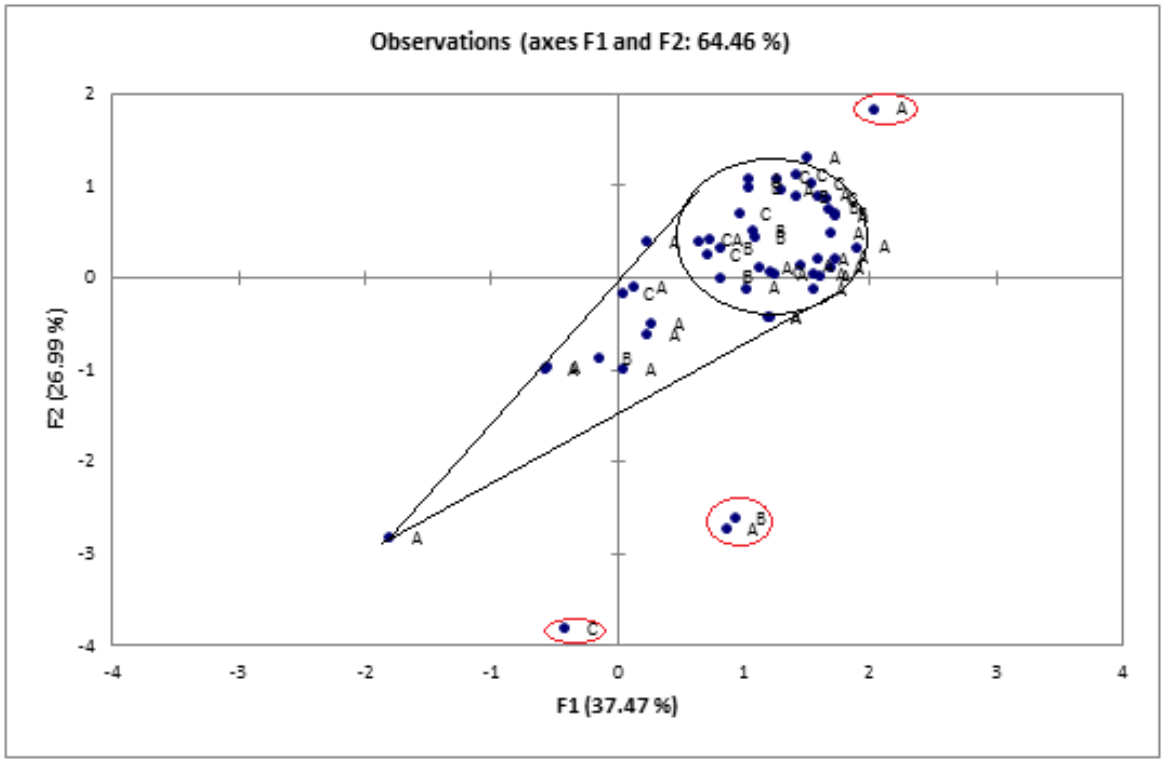

Figure 6.5: Data sets as they appear when projected to F1 and F2 Components.

Figure 6.5 shows the sample space of the datasets and their category (Table 6.14) when represented in the first two principal components. The samples not being shown with the majority are considered as outliers, they show an extreme low and high BER, lower than 10^{-11}, and higher than10^{-06}, for the 3A, 1C, and 1B samples. The 1B sample is not clearly justified, which leaves the discussion that the pattern that it has in the parameters is a bit stranger from the rest of the samples. However, the majority of the samples could be represented in a cone shape in the right-upper part of the plane which means that most samples have similar pattern and could also be followed if 65% accuracy is enough for the considered application.

6.3.4 Interpretation of Results as Reflected on Link Parameters

The data sets used for this analysis are restricted to the ones that lead a BER less than 10^{-06} at the receiver photodiode. The objective here is to extract the implied relationships among parameters based on the genetic selection algorithm implemented in chapter 5. The purpose is to set up certain criteria of selection, which at pre-installation, makesthe designer aware of certain considerations while selecting the parameters of an optical wireless link in the outdoors environment. The percentage contribution of every parameter is studied and shown in Table 6.15. Being represented in the factor analysis, Table 6.12 has shown the correlation of each variable with the principal component. Although some results are relatively similar such as:$Tx\_APP, Rx\_App, Tx\_P, and\ \alpha\_tot$, the effects of Bw and B_div have not been given enough interest, which makes the analysis on the correlation matrix itself more reliable. The correlation matrix correlates two variables at their intersection point. For instance, the i^{th} parameter is correlated to the j^{th} parameter, or vice versa, by the $[i, j]$ entry of the correlation matrix. Data analysis of the correlation matrix and Figure 6.4, shows that the receiver aperture is negatively correlated with the distance between the transmitter and the receiver. It doesn't mean that they are almost inversely proportional, but the overall contribution of these two parameters when compared against each other is differed by a factor of (-0.147). So that in most of the times, when the whole set is considered, a change factor of one of them implies a force on the change of the other by a value of -0.147. In the same time, the change in the receiver aperture is highly correlated with a factor of 0.716 to the change of the transmitter aperture for maintaining a low BER, which also makes sense. Moreover, the transmitted power is highly correlated with the receiver aperture,

transmitter aperture, and the total attenuation with factors of 0.628, 0.597, and 0.663 respectively, which means that the three of them are to be considered relatively equally when deciding about the channel parameters. The electrical bandwidth used in the channel has low correlations with all the variables, except the total attenuation and the range, which makes the selection of bandwidth more restricted to one parameter, that is; the distance between transceivers. Similar analysis goes for the beam divergence, being highly correlated to the distance as well with a factor of (-0.634). The responsivity of the receiver is mostly correlated to the transmitter and receiver aperture with factors of 0.413 and 0.298; however Figure 6.4 shows that it has minimal correlation, being orthogonal, with the range of the optical wireless link and the beam divergence. The bandwidth and the beam divergence are oppositely correlated with ($\theta = 180°$) and so is the range and the total attenuation, which both make sense in the optical wireless link. Therefore, the magnitude of the vector shows the variability or the effect that each parameter adds to the channel and the angle (θ) determines how correlated are the variables. Consequently, Figure 6.4 and Table 6.13 show good illustration of the parameters in the channel, which when selected accordingly, leads the maximum likelihood for the channel to achieve a BER lower than 10-6. As a conclusion PCA is not intended to show the real relations of the parameters as they exist in the channel, but it is more restricted to forcing a correlation among them that achieves an acceptable channel performance.

Table 6.15 Percentage Contribution of Parameters.

Parameter	Tx_APP	Rx_App	B_Div	Tx_P	Rs	α_tot	R	Bw
Summative Contribution	3.463	3.076	2.639	3.508	2.199	3.599	3.428	2.592
% Contribution	0.141	0.125	0.107	0.143	0.089	0.146	0.139	0.105

6.3.5 Validation of Results

It is in the designer's interests to realize the direction (increase, decrease) of the correlation. The matrix shows the correlation recommended when choosing parameters, but doesn't specify whether the designer has to increase or decrease the value. It also satisfies the results obtained in Figure 6.1 about the strength of each parameter but with more detail. The negative and positive signs that appear next to the correlations are mostly logical, as in real optical wireless channels, but the selection also requires enough experience when managing the correlations. There could be more than one combination that leads to a $BER < 10^{-06}$, but, as long as a promising result is achieved, it means that the solutions recommended from the correlation matrix are verified. The data samples chosen for testing here start with an arbitrary value, and since analysis is limited to some practical parameter ranges in the optical wireless channel, it is mostly unlikely that the designer wishes to increase the RX_APP with a factor of 0.716 (or any other factor) if the obtained value will exceed the channel constraints (say more than 40cm as RX_APP). For the analysis carried out in this chapter, a table of parameter industrial ranges that are considered appears in Table 6.16.

Table 6.16 Range of Considered Link Parameters.

X1: Tx aperture (cm)	2 - 16
X2: Rx aperture (cm)	7.5 - 40
X3: Beam divergence(mrad)	0.5 - 5
X4: Transmitted Power	15.6 – 480 mW
Wavelength (nm)	700 - 1600 (X5-related)
X7: Range (km)	0.01 - 3 or more
Bitrate (Mbps)	BW dependent (>100Mbps)
X5: Rx responsivity (A/W)	0.4-0.8
X6: Overall Attenuations (dB/km)	1-40
X8: Bandwidth (MHz)	100-500Mhz

The correlation matrix was tested on a data sample and applied to the optical wireless model following an OOK-modulation technique, the Signal to noise ratio being calculated from the proposed parameters according to (6.8), and then a complementary error function converts it to BER. The results appear in Table 6.17, where σ_1 and σ_0 are functions of X_8 and other parameters explained in chapter 5.

$$SNR = \frac{\left(2\, X_5 \left(X_4 \cdot \frac{{X_2}^2}{(X_1 + X_3 * X_7)^2} . 10^{\left(-X_6 \frac{X_7}{10}\right)}\right)\right)^2}{\sigma_1^2 + \sigma_0^2} \qquad (6.8)$$

The testing presented in Table 6.17 shows results based on which parameters the designers have restrictions. In some optical wireless applications, the channel could be constrained at certain RX_APP, TX_APP, etc, which means that all other parameters are adjusted, based on the initial consideration. Assuming there is more than one constraint, the designer has to find a way between the corresponding rows of correlation entries between the variables. In case the channel is equipped with a re-configurable hardware,

adjusting all parameters would not be a problem, which will help the channel to remove all the link constraints and achieve the best of this work.

Table 6.17 Validation of the correlation Matrix Results.

Validation Using Correlation Matrix	**Parameter Values After correlations applied**	**BER and Remarks**
Using advice of TX_APP	X1 = 0.1474; X2=0.636; X3=2.24; X4=446.7; X5=0.693; X6=25.49; X7=1.5821; X8=2.24;	3.2875e-05. The BER could be better but analysis began with a large transmitter aperture, which led to a very large RX_APP, which is a practically difficult case. Moreover, the category falls beyond the guaranteed margin achieved in section 6.2.8.
Using advice of RX_APP	X1=0.041; X2=0.3708; X3=1.89; X4=438.25; X5=0.637; X6=25; X7=1.51; X8=1.71;	8.8779e-06. There are also other combinations that might lead to similar or better results following the same correlation row, but as long as the correlations is giving a 10^-06 range means that PCA analysis is reliable.
Using advice of TX_P	X1 = 0.054; X2=0.15; X3=1.86; X4=274.42 compensated to 30; X5=0.581; X6=6.8; X7=2.07; X8=2.10;	Achieves very low BER, which means that Tx_P could be well compensated to 30mW and still achieves 5.9265e-008.
Using advice of Rs	X1= 0.087; X2=0.2603; X3=2.537; X4=247.25; X5=0.491; X6=19.28; X7=1.453; X8=1.808 ;	1.0389e-008.

Using advice of BW	X1= 0.125; X2=0.325; X3=2.787; X4=253.64; X5=0.45; X6=27.56; X7=1.003; X8=1.9551 ;	Ideal BER< 1.00e-009, which means that the range could increase about 100m, or even worse weather conditions could be handled.
Using advice from B_DIV	X1= 0.108; X2=0.279; X3=2.43; X4=92.47; X5=0.514; X6=20.183; X7=0.54; X8=2.71 ;	Ideal BER< 1.00e-009, which means that more bandwidth could be used, and thus better bit rate.

6.4 Conclusion

This chapter aimed at showing the percentage contribution of each parameter to the channel performance. In the first part of the chapter, each parameters' effect on channel performance is recorded separately by narrowing the range of all other parameters so that the UBs and LBs are very close. It also analyzed the implicit relations that exist among data sets to achieve a certain bit-error-rate using multivariate statistical analysis. The analyses show that the study done in section 6.2 conforms with the multivariate analysis in evaluating the parameter's effect on channel performance, but the latter gives more detailed and numerical information. All parameters that could be controlled are considered, and the correlations could be utilized for advice at a pre-installation stage or at run-time if a reconfigurable hardware is controlling the change in parameter values. Chapter 7 will show a 2-stage modeling utilizing fuzzy-neuro hybrid algorithm to adapt the channel with the best-fit (optimal) parameters studied using the ASGA generated data.

References

[6.1] K. V. Mardia, J. T. Kent, and J. M. Bibby, "Multivariate Analysis", *Academic Press*, London, 1979.

[6.2] R. Wang, "Introduction to Orthogonal Transformswith Applications in Data Processing and Analysis"*Cambridge University Press*, Cambridge, 2012.

[6.3] S. Wold, K. Esbensen, and P. Geladi "Principal component analysis Original Research Article", *in Journal of Chemometrics and Intelligent Laboratory Systems*, Volume 2, Issues 1–3, 1987, pp. 37-52.

[6.4] The Pennsylvania State University, "Principal Components Analysis (PCA)", in STAT 505 - Applied Multivariate Statistical Analysis, 2013.

[6.5] A. El. Yakzan, R.J. Green, E.L. Hines and M. Ali, "An Intelligent Approach to Link Parameter Estimation for Outdoor Optical Wireless Channels", *in Proc. Of IEEE Conference Mediterranean Conference on Embedded Computing,* Montenegro, 2012.

[6.6]J. Shlens, "A Tutorial on Principal Component Analysis" Salk Insitute for Biological Studies and Institute for Nonlinear Science, University of California, San Diego, 2005.

[6.7] M. Richardson, "Principal Compnent Analysis". May 2009, Available: <http://people.maths.ox.ac.uk/richardsonm/SignalProcPCA.pdf>, Accessed [17 May 2013]

Chapter VII: Two-Stage Modelling: Artificial Neural Network for BER Prediction, and Adaptive Neuro-Fuzzy Inference System (ANFIS) for Channel Adaptation, Utilizing ASGA Generated Data

7.1 Introduction

Two techniques are proposed in this chapter: an artificial neural network, and an adaptive neuro-fuzzy inference system (ANFIS). The neural network is used for bit-error-rate prediction in the LOS outdoors optical wireless channel; the technique gives an estimation of the channel performance at pre-installation and at run-time. The ANFIS adapts the channel by looking attwo parameters: the distance between transmitter and receiver, and the total attenuations caused by the weather condition benefiting from the results achieved in chapter 6, section (6.2.8). Adaptation of the channel targets in this chapter the set of samples that lead a satisfactory performance at a minimum transmitted power, knowing that, in this technique, a re-configurable hardware is considered to be employed in the channel. The two stages are related, where the first can validate the choices of the second.

7.2 Artificial Neural Networks (ANNs)

Artificial neural networks (ANNs) are information processing systems that roughly simulate the biological neuron network system. It began in the 1950s by Frank Rosenblatt and his colleagues when they demonstrated the first application of pattern recognition using artificial neural networks. The usage of neural networks was limited because of the lack of ideas and powerful computers [7.1]; however, at the beginning of

the 1980's, the development of the back propagation algorithm for training multilayer perceptron networks (MLP) has increased their benefit, and, consequently, started to be applied in various areas of application, including aerospace, automotive, medical, agricultural, electronics, manufacturing, and telecommunications. Artificial neural networks have the ability to understand complex patterns with a high degree of accuracy, without any prior assumptions about the nature or distribution of data. They have non-linear tools that are good at predicting non-linear behaviours. Nowadays, neural networks solve several types of problems such as pattern classification, pattern association, pattern completion, filtering, optimization, adaptation, and automatic control. Neural networks are made up of two primary elements: the processing elements (neurons), and interconnections (links). Information processing occurs in the neurons which are grouped into hidden layers. Signals are passed between neurons over the connecting links, as shown in Figure 7.1[7.1].

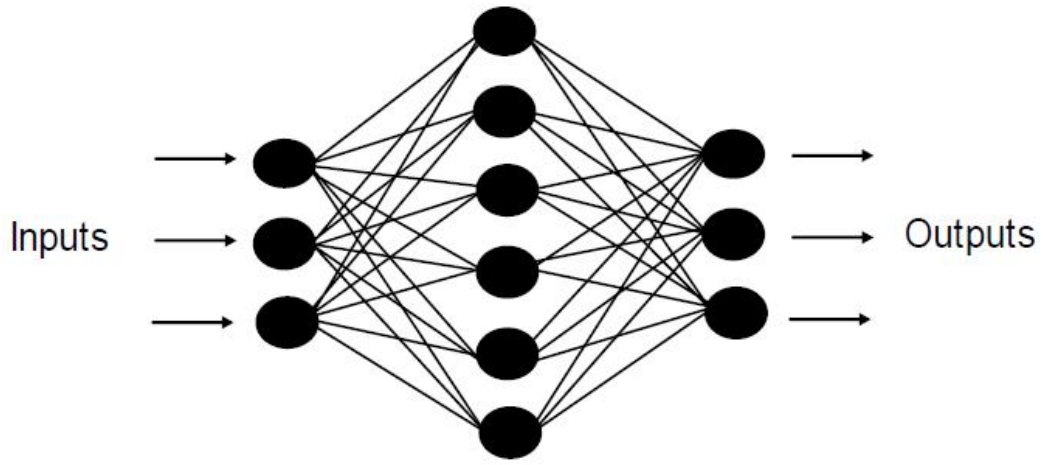

Figure 7.1A3-layer neural network. Inputs, middle layer, and outputs. The middle layer provides the connecting link between the input and output layers.

Example in Figure 7.1 shows three input neurons and three output neurons linked by a middle layer or layers, whose neurons are determined by trial and error during the

training or learning process. Each connecting link has an associated weight that multiplies the signal being processed, and each neuron applies an activation function to its net input to determine its output signal [7.1]. The middle layers are responsible for developing a relationship between the variables to satisfy a specific problem that the neurons are attempting to solve. This process is known as training, where the outputs are trained and react to the stimulus represented to the input neurons.

Neural networks are classified into two major categories on the basis of training methods: supervised and unsupervised. Unsupervised neural networks are those algorithms that deal with input data sets only where no feedback is provided to the network. Supervised Learning, on the contrary, requires both input and output to be presented to the network, in order to permit learning on a feedback basis and develop the desired network. The training process adjusts the weights of the links that give the desired output for the corresponding inputs. After the network is trained and the magnitudes of the weights that produce the desired output are setup, the resulting network can be used for prediction [7.2], [7.3]. Generally, a basic neural network looks like Figure 7.2.

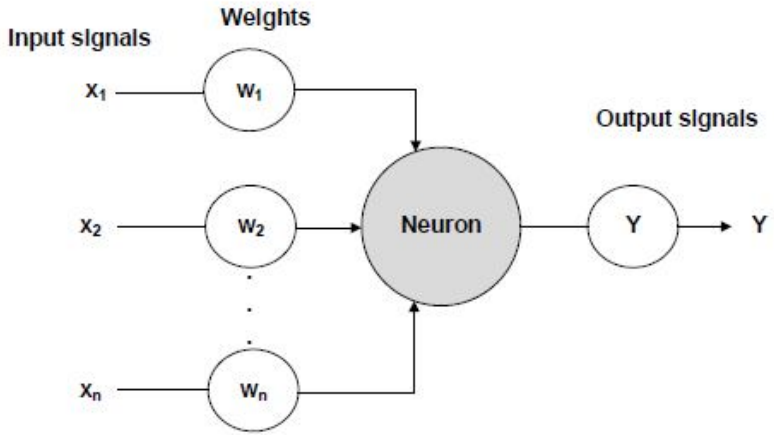

Figure 7.2 Basic single Artificial layer Neural Network (ANN) (adapted from [7.4]).

There are many types of neural networks, each targeted for special purposes [7.4], but the attention will be given to 'back propagation feed forward' network, where the input pattern is applied and forward propagated through the network using the initial node connection weights [7.6]. In this training algorithm, the weights and thresholds (if any) are initialized to a random value and activation functions are applied to the neurons. Consequently, the weights are updated accordingly to minimize the sum square error fed back in the network, using many different ways [7.7], and based on the number of neurons for each layer. All the above process is repeated until the sum square error is minimized to 0.001 or less [7.4], [7.5].

Generally, hidden layers increase the processing time, which means that the neural network is constructed so that it achieves a high level of accuracy at the minimum number of layers. According to a research studied in [7.8] and [7.9], one hidden layer could be sufficient to approximate any function, which contains a continuous mapping from one space to another in solving real life problems. The activation functions used with artificial neural functions are many, but only few are frequently applied in real applications, the activation functions are described in Figure 7.3 [7.4], [7.13].

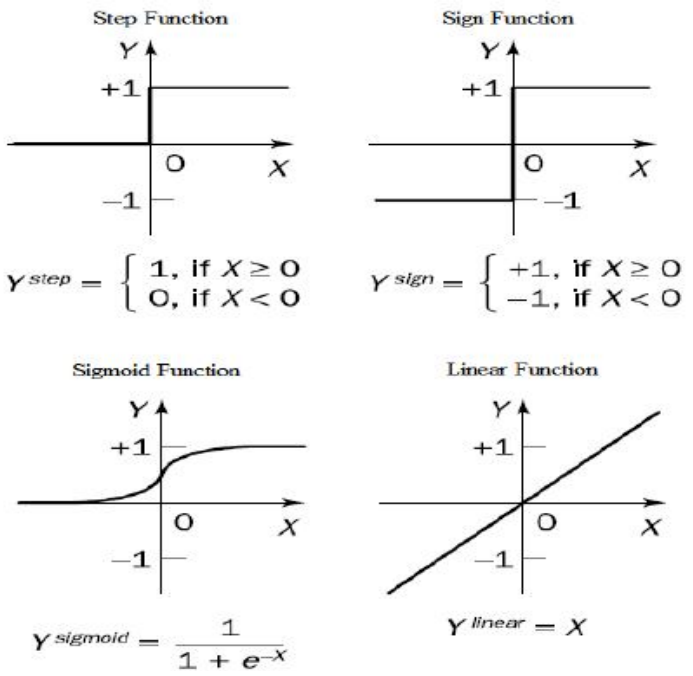

Figure 7.3 ANN activation function (adapted from [7.4], [7.13]).

Sigmoid and linear functions are mostly used as activation functions for the learning processes. As far as prediction is concerned, the most applicable technique for training the neural network is called the Levenberg-Marquadt (LM) technique. It is characterized by accuracy and fast performance; however, it explodsthe memory usage if the network is too complex. Although many learning techniques have been discussed in [7.7], the best training method, according to [7.14], is a multilayer network described by a 'steepest descent' method; but the final decision on the most appropriate neural network to use remains subject to the trial and error process that only depends on the problem itself, bearing the negative consequences that would arise from "overfitting" and causes the network to give a low learning rate and bad prediction [7.15], [7.16].

7.2.1 Why Use Artificial Neural Networks (ANNs)

Artificial Neural Networks (ANNs) are used in the LOS outdoors optical wireless channel because of theirreliability and performance in analysing a number of datasets that describe the parameters in the real channel. As they were successfully implemented in [7.17] and [7.18] and achieved reliability, it is of a great interest to design a prediction technique that is able to forecast the behaviour of the channel given some major link parameters. ANNs offer a very good local search method for finding a solution, and can be considered as a reliable method for BER prediction. After trying several techniques with a multilayer network, the highest regression rate was achieved with the Levenberg-Marquadt (LM) technique, and sigmoid activation functions. LM offered a fast convergence and low mean square error (0.01539). The sigmoid activation function provided a smooth non-zero derivative with respect to input data and also accelerated the learning rate of the network, which added efficiency to the system and resulted in a faster processing speed for the prediction system. The number of neurons used was 8, benefiting from [7.10], [7.11], [7.12], and decided after several training processes based on a 'rule of thumb'.

7.2.2 Prediction Technique Using ASGA Datasets

162 data samples are generated by the application-specific genetic algorithm with combinations that lead good and bad solutions, in order to teach the neural network the different parameters affecting the performance of the outdoors optical wireless channel. The data sets are samples covering the overall combinations of parameters. Unlike PCA, the prediction technique achieved by artificial neural networks is not based on statistics,

but on non-linear relationships that the network extrapolates from inputs and outputs. The samples are standardized and the network applies a supervised learning process benefiting from the ASGA data. The network learns how to calculate the signal-to-noise ratio from several combinations of inputs, which is then transformed to BER for comparison, using the complementary error function. After trying different training, adaptation, performance, and transfer functions, the specifications of the neural network that were most appropriate to BER prediction appear in table below:

Table 7.1 Specifications of ANN used for BER prediction.

Network Type	Feed-Forward Back Propagation
Training Function	TRAINLM
Adaptation Learning Function	LEARNGDM
Performance Function	MSE
Number of Layers	2
Number of Neurons	8
Activation Transfer Function	TANSIG

7.2.3 Simulation Results: Training, Validation, and Testing

The neural network consists of 3 layers; one input layer, one hidden layer, and one output layer. This doesn't contradict the result producted by the neural network toolbox in matlab (Table 7.1). This is because Matlab considers an output layer before data are processed to the output, where this layer has the same dimensions of the output.The division of data sets for the training process uses 70% for training, 15% for validation, and 15 % for testing using the LM learning method. The ANN is modelled with 8 neurons in the hidden layer, and one neuron at the output layer, both layer having the

same activation function (the tangent sigmoid function), which is capable of finding the solution in wide range of –1 to 1. The number of iterations of the ANN was set to 1000 epochs; it terminated at 25 epochs after the result of the validation error check reaches as low as possible. Validation of error check occurs to prevent the over-fitting of the network by stopping the training at the minimum of the validation error [7.7], showing 6 validation checks in figure 7.6, the summary of the ANN simulation model appears in Figure 7.4 and the best validation performance happens at epoch 19 as shown in Figure 7.5.

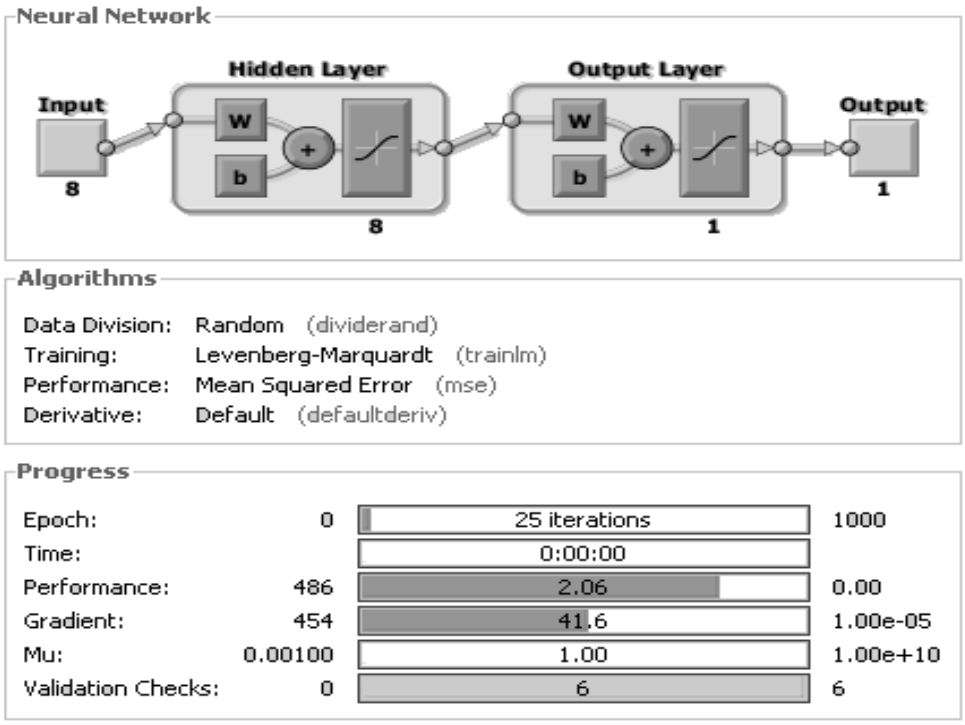

Figure 7.4 Modelling Summary of ANN.

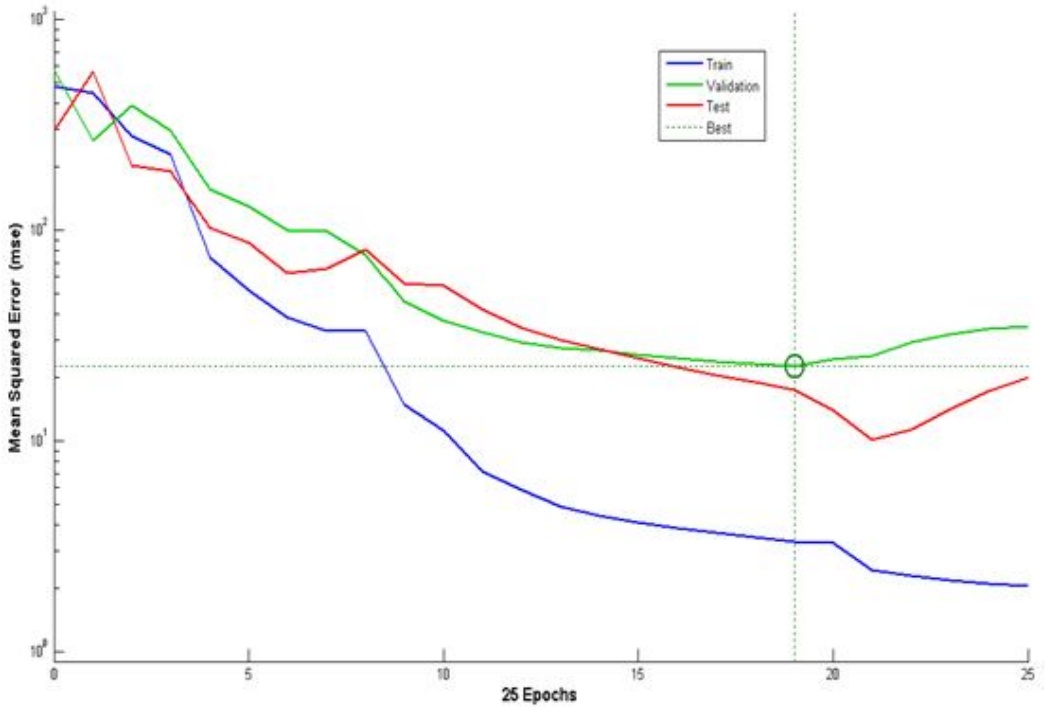

Figure 7.5 Best Validation Performance is 22.627 at Epoch 19.

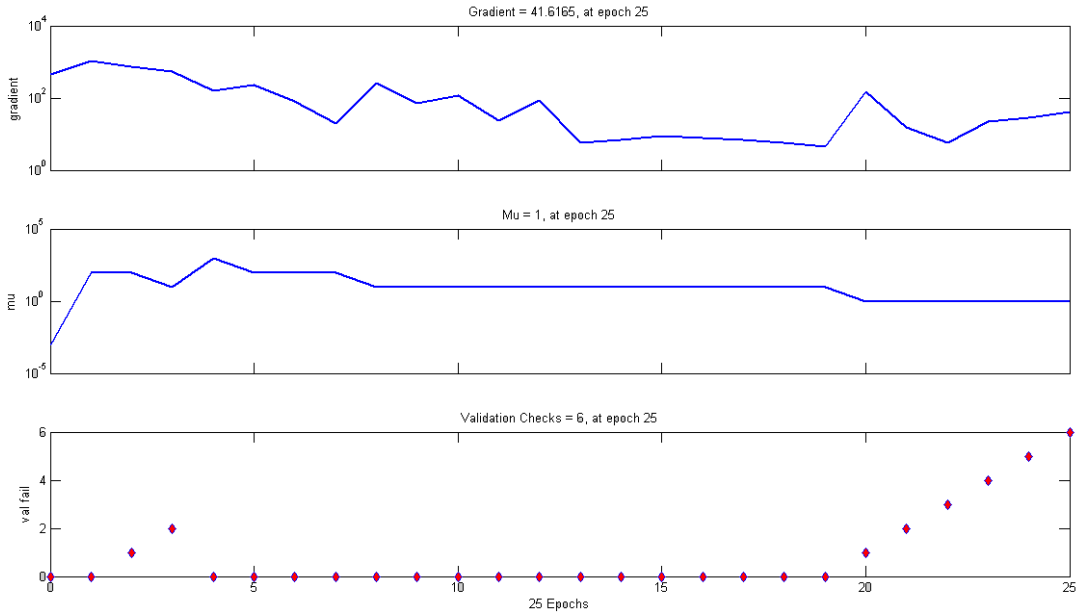

Figure 7.6 Validation Checks after ANN Modeling.

The performance of the ANN model shown in Figure 7.7 shows a satisfactory overall regression rate of 98.46%. The performance of the ANN used for BER prediction aims at minimizing the mean square error (MSE) by iterative learning in the feed-forward

back propagation network. The MSE at each iteration is calculated from the square difference between the predicted (estimated) value ($\breve{y}_i$) of BER and the actual value (Y_i), such as:

$$MSE = \frac{1}{n}\sum_{i=1}^{n}\left(\breve{y}_i - Y_i\right)^2 \tag{7.1}$$

The regression model is able to identify the extent to which the mean square error is reduced. In other words, the higher the regression rate (R), the lower the error. Figure 7.7 shows the regression (R) performance plot. This shows that the model gives good accuracy in predicting the BER, based on the parameters of major link importance in the optical wireless channel.

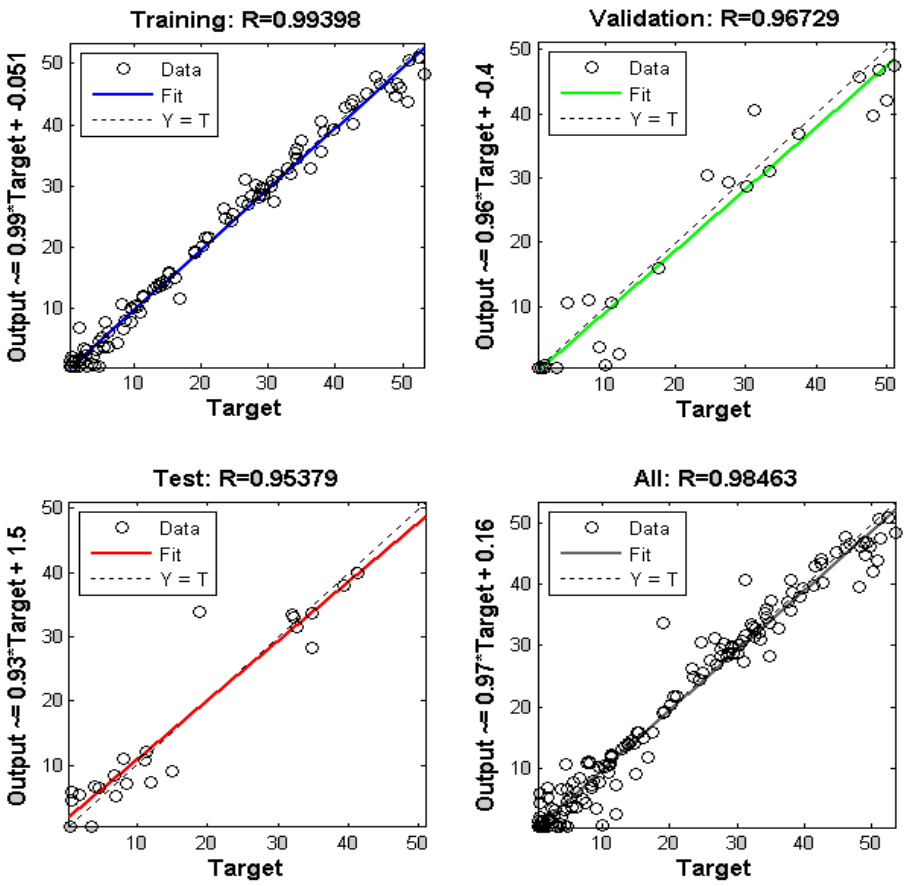

Figure 7.7 Overall regression for: Training, Validation and Testing.

7.2.4 Validation of Results

Table 7.2 ASGA Parameters Used for ANN Result Validation.

S1	0.147	0.37	1.955	274.428	0.491	20.183	1.582	195.5
S2	0.156	0.3927	1.9888	293.6	0.4978	20.1957	1.5955	359.55
S3	0.139	0.3521	1.9263	258	0.4853	20.172	1.5205	437.05
S4	0.14	0.355	1.9307	260.5	0.7446	20.1737	1.7446	499.72
S5	0.109	0.2826	3.7353	6.74	0.6555	20.1313	0.8466	446.39
S6	0.082	0.3831	3.0681	48.96	0.6896	20.0951	2.0896	308.96
S7	0.143	0.3516	2.2766	192.55	0.7851	20.1717	1.6053	242.55
S8	0.032	0.0901	2.3011	72.04	0.5903	20.1244	1.0204	230.11
S9	0.024	0.2472	4.003	5.14	0.412	10.003	1.06	100.03
S10	0.106	0.2768	4.0621	8.1	0.6484	10.0621	1.2418	100.62
S11	0.0202	0.3521	0.5055	300.5528	0.7011	20.0121	2.7033	100.11
S12	0.1228	0.3136	4.4685	7.6083	0.6937	10.0734	1.4685	100.73

Table 7.3 Validation: ANN-BER and SNR Prediction as Compared to Actual Values.

Sample	**ANN Predicted SNR**	**Actual SNR**	**ANN Predicted BER**	**Actual BER**
S_1	43.76	42.96	1.85E-011	2.78E-011
S_2	29.80	27.78	2.39E-008	6.77E-008
S_3	31	31.45	1.29E-008	1.01E-008
S_4	3.37	3.30	0.032	0.0345
S_5	4.925	4.93	0.0132	0.0132
S_6	8.80E-04	8.82E-04	0.4882	0.4881
S_7	10	10.06	7.8270e-004	7.53E-004
S_8	7.19	7.22	0.0037	0.0036
S_9	30	30.86	2.1602e-008	1.38E-08
S_{10}	38.03	37.97	3.47E-10	3.58E-010
S_{11}	0.13	0.1357	0.3592	0.3563
S_{12}	7.216	7.22	0.00361	0.0036

7.3 Adaptive Neuro-Fuzzy Inference Systems (ANFIS)

Adaptive Neuro-Fuzzy Inference Systems are hybrid algorithms combining the high level reasoning capacility of the Fuzzy Inference System (FIS), and the low level computational power of a Neural Network (NN) [7.21]. Using this hybrid algorithm, the NN can recognize patterns and help with the adaptation of the environment, whilst the FIS will incorporate human knowledge and perform decision making.

The ANFIS architecture consists of five layers as shown in Figure 7.8. The first layer is an 'If' layer (fuzzification layer), and functions as an adaptive node. It converts crisp inputs to fuzzy inputs, and it also generates the membership function (MF) for each of the inputs [7.19]. The most common MFs being used are the trapezoidal and triangular functions (*trapmf, trimf*). In ANFIS however, the most common MF is the generalized bell function (*gbellmf*), which is shown in equation (7.2), [7.20]. The type of MF can also be varied depending on the data being applied to the system.

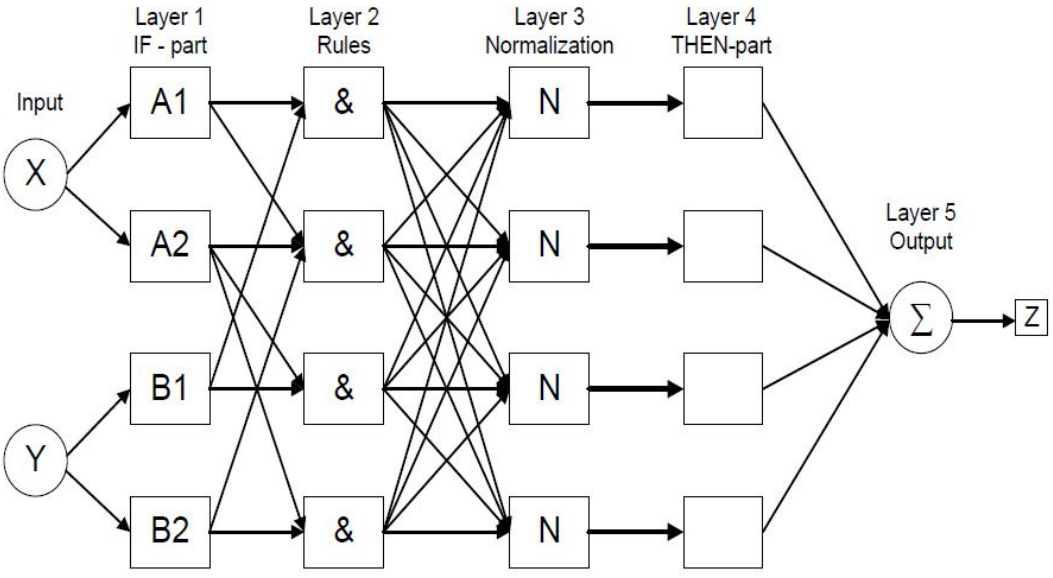

Figure 7.8 Architecture of a 2 input ANFIS (adapted from [7.20]).

$$\mu_A(x) = \frac{1}{1 + |\, x - c_i|^{2b_i}}$$

$$O_{1,i} = \mu_{ai}(x), i = 1,2$$

$$O_{1,i} = \mu_{bi-1}(y), i = 3,4 \tag{7.2}$$

where$x$ or y is the input node i; $ai, bi\ and\ ci$ are the parameter set and O is the output for the node. The next layer is a simple multiplier that represents the firing strength of each rule generated in layer 1 using "AND" as a connective product.

$$O_{2,i} = W_i = \mu_{Ai}(x), \mu_{Bi}(y), i = 1,2 \tag{7.3}$$

In layer 3, each output of the second layer will be normalized based on the ratio of each of the firing strengths divided by the total rule of the firing strength [7.13], [7.21], the normalization is based on equation (7.4).

$$O_{3,i} = \overline{w_i} = \frac{w_i}{W_{1+}\, W_2} = ,\ i = 1,2 \tag{7.4}$$

Layer 4 consists of a Takagi-Sugeno type of output which converts all fuzzy data to crisp data, and the output is therefore represented as (7.5) [7.13], [7.21].

$$O_{4,i} = \overline{w_i} = \overline{w_i} f_i = \overline{w_i}\ (p_i\, x + q_i\, y + r_i\,) \tag{7.5}$$

Where $[p_i\,, q_i\,, r_i\,] = consequent\ parameter$. Finally, the total of all neurons in layer 4 forms the output of the ANFIS.

7.3.1 Why Use ANFIS?

The selection has been previously verified in chapter 5 with an application-specific genetic algorithm, which basically works at pre-installation level and suggest appropriate changes at run-time. However, there was a necessity to use the datasets suggested by ASGA to adapt the optical wireless channel. The selection of the parameters for adaptation is not a pre-defined process, and could always change with the

limitations of the link itself. Knowing that there's a mutual agreement that the transmission power is an important factor such that most companies, like CableFree and LightPointe, try to minimize, due to optical legislations and eye safety regulations, it is important to design an adaptive model that works at state-of-the art technology, transferring 1Gbps at the minimum transmitted power. However, to maintain the transmission at optimal power costs, there should be a possibility of having an adaptive hardware able to control 4 parameters, being: the transmitter aperture, the receiver aperture, beam divergence, and responsivity of the photodiode (wavelength related). Consequently, fuzzy logic is used for decision making, based on monitoring the range-attenuation characteristics benefiting from results obtained in section 6.2.8, to decide about the 4 mentioned parameters plus the minimum power needed for obtaining an acceptable channel performance ($BER \leq 10^{-09}$).

Using a Fuzzy Inference System (FIS), the channel computes the membership function parameters that best allow the system to track the given input/output data and chooses correspondingly the appropriate solution sets at certain range-attenuation characteristic. The membership functions are tuned (adjusted) using a hybrid algorithm that combines "gradient descent" and "the least-square" methods. This adjustment allows the fuzzy system to learn from the data being modeled, knowing that the ANFIS may encounter slow learning and will use up its available memory if more than 9 inputs are used, where the generated rules for the system may become more than 2000 [7.21].

7.3.2 Implementation of Fuzzy Inference System (FIS)

The block diagram of the FIS consists of two parameters and one output. The output could be one of 12 suggested samples, the criteria of decision are obtained based on

minimum power requirements, and the channel is adapted according to the range-weather fuzzy rules from a sugeno-type system that appears in Figure 7.9.

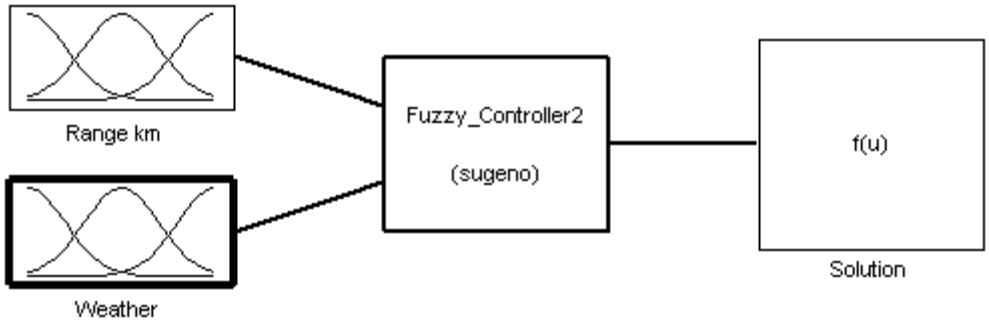

Figure 7.9 Block Diagram of FIS Controller.

The membership functions of the input variables are bell-shaped *(gbellmf)*, the range has 3 states: Low (0.5-1km), Medium (1-1.5km), and High (1.5 to 2km), and the weather is classified according to a visibility model discussed in chapter 4 with 4 states: Clear (1-3 dB/km), Haze (3-17dB/km), Fog (17-29dB/km), and Thick Fog (29-40dB/km). The input variables are shown in figures 7.10 and 7.11. The fuzzy rules used in decision making are shown in figure 7.12.

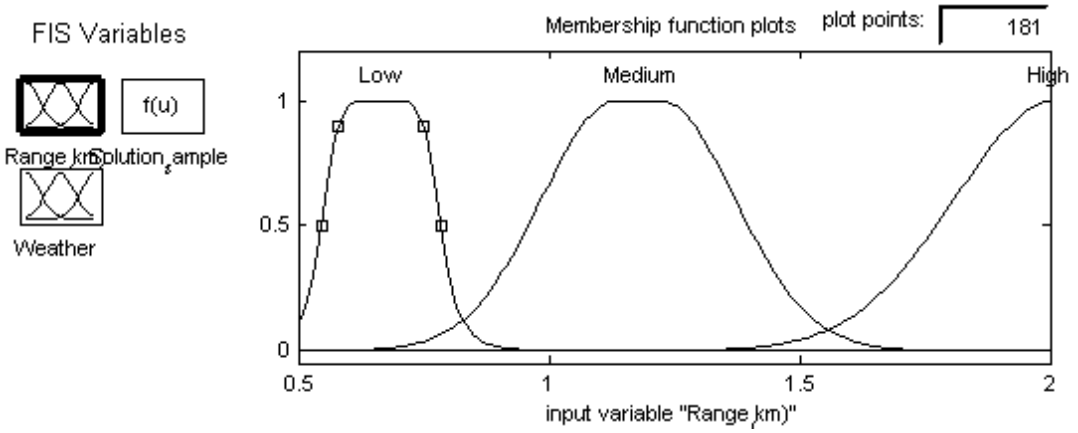

Figure 7.10 Membership Functions of Input Variable1 Range (Km).

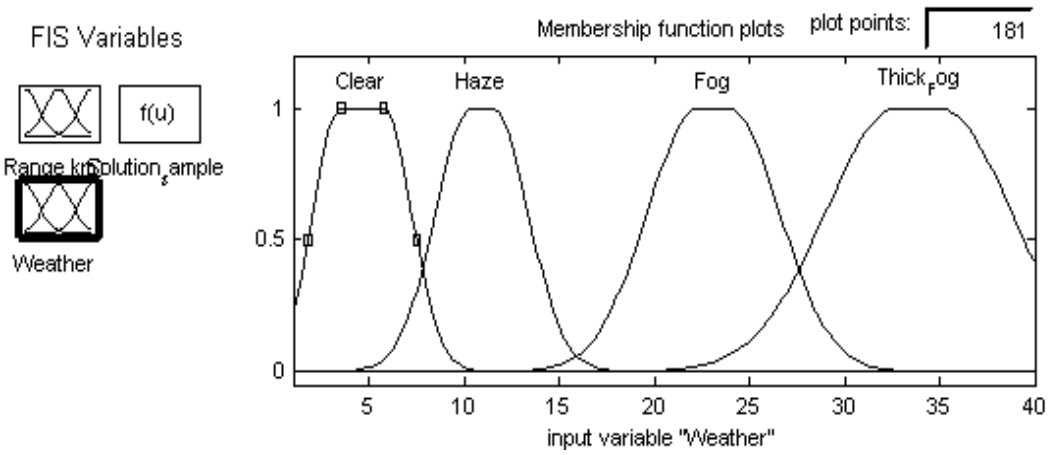

Figure 7.11 Membership Functions of Input Variable2 Attenuation (dB/km).

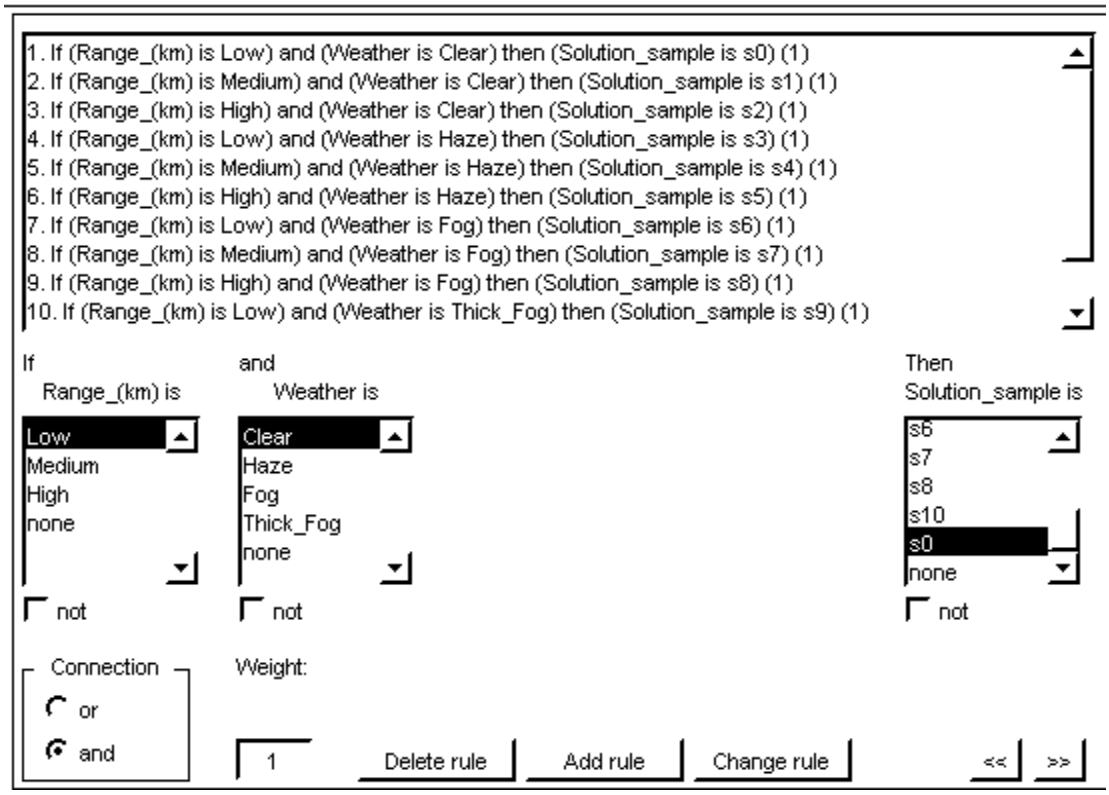

Figure 7.12 Fuzzy Rules of for Range-Weather Control.

The Output of the fuzzy inference system is described in a 3D-shape surface, linking the change of output samples with the range-weather fuzzy rules, as shown in figure 7.13.

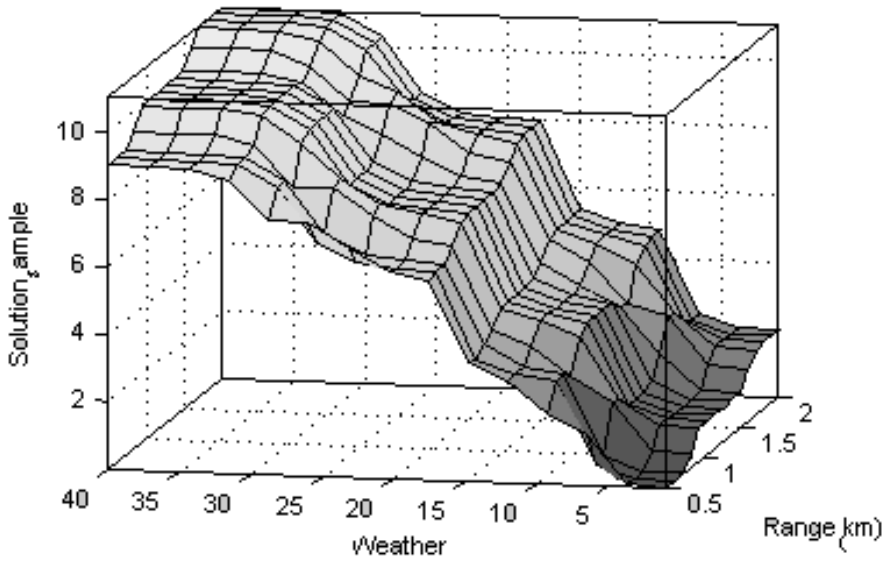

Figure 7.13 Surface Viewer of the Fuzzy Controller.

The sugeno-type FIS used as a decision maker of ANFIS is modeled to give a constant output, where it refers to the number of sample solution made from decision making. The testing of FIS appears below.

Table 7.4 Testing of FIS on Independent Data.

Weather (dB/km)	Range (km)	Decision	Actual
31	1.94	10.7	11
10	0.6	2.9	3
9	1.2	4	4
8	1.8	5	5
15	0.9	2.85	3
21	1.5	7	8
39	0.71	9	9
29.5	1.01	10	10
36	1.5	11	11
23	1.4	6.9	7
20	0.9	5.5	6
2	0.5	0	0
38	0.93	9	9
30	1.67	11	11
20	1.42	7	7
10.8	0.78	3	3
2.6	1.6	2	2
1.5	1.3	1	1

Table 7.4 Testing of FIS on Independent Data

(Contd.).

Weather	Range	Decision	Actual
10	1.6	5	5
2.5	0.9	0	0
3.2	1.7	5	5
10.5	0.8	3	3
3.2	1.5	4	4

7.3.3 Training Data with ANFIS

The data inputted to the ANFIS system are generated by the ASGA for different types of weather conditions, based on an attenuation factor. The sample decided in solutions of Table 7.4 are generated according to the best-fit parameters at a minimum transmitted power; knowing that the electrical bandwidth is fixed to 500MHz aiming at 1Gbps bit-rate for a state of the art transmission in the optical wireless channel. The ANFIS structure for the channel adaptation is shown in figure 7.14.

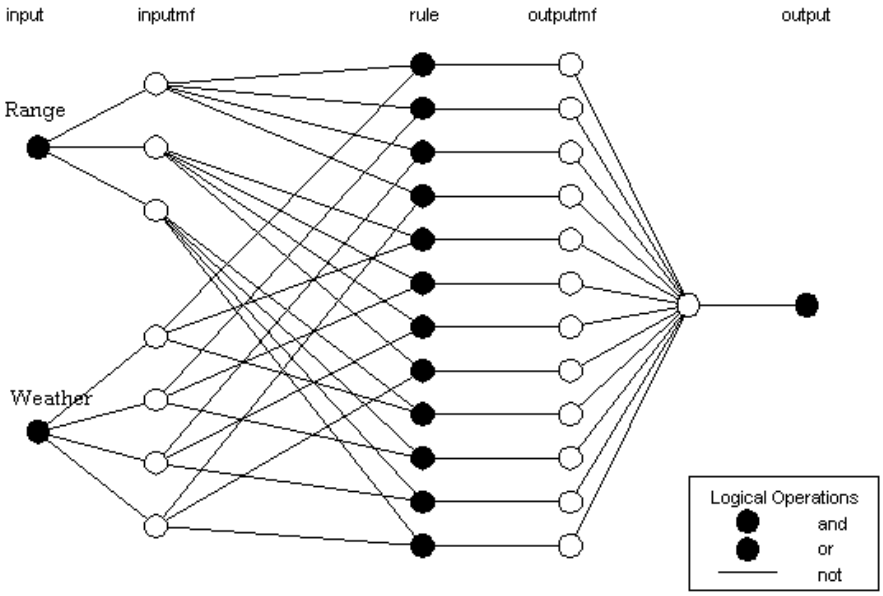

Figure 7.14 Structure of ANFIS after modeling.

The system is ready for training, the data are standardized and fed to the ANFIS system, and they appear as in Figure 7.15. The data is trained, by loading the FIS system built before to the system. The training process happens during 100 epochs, where the training error reaches a global minimum at about 34 epochs, where it continues constantly until the end of the training process. The ideal error usually targeted by ANFIS is zero; however, this is not practically achievable.

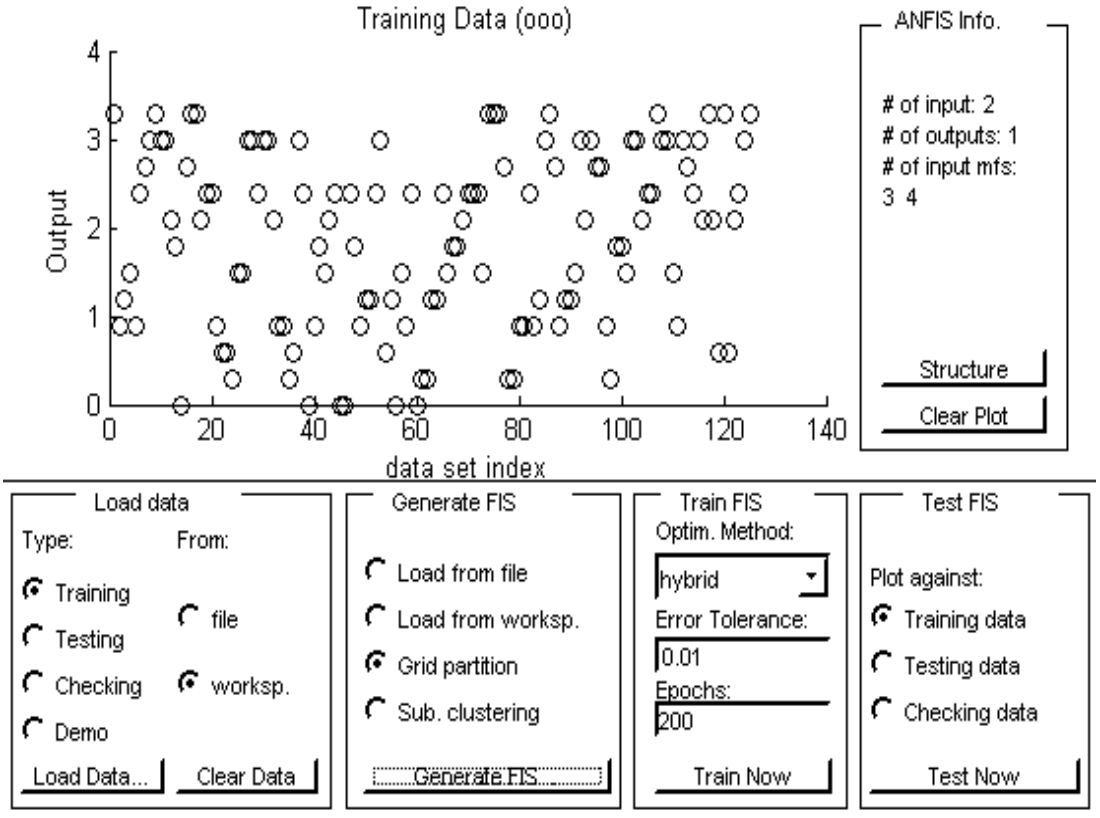

Figure 7.15 Training Data to ANFIS.

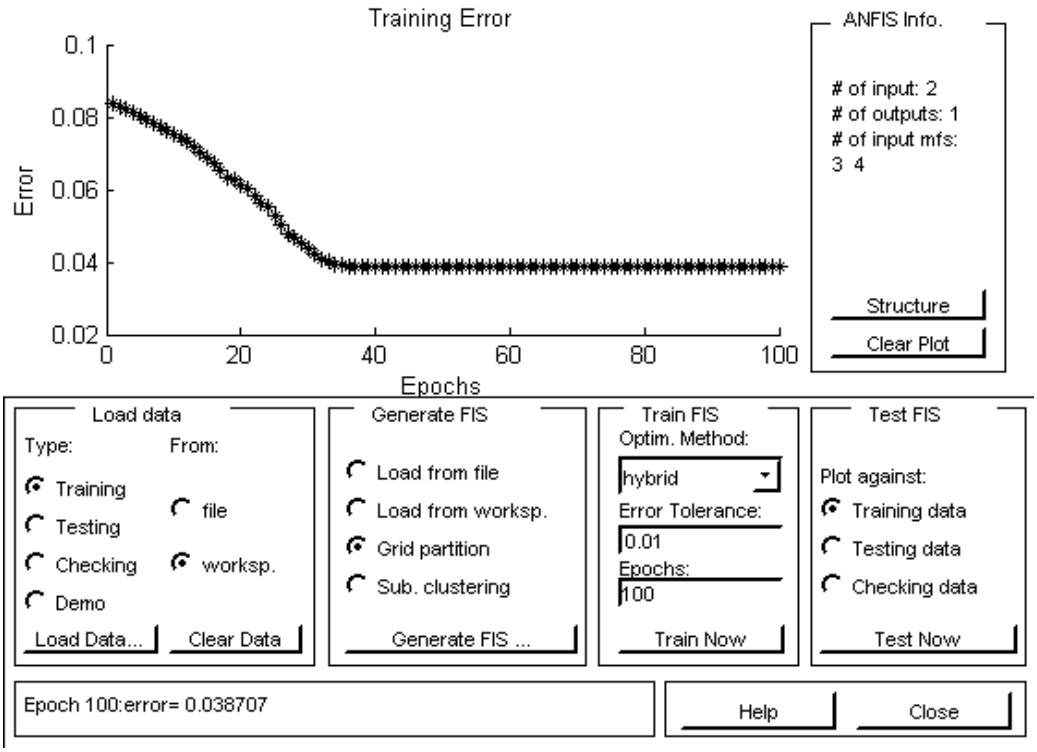

Figure 7.16 Performance of Training Error Versus Epochs.

By applying independent testing data to the ANFIS, it is shown that the channel adapts itself at approximately 97% of the data, which verifies its reliability for future use in the optical wireless channel if a reconfigurable hardware is deployed by subsequent researchers.

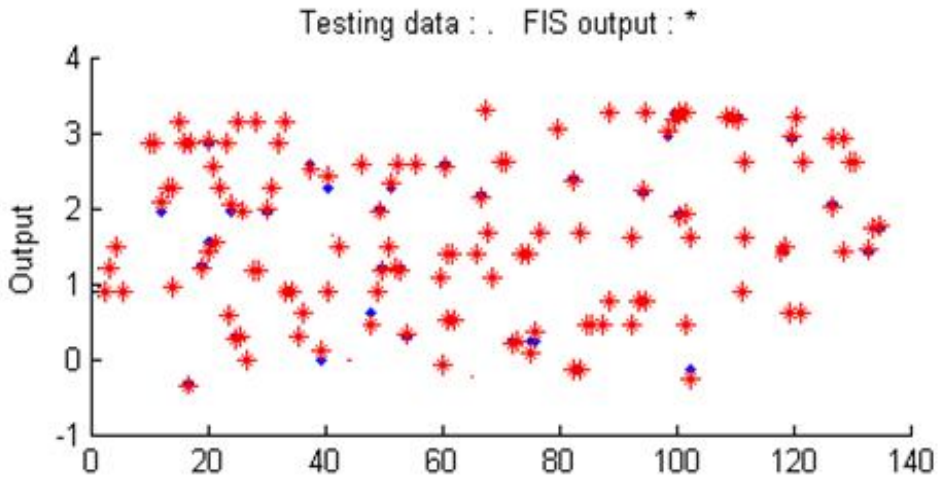

Figure 7.17: Testing Data on ANFIS.

7.3 Conclusion

This chapter presented two intelligent techniques to maximize the benefit of the results obtained from the application-specific genetic algorithm. The artificial neural network in the first part is capable of estimating the BER for any shape of optical wireless transceivers having the same effective area. The adaptive neuro-fuzzy inference system (ANFIS) is used for adaptation at run-time with adaptive hardware. This opens a new area of research for building hardware able to adapt its shape with the needs of the channel.

References

[7.1] M.T. Hagan, H.B. Demuth, M. Beale, "Neural Network Design", *PWS Publishing Company*, 1996.

[7.2] E. Llobet, E. L. Hines, J. W.Gardner, and S. Franco, "Non-destructive banana ripeness determination using a neural network-based electronic nose", *in journal of Measurement Science and Technology*, Vol. 10 538, 1999.

[7.3] J.W. Gardner, E.L. Hines and H.C. Tang, Detection of vapours and odours from a multisensor array using pattern-recognition techniques: Part 2: Artificial neural networks 1991, Sensors & actuators B, Vol 9, No 1, pp9-15.

[7.4] M. Negnevitsky, "Artificial intelligence A guide to intelligent systems", *Addison-Wesly*, 2005.

[7.5]S. Judd, Learning in neural networks, in Proc. 1st Annual Workshop on Computational Learning Theory, Morgan Kaufmann, San Mateo, CA, 1988, pp. 2-8.

[7.7] H. Demuth, M. B. 2004. Neural Network Toolbox: For use with Matlab.

[7.6] S.A. Shearer, T. F. B., J.P. Fulton, S.F. Higgins, "Yield Prediction Using A Neural Network Classifier Trained Using Soil Landscape Features and Soil Fertility Data", *in ASAE (ed.) Annual International Meeting. Midwest Express Center, Milwaukee, Wisconsin: ASAE*, 2000, Ch2, pp. 56.

[7.8] D.Foster, J. Mccullagh, & T. Whitfort, "Evolution versus training: an investigation into combining genetic algorithms and neural networks": in Neural Information Processing, *Proceedings of International Conference on Neural Information Processing, 1999* , 848-854 vol.3.

[7.9] F. Zhang, "Intelligent Feature Selection for Neural Regression Techniques and Application", Doctor of Philosophy, University of Warwick, 2011.

[7.10] A. Weigend, "On overfitting and the effective number of hidden units", *in Proceedings of the 1993 Connectionist Models Summer School*, 1994.335-342.

[7.11] S. Geman, E. Bienenstock, R. Doursat, "Neural networks and the bias / variance dilemma, *in journal of Neural Computation*, *MIT Press Cambridge*, MA, USA, 1992, vol.4, pp. 1 – 58.

[7.12] I. V. Tetko, D.J. Livingstone, and A.I. Luik, "Neural Network Studies.1. Comparison of Overfitting and Overtraining", *in journal of J. Chem. Info. Comp. Science*, 1995, 35**,** 826-833.

[7.13] J.-S.R. Jang, C.-T.Sun., E. Mizutani, "Neuo-Fuzzy and Soft Computing", *Prentice Hall*, 1997.

[7.14] B. Safa, A. Khalili, A.M. Liaghat and M. Teshnehlab, "Persentation Entitled Prediction of Wheat Yield Using Artificial Neural Network", *in poceedings of Conference on Agricultural and Forest Meteorology*, American Meteorological Society, 2003 .

[7.15] B. G. Kermani, S. S. Schiffman, & H. T. Nagle, "Performance of the Levenberg-Marquardt neural network training method in electronic nose applications", *Sensors and Actuators B: Chemical*, 2005, 110**,** 13-22.

[7.16] M. I. A. Lourakis, "A brief description of the Levenberg-Marquardt algorithm", 2005, Available: <www.ics.forth.gr/~lourakis/levmar/levmar.pdf>,Accessed[May 30, 2013].

[7.17] R. J. Pratap, S. Sarkar, S. Pinel, J. Laskar, and G. S. Ma, "Modeling and Optimization of Multilayer LTCC Inductors for RF /Wireless Applications Using Neural

Network and Genetic Algorithm", *in IEEE proc. of Electronic Components and Technology Conference*, 2004.

[7.18] S. Rajbhandari, M. Angelova, "The Bit Error Performance of Diffuse Indoor Optical Wireless Channel PPM System Employing Artificial Neural Networks for Channel Equalization", *Intelligent Modeling lab*, Northumbria University, UK, 2009.

[7.19] Y.-M. Wang & T. M. S. Elhag, "An adaptive neuro-fuzzy inference system for bridge risk assessment", *Expert Systems with Applications*, 2008, 34**,** 3099-3106.

[7.20] M. K. Abdul Kadir, E.L.Hines, S. Arof, D. Iliescu, M. Leeson, E. Dowler, R. Collier, R. Napier, K. Qaddoum, R. Ghaffari, "Grain Security Risk Level Prediction Using ANFIS", *in proceedings of 3rd International Conference on Computational Intelligence, Modelling& Simulation*, Malaysia, 2011.

[7.21] C. Potter, M. Negnevitsky, "ANFIS application to competition on artificial time series (CATS)", *In: Fuzzy Systems, 2004. Proceedings.2004 IEEE International Conference on*", July 2004, 469-474 vol.1.

Chapter VIII: Conclusions and Future Work

8.1 Introduction

This Chapter summarises the main findings of this research and presents the conclusions. It also includes suggestions for further research in the future.

8.2 Overview of the Main Research

The genetic algorithms (GAs) used in this thesis have demonstrated their adaptability and flexibility in the selection problem of the outdoors optical wireless channels. Also, the efficiency, in terms of time processing of the proposed genetic algorithm in tackling the specific problem, was verified.

This thesis has addressed its objectives by solving the problems below:

1) A first attempt has been verified with a genetic algorithm based selection technique for the transmission wavelength in the line-of-sight (LOS) optical wireless channels. It showed that a genetic algorithm is able to understand the instantaneous changes in the weather and apply it to select the most appropriate wavelength for transmission.
2) The genetic algorithm implemented in (1) was extended to include several parameters of link importance, and an application-specific genetic algorithm is defined for fast prototyping and ease of use with the specific problem. It has been compared against the complexity and reliability of the Matlab2011a GA Toolbox, and it has shown similar results in processing time and performance.

3) The ASGA was beneficialfor the selection of parameters that lead to an optimal performance at pre-installation stages and run-time if adaptive hardware is employed.
4) Principal Component Analysis (PCA) has been applied to study the effects of parameters on the bit-error-rate performance, and then define a correlation matrix that always lead a BER less than or equal to 10^{-6}.
5) An Artificial Neural networks (ANN) has been applied, benefiting from the ASGA data sets, to predict the channel performance based on signal-to-noise ratio, which can also verify the advice given by (4).
6) A Fuzzy-Neuro approach is done for channel adaptation at state-of-the art transmission of 1Gbps bit rate. The fuzzy part selected the samples that can best suit the neural network for parameter adaptation at different weather and link-range characteristics.

8.3 Addition of Adaptive Hybrid Modulation Technique

Future further work in this research would target the adaptive hybrid modulation technique proposed in [8.1], and utilize it for the ASGA selection algorithm. An additional input parameter will be added, where the three major modulation schemes in the optical wireless channel will be studied: On-off keying (OOK), pulse amplitude modulation (PAM), and pulse position modulation (PPM), according to their power and bandwidth requirements. The system is estimated to have an enhanced performance by adaptively employing amplitude and position modulation, which may lead to channel improvement, the compromises added by different modulation techniques, when compared to On-Off Keying (OOK) being summarized in Table 8.1.

Table 8.1 Comparison of Intensity Modulation Techniques (Benefited from [8.2])
R_b: Bit rate, P_{OOK}: average power requirements for OOK Modulation.

Modulation Scheme	Average Optical Power Requirement	Optical Power Penalty (Relative to OOK)	Bandwidth Requirement
OOK	P_{OOK}	0 dB	R_b
2-PPM	P_{OOK}	0 dB	$2R_b$
L-PAM	$\frac{L-1}{\sqrt{log_2 L}} P_{OOK}$	$\frac{5log_{10}(L-1)^2}{log_2 L}$ dB	$\frac{R_b}{log_2 L}$
L-PPM	$\frac{1}{\sqrt{0.5 L log_2 L}} P_{OOK}$	$-5log_{10}(\frac{1}{2} L log_2 L)$	$\frac{LR_b}{log_2 L}$

8.4 Application of Intelligent Systems in Underwater Wireless Optical communication

Wireless communication "underwater" has recently been a hot area of research and interesting applications have been implemented, such as unmanned underwater vehicles, communication among divers, ships, submarines, and under water sensors for other applications. Therefore, there's a great necessity of having efficient and high speed communications enabling the underwater data transmission of large amounts of data. In several applications, the communication has employed acoustic waves because of the low attenuation effects and long-range capability they have when transmitted in the water medium [8.3]. However, acoustic waves have narrow bandwidth, which means that they can't handle high data-rate transmissions, and the fact that its speed is as low as (1.5Km per second) causes latency in communication [8.4], [8.5]. Consequently, optical wireless communication under water is considered for using different frequencies that

can handle higher bit rates. Nevertheless, scattering and absorption effects in the underwater communication have adverse effects on the signal-to-noise ratio. This requires an appropriate selection of wavelength which might verify the need of [8.6] to satisfy the problem discussed in [8.7], it could then utilize the ASGA implemented in [8.8] if more parameters are required to be controlled and monitored. The BER prediction algorithm implemented in chapter 7 might be utilized as well, for performance prediction in the underwater communication channel. Also, due to multiscattering effects, fuzzy logic could be used at the receiver side so that it adapts itself by changing its sensitivity based on the value of received power and Signal to Noise Ratio (SNR) levels [8.9], or an ASGA could be proposed, which has carefully selected the responsivity of the receiver, given that an adaptive hardware is required at channel run-time.

8.5 Suggestions for Further Work

The further work that could be benefited from this research is the use of the ASGA in other areas of research that target selection problems. Although it is an application-specific algorithm, it could be applied to other similar purposes by changing the number of parameters, mapping them to their corresponding upper and lower bounds, and writing the appropriate objective function (model) that describes an optimized behaviour of the system. The achievement is more suitable for selection problems rather than optimization; the latter is a very general term, which makes it worthy to apply the options offered by several GA Toolboxes in terms of selection functions, mutation, and cross over, which all remain a decision of trial and error related to the optimization problem itself.

References

[8.1] Y.Zeng, R.J.Green, M.S. Leeson, "Adaptive Pulse Amplitude and Position Modulation for Optical Wireless Channel", *in proceedings of the 2nd Institution of Engineering and Technology International Conference on*, 2006.

[8.2] J. R. Barry, "Wireless Infrared Communications", *Kluwer Academic Publishers*, Boston, 1994.

[8.3] H. Ochi, Y. Watanabe, and T. Shimura, "Experiments of underwater acoustic communication using 16-QAM," *in Proceedings of 8th International Congress on Acoustics*, Kyoto, Japan, 2004.

[8.4] T. J. Hayward and T. C. Yang, "Underwater acoustic communication channel capacity: a simulation study," *in Proceedings of AIP Conference*, La Jolla, CA, USA, pp. 114–21, 2004.

[8.5] I. F. Akyildiz, D. Pompili, and T. Melodia, "Underwater acoustic sensor networks: research challenges," *in Proceedings of Journal of Ad Hoc Networks*, Vol. 3, pp. 257–79, 2005.

[8.6] A. El. Yakzan, R.J. Green and E. L. Hines, "A Genetic Algorithm based Selection of a Transmission Wavelength in the LOS Optical Wireless Channel", *International Conference on Transparent Optical Networks*, University of Warwick, UK, July, 2012.

[8.7] K. S. Shifrin, "Physical Optics of Ocean Water", *American Institute of Physics*, New York, 1988.

[8.8] A. El. Yakzan, R.J. Green and E. L. Hines, "Application-Specific Genetic Algorithm Targeting the Complexity of Parameter Selection in LOS Outdoors Optical Wireless Channel",*UKSim 15th International Conference on Mathematical/Analytical Modelling and Computer Simulation,* Cambridge, UK, 2013

[8.9] L. R. D. Suresh, S. Sundaravadivelu, "Real Time Adaptive Nonlinear Noise Cancellation using Fuzzy Logic for Optical Wireless Communication System with Multi-scattering Channel Member", *Engineering Letters, Advance Online Publication*, November 2006.

APPENDIX –A

Functions programmed for Selection Algorithm

```
% GENETIC. M %
%**********************************************
%ASGA Code

clc;                    % Clears the screen
clear all;              % Clears the memory
close all;
global Solution def LB1 UB1 LB2 UB2 LB3 UB3 LB4 UB4 LB5 UB5 LB6 UB6 LB7 UB7 LB8
UB8; % 8 Variables
gen=0;
def=1e150; % one with a hundredfifty zeros after it, def is the minimum error in each iteration.
FVAL=1e150; % global minumum error
N=20;     %Number of  phenotypes ina paramter, means we have 20sets of parameters
(chromosomes)
        %Number of solutions in each iteration,
        %Means the program starts with 20 possible solutions for each
G=500;   %Number of Generations, it means how manytimes you wish to iterate for each
solution
k=8;     %Number of Parameters, number of GENOTYPES

% Entering four intitial phenotypes

x=rand(k,N);%between 0 and 1 -, matrex of 2x100 (2 rows, 100 columns)
X(1,:)=mapping(x(1,:),LB1,UB1);%map row1                % Mapping the values to upper and
lower bounds
X(2,:) = mapping(x(2,:),LB2,UB2);%map row2
X(3,:) = mapping(x(3,:),LB3,UB3);%map row3
X(4,:) = mapping(x(4,:),LB4,UB4);
X(5,:) = mapping(x(5,:),LB5,UB5);
```

```
X(6,:) = mapping(x(6,:),LB6,UB6);

X(7,:) = mapping(x(7,:),LB7,UB7);
X(8,:) = mapping(x(8,:),LB8,UB8);
[p err CSolutionCdef]=FunGen(X);       % Calculating the probabilities
Solution=CSolution.';%selects solution with lowest error found in the first iteration only since
we started with 1e150
% we suppose that the best solution and best cdef (error) is found in the first iteration and
% base our iterations on, if we get lesser value, we replace it, &% continue.
% Global Loop Starts
%t=0;% while def>3%     t=t+1;
tic % shows the time it takes to do computations, see them in command window when running
for t=1:G % for t = 1 -> number of generations (500)

%tournament selection
tempPopulation = x;
   for i = 1:2:N
       i1 = TournamentSelect(err,p(1:i));
       i2 = TournamentSelect(err,p(1:i));
       chromosome1 = x(i1,:);
 chromosome2 = x(i2,:);
tempPopulation(i,:) = chromosome1;
tempPopulation(i+1,:) = chromosome2;
 end
sn = tempPopulation;

% Crossover Operator
cross=RandDif(N,k);
   [r c]=size(cross);
 for i=1:r
       pc(i)=rand;
       if pc(i)<=0.4 %crossover rate
          dum1=zeros(k,1);
```

```
dum2=zeros(k,1);
dum1=x(:,cross(i,1));
          dum2=x(:,cross(i,2));
          x(1:(cross(i,3)),cross(i,1))=dum2(1:(cross(i,3)));
          x(1:(cross(i,3)),cross(i,2))=dum1(1:(cross(i,3)));
     end
 end

% Mutation Operator
sn=ceil(sn.*4.2950e+009);
   for i=1:1:N
       pm(i)=rand;
       if pm(i)<=0.02 % mutation rate
dum=random(32*(k)-1);
          bit=bitget(sn(ceil(dum/32),i),mod(dum,32)+1);
          if bit
sn(ceil(dum/32),i)=bitset(sn(ceil(dum/32),i),mod(dum,32)+1,0);
          else
sn(ceil(dum/32),i)=bitset(sn(ceil(dum/32),i),mod(dum,32)+1,1);
          end
      end
 end
 x=sn./4.2950e+009;
% Display and Comparison

   X(1,:)=mapping(x(1,:),LB1,UB1);%map row1                % Mapping the values to upper and
lower bounds
   X(2,:) = mapping(x(2,:),LB2,UB2);%map row2
   X(3,:) = mapping(x(3,:),LB3,UB3);%map row3
   X(4,:) = mapping(x(4,:),LB4,UB4);
   X(5,:) = mapping(x(5,:),LB5,UB5);
   X(6,:) = mapping(x(6,:),LB6,UB6);
   X(7,:) = mapping(x(7,:),LB7,UB7);
```

```
 X(8,:) = mapping(x(8,:),LB8,UB8);



[p err CSolutionCdef]=FunGen(X);            % Calculating the probabilities
    hold on;

   if FVAL>Cdef % if current error < global error, save current error and current values
       Solution=CSolution.' %def changes in every iteration, but Fval changes only if found
better solution, more global
      FVAL=def   % best solution  = Csolutionbecausse current error is less than Fval
gen=t; % save the generation that made best solution.
         plot(t,Cdef, 'x')%generations vslamda
xlabel('generations')
ylabel('BER')
   end
end
gen % print generation that resulted in best value
Final_Error=FVAL %display final error
toc
X=Solution;
disp('  tx_app(m)   rx_app(m)  b_div(mrad)   tx_PRsalpha_sc  Range(km)   Bandwidth (MHz)')
disp(Solution)


%mapping
function X=mapping(x,LB,UB)
X=((UB-LB)*x+LB);


%Fitness Function
function [p, err, CSolution, Cdef]=FunGen(x)
global  def Solution  LB1 UB1 LB2 UB2 LB3 UB3 LB4 UB4 LB5 UB5 LB6 UB6 LB7 UB7 LB8
UB8;
Cdef=1e150;
[r c] = size(x); % returns r as # of rows, c as # of cloumns
```

```
X=x;
for val=1:c % for val = 1-> 100
   if ( X(1,val)> LB1 && X(1,val) <UB1 && X(2,val)>LB2 && X(2,val)<UB2...
&& X(3,val)>LB3 && X(3,val)<UB3 && X(4,val)>LB4 && X(4,val)<UB4...
&& X(5,val)>LB5 && X(5,val)<UB5 && X(6,val)>LB6 && X(6,val)<UB6...
&& X(7,val)>LB7 && X(7,val)<UB7 && X(8,val)>LB8 && X(8,val)<UB8)
Pr = 0.001*X(4,val)* X(2,val)^2 * 10 ^(-0.1*X(6,val)*X(7,val) ) /  ( X(1,val) + X(3,val)*X(7,val)
)^2;
   %Pr is multiplied by 0.001 here becoz in the ranges defined in Genetic, we multiplied them by
1000.
   % So Now, the value of Ptx that the GA generates should be divided by
   % 1000.
   T = 298; % Room Temperature (K)
   R = 1000; % Load resistance (Ohms)
   Kb = 1.38 * 10^-23; % Boltzmann's constant (J/K)
   q = 1.6 * 10^-19; % Electron Charge
   Sigma1= sqrt (2 * q * X(8,val)*10^8* 2 * X(5,val) * Pr + (4 * Kb*T*X(8,val)*10^8/R) );
   Sigma0= sqrt ( (4 * Kb*T*X(8,val)*10^8/R) );
   SNR= (4 * X(5,val) * Pr^2 ) /(Sigma1^2+Sigma0^2);
      err(val)= 0.5 * erfc ( sqrt (SNR/2) );
   else err(val) = 100000;
   end
end

% err=(1/6.931-X(1).*X(2)/(X(3).*X(4))).^2;

def=min(err);       % min returns a row vector from err, containing the minimum element from
each column,
Cdef=def(1);        % the first valuee in the vector, which is the minimum.
selected=find(err==Cdef); % returns the vector row positions that are equal to Cdef, so
selected is a 1xCdef if Cdef is found or its zero.
selected=selected(1); % first value of the selected data
CSolution=X(:,selected); % Csolution is a vector of X, formed from column number "selected"
```

```
c=0;
p1=(1./(err));              % Calculates the probability of reproduction of each phenotype
c=sum(p1);
p=p1./c;
d=sum(p); % is always equal to 1 (sum of all probabilities)

%Fitness Function for Wavelength Selection

function [cost1]=fitness2(in)
v=in(1,1)*3;
lambda=in(1,2)*10;
if (lamda<=10 && v<=3)
   cost=(17/(v))*(550/labmda)^(0.585*(v)^0.333);
else
   cost=10000;
end
cost1=cost;

%Randif Function
function [mat]=RandDif(N,k)
c=0;
mat=[];
while c<(N)
   [r c]=size(mat);
num=ceil(N*(rand));
   dummy=find(mat==num);
   if dummy
   else
      mat=[mat num];
   end
end
for i=1:N/2
```

```
index(i)=ceil((k-1)*rand);
end
mat=[mat index];
mat=reshape(mat,N/2,3);
% random function
function [num]=random(x)
num1 = x*rand;
num = ceil(num1);

%simple objective function
function y = simple_objective(x)
  y = (4 - 2.1*x(1)^2 + x(1)^4/3)*x(1)^2 + x(1)*x(2) + ...
      (-4 + 4*x(2)^2)*x(2)^2;

%Tournament Select
function iSelected = TournamentSelect(error,tournamentSelectionParameter);
populationSize = size(error,1);
iTmp1 = 1 + fix(rand*populationSize);
iTmp2 = 1 + fix(rand*populationSize);
r = rand;
if (r <tournamentSelectionParameter)
   if (error(iTmp1) < error(iTmp2))
iSelected = iTmp1;
   else
iSelected = iTmp2;
   end
else
if (error(iTmp1) < error(iTmp2))
iSelected = iTmp2;
   else
iSelected = iTmp1;
   end
end
```

APPENDIX-B

GA Simulations on Particular Wavelengths:

Wavelength	Visibility (km)	Attenuation (dB/km)	***Wavelength***	Visibility (km)	Attenuation (dB/km)
1064nm	0.880	17.00	***10 µm***	0.69	17.00
	0.875	16.00		0.75	15.00
	1.00	15.00		0.875	12.00
	1.067	14.00		1.00	9.68
	1.125	13.00		1.125	8.00
	1.20	12.00		1.25	6.80
	1.33	11.00		1.375	5.78
	1.395	10.00		1.50	4.95
	1.54	9.00		1.675	4.30
	1.69	8.00		1.75	3.60
	1.88	7.00		1.875	3.15
	2.130	6.00		2.00	2.75
	2.40	5.00		2.125	2.40
	2.88	4.00		2.25	2.10
	3.00	3.85		2.375	1.85
				2.50	1.50
				2.625	1.35
				2.75	1.20
				2.825	1.15
				3.00	1.00
	0.87	17.00		0.868	17.00
850nm	0.98	16.00	***1550nm***	1.00	14.00
	1.05	15.00		1.125	12.00
	1.123	14.00		1.25	10.60
	1.20	13.00		1.375	9.35
	1.28	12.00		1.50	8.42
	1.375	11.00		1.675	7.67
	1.50	10.00		1.75	6.90
	1.625	9.00		1.875	6.30
	1.82	8.00		2.00	5.70
	2.04	7.00		2.125	5.35
	2.32	6.00		2.25	4.85
	2.68	5.00		2.375	4.60
	3.00	4.40		2.50	4.15
				2.625	3.80
				2.75	3.68
				2.825	3.40
				3.00	3.82

APPENDIX-C

DataSets

Chapter 5, BER Calculation : Noise Analysis

Section 5.6.2

Solution =

0.1500 0.3768 2.9286 147.8573 0.7714 40.0929 1.0929 1.0093

FVAL =

0.3456

Gen= 1

Solution =

0.0955 0.2502 2.0390 136.1709 0.6156 40.0539 1.0539 1.0054

FVAL =

0.3216

Gen= 20

Solution =

0.0843 0.3868 2.4595 133.7857 0.5838 40.0460 1.0460 1.0046

FVAL =

0.2077

Gen= 147

Solution =

0.0756 0.3666 2.3972 193.9720 0.5589 40.0397 1.0397 1.0040

Final_Error =

0.1196

Gen= 152

Solution =

0.1557 0.3901 1.4847 199.6942 0.7878 40.0969 1.0469 1.0097

Final_Error =

3.3238e-004

Gen= 176

Solution =

0.0457 0.2972 1.0918 191.8362 0.4734 40.0184 1.0184 1.0018

1.1943e-005

Gen= 241

Solution =

0.0843 0.3868 1.2296 194.5929 0.5837 40.0459 1.0459 1.0046

Final_Error =

4.2941e-006

Gen= 343

Solution =

0.0820 0.3814 1.2213 222.1330 0.5771 40.0443 1.0443 1.0044

Final_Error =

1.8512e-007

Gen= 380

Solution =

0.0258 0.2511 1.0209 270.8348 0.4167 40.0042 1.0042 1.0004

FVAL =

1.6781e-008

Gen=398

tx_app(m) rx_app(m) b_div(mrad) tx_PRsalpha_sc RangeBandwidth

0.0694 0.3521 1.1763 277.0532 0.5411 40.0353 1.0353 1.0035

FVAL =

1.2302e-010

Gen=413

0.0780 0.3721 1.2071 278.2826 0.5657 40.0414 1.0414 1.004

FVAL =

9.3283e-011

Gen=462

RK: All Bandwidth Values are multiplied by 1E08.

Sections 5.6.3-5.6.4

GEN	*S_N*	*BER*	*tx_P*
4.40E+01	*2.58766E-07*	*0.0843*	*54.8633*
6.50E+01	*2.23754E-07*	*0.0743*	*79.3004*
1.00E+02	*2.06095E-07*	*0.0287*	*62.1238*
1.09E+02	*2.19472E-07*	*0.0212*	*251.7673*
1.65E+02	*2.73836E-07*	*0.0095*	*251.7673*
2.00E+02	*2.11781E-07*	*0.0087*	*114.1483*
2.10E+02	*2.172E-07*	*0.0024*	*59.0569*
2.27E+02	*2.53976E-07*	*0.00093093*	*179.1285*
2.29E+02	*2.62867E-07*	*0.00049154*	*210.9048*
2.40E+02	*2.06654E-07*	*0.00022935*	*170.3812*
3.13E+02	*2.50527E-07*	*1.85E-05*	*23.546*
3.52E+02	*2.3391E-07*	*1.76E-05*	*111.1913*
3.94E+02	*2.06816E-07*	*3.24E-06*	*28.2403*
3.99E+02	*2.05185E-07*	*8.58E-07*	*23.546*
4.01E+02	*2.50527E-07*	*4.39E-07*	*175.3349*
4.05E+02	*2.03288E-07*	*2.42E-07*	*18.1351*
4.11E+02	*2.35565E-07*	*7.92E-09*	*116.3598*
4.36E+02	*2.11019E-07*	*1.76E-09*	*40.2858*
4.63E+02	*2.51104E-07*	*1.32E-10*	*168.7134*
4.92E+02	*2.34318E-07*	*1.81E-10*	*17.455*
4.51E+02	*2.20229E-07*	*2.69E-11*	*67.8051*

Section 5.6.5

Data Sample:

0.0459 0.1352 1.3338 67.8051 0.4741 40.0414 0.65 4.983 2.69E-11

Gen=492

Section 5.7

Final_Error =

7.5344e-010

tx_apprx_appb_divtx_PRsalpha_sc Range Bandwidth

0.0215 0.2411 4.0011 5.0550 0.4044 10.0011 1.0220 1.0001

Gen =

468

Final_Error =

7.9808e-009

tx_apprx_appb_divtx_PRsalpha_sc Range Bandwidth

0.0996 0.2598 3.8412 69.3697 0.6274 20.0569 1.1372 1.0057

Gen =

342

Final_Error =

1.3783e-009

tx_apprx_appb_divtx_PRsalpha_sc Range Bandwidth

0.1559 0.3905 2.7207 149.1197 0.7883 30.0971 1.0971 1.0097

Gen=

267

Chapter 6

Data Sets in A, B, and C for different BER values.

Contribution of the observations (%):

	F1	F2	F3	F4	F5
A	0.800	0.000	0.099	0.074	1.270
A	0.901	0.006	0.092	0.063	1.418
A	1.131	0.049	0.090	0.024	1.599
A	0.938	0.021	0.112	0.042	1.333
A	0.758	0.001	0.115	0.044	1.085
A	0.451	0.081	0.103	0.220	0.951
A	0.452	0.082	0.103	0.219	0.950
A	0.762	0.006	0.078	0.170	1.472
A	0.783	0.020	0.151	0.001	0.823
A	0.329	0.005	0.322	0.107	0.301
A	0.000	0.423	0.342	0.158	0.822
A	0.655	0.010	0.171	0.004	1.121
C	0.456	0.002	0.244	0.015	0.232
B	0.007	0.335	0.494	0.010	0.254
A	0.489	0.001	0.250	0.020	0.219
A	0.902	0.107	0.194	0.045	0.636
A	0.022	0.112	0.433	0.000	0.596
B	0.941	0.212	0.246	0.178	0.421
A	0.397	0.005	0.332	0.110	0.044
A	0.927	0.201	0.249	0.178	0.403
A	0.016	0.167	0.538	0.118	0.303
B	0.869	0.253	0.301	0.317	0.227
B	0.207	0.044	0.658	0.148	0.049
C	0.853	0.332	0.360	0.489	0.119
B	0.208	0.000	0.454	0.242	0.031
B	0.366	0.084	0.701	0.098	0.006
A	0.005	0.005	0.740	0.349	0.021
B	0.360	0.116	0.556	0.773	0.088
A	0.523	0.402	0.697	0.534	0.017
C	0.741	0.464	0.509	0.814	0.002
B	0.632	0.350	0.514	0.972	0.008
C	0.162	0.029	0.646	0.776	0.335
A	0.335	0.502	0.052	0.204	2.527
A	0.713	0.751	0.344	0.100	4.527
A	1.306	1.481	0.719	0.065	3.944
C	0.000	0.013	0.949	1.111	1.697

C	0.130	0.072	0.792	1.278	0.722
C	0.291	0.221	0.970	0.561	0.146
C	0.625	0.553	0.613	1.511	0.087
C	0.499	0.519	0.751	1.258	0.161
A	0.163	0.077	0.795	1.338	0.704
B	0.335	0.427	0.914	1.001	0.318
A	0.016	0.068	0.995	1.231	0.046
A	1.034	3.457	0.921	0.655	8.482
C	0.057	6.320	0.140	0.225	0.662
B	0.270	2.970	3.812	0.169	0.000
A	0.231	3.260	3.509	0.179	0.001
A	0.786	0.354	1.675	1.964	0.615
A	0.104	0.434	0.074	5.782	3.456
A	0.096	0.411	0.079	5.790	3.332
C	0.205	3.760	0.797	0.837	9.653
A	0.158	3.670	1.020	0.850	10.522
C	0.267	5.664	1.621	1.320	2.543
B	0.005	2.838	7.749	1.158	0.473
B	0.290	5.925	1.498	1.345	2.454
A	0.316	6.231	1.361	1.374	2.356
A	0.010	2.364	7.911	0.926	0.504
A	0.515	0.108	0.021	3.887	0.004
B	0.567	0.139	0.018	3.956	0.011
C	0.008	1.853	0.348	2.074	3.733
A	0.099	3.570	0.370	0.006	0.523
A	1.235	0.517	0.011	0.001	0.004
B	1.387	0.387	0.034	0.002	0.006
C	1.904	2.883	0.020	0.049	0.227
C	3.997	0.001	0.004	0.103	0.520
C	3.925	0.002	0.002	0.123	0.549
A	2.360	0.372	0.161	0.980	0.195
C	3.996	0.000	0.010	0.244	0.028
C	1.923	0.459	0.358	1.644	0.425
A	2.335	0.377	0.170	1.012	0.205
A	3.435	0.000	0.036	0.004	0.137
A	3.519	0.000	0.053	0.001	0.128
A	3.515	0.003	0.203	0.016	0.070
A	3.461	0.002	0.180	0.011	0.073
A	3.307	0.001	0.123	0.003	0.085
A	3.926	0.137	0.246	0.038	0.212
C	3.499	0.041	0.105	0.045	0.394
A	2.028	0.049	0.008	0.324	0.038
C	3.245	0.001	0.587	0.000	0.028

C	0.024	2.401	3.491	0.088	0.264
B	0.008	2.642	4.159	0.085	0.390
A	0.039	2.285	3.699	0.083	0.418
C	0.268	1.343	1.431	0.101	0.039
A	0.017	2.792	3.629	0.018	0.491
C	0.063	2.484	1.493	0.001	0.001
C	0.025	2.747	2.732	0.000	0.265
B	0.409	1.371	0.204	0.004	0.236
C	0.000	3.779	3.147	0.027	0.276
A	1.750	0.557	0.884	0.595	0.020
A	1.460	0.768	0.631	0.579	0.010
A	2.282	0.283	1.393	0.621	0.044
C	0.454	2.213	0.013	0.500	0.009
A	2.499	0.204	1.610	0.635	0.055
A	1.651	0.623	0.795	0.589	0.016
C	0.510	0.061	0.198	7.042	2.619
A	0.563	0.020	0.534	7.616	2.473
C	0.242	0.311	2.265	3.401	0.643
C	0.340	0.446	2.653	3.373	0.707
A	0.279	0.339	0.216	3.292	2.307
B	0.792	0.430	2.102	2.019	0.025
A	0.216	0.041	0.368	2.048	0.359
A	1.023	0.635	2.576	1.979	0.039
A	2.290	0.345	0.004	2.671	2.507
A	0.898	1.345	1.995	2.734	0.377
A	0.514	2.090	2.986	2.834	0.504
A	1.911	0.271	0.765	2.998	0.221

Chapter 6 Section 6.2:

Guaranteed Margin,

Data Set:

0.0430 0.2908 0.5820 258.1983 0.4656 12.164 3.0164 1.82

BER= 6.8167e-009.

Section 6.3.4:

Data Set:

0.1474 0.3708 1.9551 274.428 0.491 20.183 1.5821 1.9551

BER = 1.19E-11

Data Sets Used for ANN –SNR Prediction

0.1474	0.3708	1.9551	274.4283	0.491	20.183	1.5821	1.9551	42.96
0.1569	0.3927	1.9888	293.6055	0.4978	20.1957	1.5955	3.5955	27.7847
0.1394	0.3521	1.9263	258.0094	0.4853	20.172	1.5205	4.3705	31.4584
0.1406	0.355	1.9307	260.5016	0.7446	20.1737	1.7446	4.9972	3.3074
0.1094	0.2826	3.7353	6.7478	0.6555	20.1313	0.8466	4.4639	4.9354
0.0827	0.3831	3.0681	48.9605	0.6896	20.0951	2.0896	3.0896	8.8E-04
0.1436	0.3516	2.2766	192.5535	0.7851	20.1717	1.6053	2.4255	10.06995
0.032	0.0901	2.3011	72.0427	0.5903	20.1244	1.0204	2.3011	7.2285
0.0242	0.2472	4.003	5.1499	0.412	10.003	1.06	1.0003	30.8687
0.1069	0.2768	4.0621	8.1045	0.6484	10.0621	1.2418	1.0062	37.9755
0.0202	0.3521	0.5055	300.5528	0.7011	20.0121	2.7033	1.0011	0.1357
0.032	0.0901	2.3011	72.0427	0.5903	20.1244	1.0204	2.3011	7.2285

APPENDIX-D

IL700A research radiometer

Sensitivity factor set to equal 1.776E-2 (cm^2/W)

Radiometer Probes